

THE USE OF SUPERCRITICAL FLUID CHROMATOGRAPHY (SFC) AND LIQUID
CHROMATOGRAPHY (LC) FOR THE SEPARATION OF PHARMACEUTICAL
PRODUCTS, NATURAL PRODUCTS AND CHIRAL
PHOSPHORIC AND SULFONIC ACIDS

by

JONATHAN PAUL SMUTS

Presented to the Faculty of the Graduate School of
The University of Texas at Arlington in Partial Fulfillment
of the Requirements
for the Degree of

DOCTOR OF PHILOSOPHY

THE UNIVERSITY OF TEXAS AT ARLINGTON

December 2013

I dedicate this dissertation to my late mother, Anna Catharina Dolphina Smuts (February, 1934 – May, 2000). “*Her children arise up, and call her blessed...*” – Prov. 31:28

Acknowledgements

I would like to thank my research professor, Dr. Daniel W. Armstrong for the honor of working in his research group and for the guidance he afforded throughout the degree. Many times I have found his patience to be a tacit rebuke to my impatience. I would also like to thank my research committee: first Dr. Sandy Dasgupta who, like my late mother, always held to me a higher standard and made sure I push myself to the limit even though I did not always make it or like it; secondly Dr. Subhrangsu Mandal who kindly chaired the committee for all my research updates. Thank you all for your time and inputs into my degree. I would also extend my thanks to the entire Armstrong research group, particularly Zach, Sophie, Eranda, Nilusha, John, Edra, Eva and Barbara. I worked closely with all of you and found you professional colleagues in our research.

To my dear family who has been closer to me than all of the above, I confess I have not always been patient and cheerful and have taken much for granted and given little in return. Thank you for your love and support in these five years of study. To Kelly, my wife, “thou art all fair, my love; there is no spot in thee” and in your mouth is “the law of kindness.” To my children, Calvin and Elizabeth, you are faithful arrows in my quiver and a heritage from the Lord.

Lastly, and most importantly, I extend my humble thanks to my heavenly Father who has been even closer to me than my own family. I owe my entire existence to Thee and yet have been an unprofitable servant who has not done his duty as he ought. I am so grateful for your abounding grace and mercy; for the parents you blessed me with, for their counsel, correction and prayers. The psalmist, David, spoke truly when he said, “The Lord is merciful and gracious, slow to anger, and plenteous in mercy. He will not always chide: neither will he keep his anger forever. He hath not dealt with us after our sins; nor rewarded us according to our iniquities. For as the heaven is high above the

earth, so great is his mercy toward them that fear him. As far as the east is from the west, so far hath he removed our transgressions from us. Like as a father pitieth his children, so the Lord pitieth them that fear him. For He knoweth our frame; he remembereth that we are dust.” – Ps. 103: 8 – 14

November 25, 2013

Abstract

THE USE OF SUPERCRITICAL FLUID CHROMATOGRAPHY (SFC) AND LIQUID
CHROMATOGRAPHY (LC) FOR THE SEPARATION OF PHARMACEUTICAL
PRODUCTS, NATURAL PRODUCTS AND CHIRAL
PHOSPHORIC AND SULFONIC ACIDS

Jonaathan Paul Smuts, PhD

The University of Texas at Arlington, 2013

Supervising Professor: Daniel W. Armstrong

This dissertation focuses on two chromatographic techniques, supercritical fluid chromatography (SFC) and high performance liquid chromatography (HPLC). The goal of the SFC work is to describe the synthesis of new stationary phases based upon ionic liquids and to discuss their application to the separation of pharmaceutical compounds. The tunable nature of immobilized ionic liquids will be demonstrated by the variation of the cation-anion combination.

The goal of the remaining chapters is to demonstrate HPLC applications for analyzing natural products and for performing enantiomeric separations. The usefulness of HPLC in separating antioxidants in rosemary and in conducting a degradation study of the main antioxidants will be demonstrated. The sections dealing with enantiomeric separations will show, firstly, the important role vancomycin-based chiral stationary phases (CSPs) play in providing answers regarding the stereoisomeric distribution of flinderole B in nature and in separating its related bisindole alkaloid enantiomers. Secondly, novel separations of chiral anionic compounds will be presented for the new cyclo-oligosaccharide, cyclofructan 6, by exploiting its ionophoric proclivity for barium

cations. The ability to tune retention and enantioselectivity of cyclofructan-barium CSPs by varying the kosmotropicity/ chaotropicity of the counter anion will be demonstrated.

Table of Contents

Acknowledgements	iii
Abstract	v
List of Illustrations	xii
List of Tables	xv
Chapter 1 Introduction.....	1
1.1 Organization of dissertation	1
1.2 Comparison of Supercritical fluid chromatography (SFC) and HPLC	1
1.3 The importance of pharmaceuticals and natural products and chromatographic techniques to characterize them.....	4
1.4 The importance of enantiomeric separations and the use of HPLC/ SFC chiral stationary phases (CSPs)	6
Chapter 2 Comparison of stationary phases for packed column supercritical fluid chromatography based upon ionic liquid motifs: A study of cation and anion effects	9
2.1 Abstract.....	9
2.2 Introduction	9
2.3 Experimental.....	12
2.3.1 Equipment	12
2.3.2 SFC Operation.....	12
2.3.3 Reagents and chemicals	13
2.3.4 Samples.....	13
2.3.5 Synthesis of ionic-liquid-based stationary phases	15
2.3.5.1 Tributylphosphonium stationary phase (PBU ₃)	16
2.3.5.2 Tripropylphosphonium stationary phase (PPr ₃)	16

2.3.5.3 Triphenylphosphonium stationary phase (PPh ₃)	18
2.3.5.4 Methyl-imidazolium stationary phase (Me-Im).....	18
2.3.5.5 Benzyl-imidazolium stationary phase (Bz-Im).....	19
2.3.5.6 4,4'-Bipyridyl stationary phase (4,4'-BiPy)	19
2.3.6 Column packing.....	19
2.3.7 Anion exchange.....	20
2.4 Results and Discussion	21
2.4.1 Cation effect study.....	23
2.4.2 Anion effect study	28
2.5 Conclusion	33
Chapter 3 Degradation study of carnosic acid, carnosol, rosmarinic acid, and rosemary extract (<i>Rosmarinus officinalis</i> L.) assessed using HPLC	34
3.1 Abstract.....	34
3.2 Introduction	34
3.3 Materials and methods	36
3.3.1 Materials	36
3.3.2 HPLC Methods	37
3.3.3 HPLC/MS/MS method	37
3.3.4 Calibrations.....	38
3.3.5 Sample preparation and storage.....	40
3.3.6 Rosemary powder extraction.....	42
3.4 Results and discussion.....	42
3.4.1 Analytical method	42
3.4.2 Degradation of carnosic acid, carnosol, rosmarinic acid, and their mixture in ethanol solutions	42

3.4.2.1 Degradation profiles of three primary phenolic antioxidants in rosemary	43
3.4.2.2 Identification of degradation products and pathways of carnosol and carnosic acid. degradation products of carnosol.....	45
3.4.2.4 Degradation pathway of carnosic acid.....	55
3.4.2.5 Degradation of the mixture.....	55
3.4.3 Degradation of rosemary extract in fish oil.....	60
3.4.4 Kinetic data.....	63
3.4.4.1 Analysis and discussion.....	64
3.5 Conclusion	68
Chapter 4 On the biosynthesis and optical activity of the flinderoles	69
4.1 Abstract.....	69
4.2 Introduction	69
4.3 Experimental.....	72
4.3.1 Synthesis of flinderole B.....	72
4.3.2 Preparative HPLC.....	72
4.3.3 Analytical HPLC.....	72
4.3.4 Mass spectrometry	72
4.3.5 Optical rotation determination	73
4.4 Results and discussion.....	73
4.5 Conclusions	75
Chapter 5 Enantioseparation of flinderoles and borreverines by HPLC on Chirobiotic V and V2 stationary phases and by CE using cyclodextrin selectors	77
5.1 Abstract.....	77

5.2 Introduction	77
5.3 Experimental	79
5.3.1 Materials	79
5.3.2 HPLC	80
5.3.3 Preparative HPLC.....	81
5.3.4 Capillary electrophoresis (CE).....	81
5.4 Results and discussion	82
5.4.1 HPLC and preparative HPLC	82
5.4.2 Capillary electrophoresis (CE) separations	91
5.5 Conclusions	93
Chapter 6 Enantiomeric separations of chiral sulfonic and phosphoric acids	
with barium-doped cyclofructan selectors via an ion interaction mechanism	95
6.1 Abstract.....	95
6.2 Introduction	95
6.3 Experimental section	98
6.3.1 Synthesis of CSA-1 – 5 and CPA-7.....	99
6.3.1.1 CSA-1 – CSA-5.....	99
6.3.1.2 CPA-7.....	100
6.3.2 HPLC	101
6.3.3 Preparative HPLC.....	102
6.3.4 van't Hoff plots.....	102
6.3.5 Barium loading and removal.....	102
6.4 Results and discussion	103
6.4.1 Effect of the counter anion of the Ba ²⁺ salt.....	107
6.4.2 Effect of the mobile phase dielectric constant.....	113

6.4.3 Retention order.....	113
6.4.4 Effect of varying concentration of the Ba ²⁺ salt in the mobile phase.....	114
6.4.5 van't Hoff plots.....	115
6.4.5.1 ln k vs. 1000/T.....	117
6.4.5.2 ln α vs. 1000/T.....	122
6.4.6 Optimized separations.....	123
6.5 Conclusion.....	125
Chapter 7.....	127
7.1 General summary.....	127
Appendix A Names of co-contributing authors.....	130
Appendix B Rights and permissions.....	132
References.....	138
Biographical Information.....	146

List of Illustrations

Figure 1-1 Phase diagram illustrating the supercritical region for CO ₂ . ¹	2
Figure 2-1 A list of basic and acidic drugs analyzed by SFC.....	14
Figure 2-2 Outline of the two possible reaction schemes for the synthesis of ILLs.....	15
Figure 2-3 Improvement in peak shape through column packing.....	20
Figure 2-4 Retention time repeatability on the PBU ₃ TFA stationary phase.	22
Figure 2-5 Anion effect for the separation of BB Mix 1 on PBU ₃	29
Figure 2-6 Anion effect for the separation of BD Mix 1 and 2 on PBU ₃	30
Figure 2-7 Anion effect for the separation of Acid Mix on PBU ₃	31
Figure 3-1 Structures of compounds for this study.	39
Figure 3-2 UV spectra of A) carnosol, B) carnosic acid and C) rosmarinic acid.....	41
Figure 3-3 Degradation profiles of three primary phenolic antioxidants in rosemary.	44
Figure 3-4 HPLC chromatograms of the degradation study.	47
Figure 3-5 Degradation products of carnosol as a function of time at 40 °C with light exposure.	48
Figure 3-6 HPLC chromatograms of carnosol ethanol solutions stored under different conditions after 13 days.	49
Figure 3-7 HPLC chromatograms of carnosic acid ethanol solutions stored under different conditions after 13 days.	52
Figure 3-8 The proposed degradation pathway of carnosic acid in ethanol solution.	54
Figure 3-9 HPLC chromatograms of carnosic acid/carnosol mixture ethanol solutions stored under different conditions after 13 days.....	58
Figure 3-10 HPLC chromatograms of A) methanolic rosemary extract, B) fish oil and C) rosemary extract in fish oil	61
Figure 3-11 Rate constant diagram of Figure 3-8.....	63

Figure 3-12 Carnosol kinetics for different simplifications of Figure 3-11.....	66
Figure 4-1 Isoprenylated indole natural products.	70
Figure 4-2 Biosynthesis of the borreverines.	70
Figure 4-3 Biosynthesis of the flinderoles.	71
Figure 4-4 HPLC separation of (-)- and (+)-flinderole B on Chirobiotic V	75
Figure 5-1 Structures of the flinderole and borreverine compounds.	78
Figure 5-2 Comparison of the 2- and 3-dimensional representations of flinderole B and C.	85
Figure 5-3 Structures of a beta-blocker (atenolol), citalopram and flinderole B	87
Figure 5-4 Enantioseparations of various flinderole and borreverine racemates on the V2 column in the polar organic mode.....	88
Figure 5-5 Flinderole C racemate on V2 (2) and V (1 , 3 and 4) columns.....	88
Figure 5-6 Preparative enantioseparation of flinderole B on V column	90
Figure 5-7 Electropherograms of the flinderole and borreverine racemates	92
Figure 6-1 Structures of the chiral sulfonic and phosphoric acid analytes.	99
Figure 6-2 Synthetic schemes for: A) CSA-1 - 5 and B) CPA-7	100
Figure 6-3 Original separation of CSA-5.....	104
Figure 6-4 Preparative HPLC separation of racemic CSA-5 on Ba ²⁺ -doped FRULIC-N	105
Figure 6-5 Barium counter anion effect on enantioselectivity	109
Figure 6-6 Effect of selective adsorption of eluent anions on the potential curve of a charged surface.	112
Figure 6-7 Change of K (blue diamond) and complexed Ba ²⁺ (red square) as a function of temperature.....	117
Figure 6-8 van't Hoff plot (lnk vs. 1000/T) for CPA-1 and CSA-5 using Ba(OAc) ₂ additive	118

Figure 6-9 van't Hoff plot ($\ln k$ vs. $1000/T$) for CPA-1 and CSA-5 using $\text{Ba}(\text{TFA})_2$ additive	119
Figure 6-10 van't Hoff plot ($\ln k$ vs. $1000/T$) for CPA-1 and CSA-5 using $\text{Ba}(\text{ClO}_4)_2$ additive	119
Figure 6-11 van't Hoff plot ($\ln \alpha$ vs. $1000/T$) for CPA-1 and CSA-5 using three different Ba^{2+} -salt additives	120
Figure 6-12 Effect of temperature on enantioselectivity for CPA-1 (entropy driven) and CSA-5 (enthalpy driven) in a methanol mobile phase containing 5 mM $\text{Ba}(\text{ClO}_4)_2$	123
Figure 6-13 Overview of the performance of commercially available cyclofructan columns (complexed with barium) in separating chiral sulfonic and phosphoric acids.	125

List of Tables

Table 1-1 Typical physical properties of gases, liquids and supercritical fluids	2
Table 2-1 Summary of reaction conditions used for the synthesis of the six stationary phases.....	17
Table 2-2 Retention factors for six beta-blockers on six cationic stationary phases.	23
Table 2-3 Retention factor data for all analytes analyzed on the cationic stationary phases.....	26
Table 2-4 Selectivity data for the separation of BB Mix 2.....	27
Table 2-5 Effect of anion variation on the selectivity for BB Mix 2.....	32
Table 3-1 Statistical figures of merit and calibration curve results	40
Table 3-2 Peak area data for epirosmanol ethyl ether and carnosol in solutions 1 – 3....	59
Table 3-3 MS and UV spectral data for rosemary compounds.....	62
Table 3-4 Summary of rate constants for the degradation of carnosic acid and carnosol, and for the formation of their degradation products.....	65
Table 4-1 Optical rotation data for (-)- and (+)-flinderole B.....	74
Table 5-1 Chromatographic parameters for the enantioseparation of flinderole and borreverine racemates on V and V2.	84
Table 5-2 Chromatographic parameters for the enantioseparation of flinderole C on V and V2 columns in the reversed phase mode.....	90
Table 5-3 Optimized CE enantioseparations of flinderole and borreverine racemates.	91
Table 6-1 Effect of barium pretreatment on the retention and enantioselectivity of chiral sulfonic and phosphoric acids on commercially available cyclofructan columns.....	106
Table 6-2 – Continued.....	107

Table 6-3 Comparison of different barium salt additives (~ 5 mM in each mobile phase) on the retention (k), selectivity (α) and resolution (R_s) of chiral sulfonic/ phosphoric acids on LARIHC-CF6-P in the polar organic mode.	111
Table 6-4 Linear regression of the log k vs. log [X] plots for CPA-1 and CSA-5 for different Ba ²⁺ salts.....	114
Table 6-5 Thermodynamic parameters calculated from the van't Hoff plots in Figures 6-8 – 6-11.	121

Chapter 1

Introduction

1.1 Organization of dissertation

This dissertation focuses primarily on HPLC and in one instance an application of SFC. Chapter 2 addresses the synthesis of new SFC stationary phases and their applicability in separating pharmaceutical products. Chapter 3 is an HPLC examination of antioxidants present in rosemary. Chapters 4 and 5 are studies on flinderole, borreverine and closely related molecules. The first of these chapters attempts to address the concern as to whether Flinderole B is naturally racemic. This was done by isolating both enantiomers from a synthetic racemic mixture and measuring the respective specific rotations and comparing them with the naturally occurring flinderole B. The second of these chapters focuses on the enantiomeric separation of the flinderole and borreverine racemates using Chiribiotic V/V2 columns. The final chapter, Chapter 6, outlines the development of a unique enantiomeric separations approach. It utilizes the crown ether like behavior of cyclofructan 6 chiral stationary phases (CSPs) to form a complex with barium cations in the polar organic mode. These CSPs exhibit retention and enantioselectivity towards chiral sulfonic and phosphoric acids according to an ion-interaction mechanism.

1.2 Comparison of Supercritical fluid chromatography (SFC) and HPLC

A supercritical fluid is a substance which exceeds its critical temperature and pressure. For carbon dioxide (CO₂), the most popular and practical supercritical fluid, these critical values are T_{crit} = 31 °C and P_{crit} = 73 atm (see Figure 1-1). The physical properties for gases, liquids and supercritical fluids are compared in Table 1-1. Since supercritical CO₂ has a viscosity more similar to its gaseous form and a density more similar to its liquid form, it may be considered as a non-viscous liquid or a solvating gas.

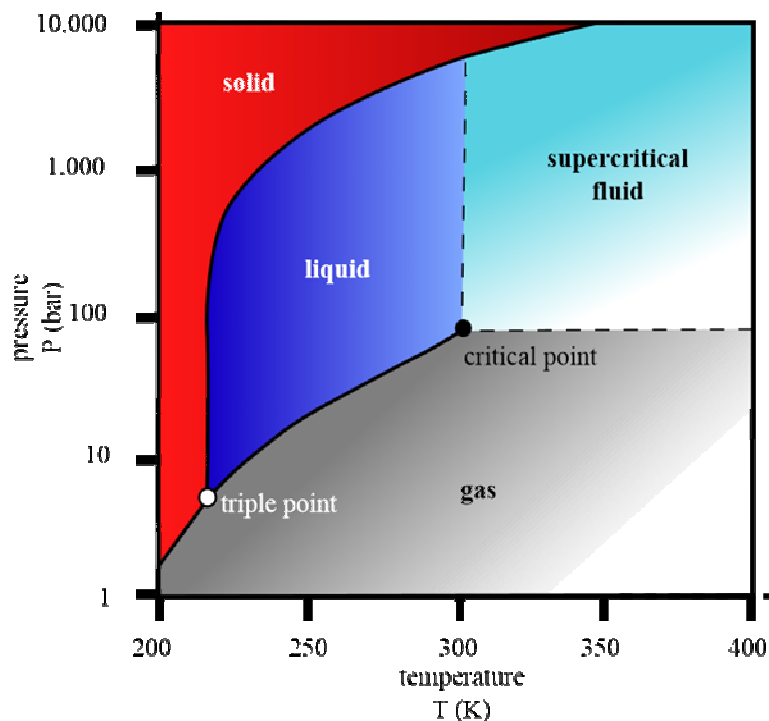


Figure 1-1 Phase diagram illustrating the supercritical region for CO₂.¹

Table 1-1 Typical physical properties of gases, liquids and supercritical fluids

Property	Gas	Supercritical fluid	Liquid
Diffusion coefficient, D _m (cm ² /s)	10 ⁻¹	10 ⁻³ – 10 ⁻⁴	<10 ⁻⁵
Density, ρ (g/cm ³)	10 ⁻³	10 ⁻¹	1
Viscosity, η (g/cm.s)	10 ⁻⁴	10 ⁻⁴ – 10 ⁻³	10 ⁻²

The use of supercritical fluids as mobile phases for chromatographic separations was first demonstrated by Klesper in 1962 for the separation of thermally labile porphyrins on a packed GC column.² Approximately two decades later SFC could have branched into two alternate areas: 1) either packed column SFC (developed by Berger et al. in the 1990s³⁻⁶) or 2) capillary SFC (Novotny et al.)⁷⁻⁹ The latter became the dominant

area of focus at that time partly because of the momentum of commercially available capillary GC columns and partly because capillary SFC was touted as having all of the benefits of GC and HPLC while being amenable to flame ionization detection (FID). Unfortunately supercritical CO₂, the most popular and practical supercritical fluid, has poor solvating power, with only the most non-polar samples, such as petrochemicals, soluble in it. The use of organic modifiers such as methanol to improve eluting power was inevitable and resulted in two things: 1) the use of FID was not possible due to increased baseline and 2) the supercritical fluid became a sub-critical fluid because of the presence of appreciable amounts of organic modifier. By the 1990s, interest faded in SFC and remained so until later in the decade when analytical chemists sought ways to increase sample throughput and reduce costs for preparative scale HPLC separations. The solution to these pressing concerns was packed column SFC, which became a boon for the pharmaceutical industry.

Packed column SFC is essentially a normal phase chromatographic technique because a polar column is used with an aprotic solvent containing a protic modifier.¹⁰ Most of the columns that are used in SFC (diol, aminopropyl, silica, 2-ethylpyridine) are normal phase columns. The contrasting differences between HPLC and SFC use and instrumentation are:

- 1) the mobile phase in SFC has a much lower viscosity than it does in HPLC and therefore can be easily operated at flow rates of up to 5 mL/min on a 25 cm column x 4.6 mm.
- 2) since CO₂ intended for SFC is a liquid, the pump head for the CO₂ must be chilled to -10 °C, requiring a chiller and a specialized pump head.

- 3) to maintain a stable supercritical fluid, the back pressure, i.e., after the detector, must be regulated above the critical pressure, usually at ~100 atm, requiring a back pressure regulator.
- 4) a high pressure UV cell is required for SFC since the high pressure is maintained across the detector cell as well.
- 5) a thermostated column chamber that can function over a 20 – 80 °C range is mandatory for SFC to control temperature effectively whereas in HPLC it is optional.

As a result, a typical SFC will be more expensive than an HPLC. This cost however is easily offset by the solvent savings in preparative SFC versus preparative HPLC. The former is amenable to 100 mg – 100 kg scale separations using appropriately sized columns and sample injection systems.¹⁰ Packed column SFC has thus gained interest in the analysis of pharmaceuticals and natural product.

1.3 The importance of pharmaceuticals and natural products and chromatographic techniques to characterize them

Many successful drugs have been developed by mimicking natural products. A case in point is Aspirin. More than 2000 years ago Hippocrates recommended chewing the bark of a willow tree to alleviate pain.¹¹ The active component in willow bark is salicin which consists of a glucose derivatized salicyl alcohol molecule. This product can be hydrolysed to salicyl alcohol which can in turn be oxidized to salicylic acid. The oxidized product was discovered to be more effective in treating pain but caused extreme irritation of the stomach lining. To circumvent this, researchers at Bayer acetylated the salicylic acid phenolic group to produce what is now called Aspirin. Other compounds in nature having high efficacy, but low abundance have to be produced synthetically. Examples of this are the very effective anti-cancer drug, Taxol,^{12,13} and the extremely powerful non-

opiate analgesic, epibatidine.¹⁴ The former is extracted from a rare and slowly growing tree whose taxol content could not possibly meet the growing pharmaceutical demand. The latter compound is found in the skin of Ecuadorian tree frogs which are a protected species. Other compounds, though, are still commercially viable as extracts; an example is quinine and its related cinchona analogs. In all these cases, the isolation of the pure, active natural component is largely dependent on both analytical and preparative chromatographic techniques.

Assays in bulk pharmaceutical and formulated products are dominated by reversed phase HPLC with diode array detection (DAD). According to recent reviews on pharmaceuticals and related drugs,^{15,16} although 2 μm particle diameter stationary phases are becoming more and more popular, a lot of work is still conducted on standard 150 mm x 4.6 mm or 250 mm x 4.6 mm containing 5 μm particle diameter C18, C8 and CN phases. Many of these methods are run with isocratic acetonitrile/ water or methanol/water mobile phases with a phosphate buffer to control pH.¹⁵ Typical reversed phase columns are relatively inexpensive, robust and have excellent efficiency and reproducibility, necessary qualities for pharmaceutical assays.

Reversed phase columns are also suitable for more complex samples such as natural product analysis, fermentation based drugs, for conducting degradation studies and purity/impurity profiling by utilizing ion-pairing, gradient and micellar RPLC conditions. In some of these cases electrospray ionization mass spectrometry (ESI-MS) together with DAD are the preferred method of detection and therefore volatile buffers such as ammonium acetate are required. Interest also has grown in monolithic columns, molecularly imprinted polymers and small particle diameter silica-based columns known as ultra-high pressure liquid chromatography (UHPLC) to decrease method run times and increase sample throughput. The increased efficiency of UHPLC is attractive for the

analysis of complex samples. Some researchers, however, have suggested that it has not been as readily adopted in pharmaceutical assays due to repeatability problems possibly arising from nonlinear heating effects.¹⁵ Regardless, UHPLC is continually gaining ground in analytical pharmaceutical applications.¹⁷⁻²⁰

A growing interest in hydrophilic interaction chromatography (HILIC) has also been observed.²¹⁻²⁴ Polar molecules that are not adequately retained and/ or do not separate on reversed phase columns are separated in this mode of chromatography. HILIC is a special class of normal phase LC (NPLC) in that it consists of a polar stationary phase (bare silica, diol, aminopropyl, cyanopropyl etc.) and analytes are retained on the basis of increasing polarity. The mobile phase consists of acetonitrile containing small amounts of (1 – 40 %) aqueous buffer which is vastly different from heptane-alcohol systems used in NPLC. The hydro-organic mobile phase of HILIC allows for the analysis of polar compounds that are insoluble in NPLC systems, e.g., amino acids, sugars, drug metabolites and peptides. Since HILIC and RPLC are complementary to each other and the respective mobile phases are miscible, the two have great potential for comprehensive LC x LC.

1.4 The importance of enantiomeric separations and the use of HPLC/ SFC chiral stationary phases (CSPs)

The importance of enantiomeric separations extends to fields such as asymmetric synthesis and catalysis, studies of biological systems, biochemistry and medicinal chemistry. The ability to separate enantiomers by HPLC was at first a challenge to separation scientists. Pure enantiomers have identical physical and chemical properties and thus cannot be separated by ordinary physical or chemical methods. Pasteur was fortunate in that the tartrate enantiomers in racemic tartaric acid crystallized with different morphologies. The mixture however was still racemic and

Pasteur had to physically separate the two enantiomers using tweezers and a magnifying glass. A chiral entity, i.e., a stationary phase substrate or pairing agent, is required to interact with the enantiomers for their separation by chromatographic means. In the case of a chiral stationary phase, the chiral entity will preferentially interact with one of the enantiomers more than the other and thus separate the two. In the case of a chiral pairing agent, the enantiomers form short-lived diastereomeric adsorbates that can be separated on an achiral column. This interaction, or chiral recognition, has been called the three point interaction model. In other words, a minimum of three simultaneous interactions is required between the CSP and the enantiomers with at least one of these interactions being stereochemically dependent, i.e. it will be present for one enantiomer but attenuated or completely absent for the other.^{25,26} In 1992 the FDA issued a policy statement for the development of new stereoisomeric drugs. The policy indicates that the stereoisomeric composition of any drug containing a chiral center must be known and quantified for pharmacological, toxicological and clinical studies. A pharmacokinetic study for each enantiomer, or for a mixture of enantiomers, would require an assay that could separate the enantiomers. This policy therefore gave additional impetus to the already growing field of enantiomeric separations.

The first chiral stationary phase (CSP) was developed by Davankov.²⁷ L-proline, immobilized on a resin, in the presence of Cu^{2+} ions in the mobile phase, forms Cu^{2+} chelate with its amino and carboxylate moieties. The resulting ternary complexes with amino acid enantiomers afforded diastereomeric complexes with different stabilities. This is known as a ligand exchange type of chromatography. Thereafter Cram and co-workers developed chiral crown ethers to separate primary amines which form complexes with the 18-crown-6 core.²⁸ Lindner and Mannschreck demonstrated the use of triacetylcellulose to separate a variety of enantiomers.²⁹ The 1980s saw an explosion in CSPs. Pirkle

developed different CSPs containing π -acidic and/or π -basic groups.³⁰⁻³⁵ Armstrong et al. published the use of the first reversed phase CSP using cyclodextrins,³⁶⁻³⁹ which contain a hydrophobic cavity. Cyclodextrin CSPs continued to be developed through derivatization of the hydroxyl groups using different selectors.⁴⁰⁻⁴⁵ Polymeric CSPs based upon proteins (BSA, ovomucoid etc.) were developed by Allenmark et al.⁴⁶ and synthetic polymeric CSPs were developed by Okamoto.⁴⁷ Polysaccharides CSPs based on derivatized cellulose and amylose were further developed by Okamoto et al.⁴⁸ In the 1990s Armstrong et al. developed the macrocyclic glycopeptide-based CSPs⁴⁹ and while Lindner et al. developed the cinchona alkaloid-based CSPs.^{50,51} In the 2000s the field of chiral separations had developed into a mature science and many of the publications were efforts to improve or better understand existing chiral selectors. Armstrong et al. developed several polymeric CSPs⁵²⁻⁵⁴ and in 2009 introduced a new oligosaccharide CSP called cyclofructan which contains a crown ether core and fructofuranose pendent moieties.⁵⁵ When derivatized, these novel cyclic oligosaccharides form exceptional chiral selectors.

Chapter 2

Comparison of stationary phases for packed column supercritical fluid chromatography based upon ionic liquid motifs: A study of cation and anion effects

2.1 Abstract

A class of stationary phases for SFC, referred to as immobilized ionic liquids (IILs), are evaluated with a two part study: 1) a cation effect study and 2) an anion effect study. The former study compares six different IILs (tripropylphosphonium, tributylphosphonium, methyl-imidazolium, benzyl-imidazolium, triphenylphosphonium and 4,4'-bipyridyl) on silica gel, evaluating their performance in SFC with all the counter anions as trifluoroacetate (TFA). In the latter study the stationary phase consisted of a bonded tributylphosphonium cation and varying counter anions (acetate, TFA, chloride, NTf₂⁻ and perchlorate). An order of retentivity was established for the cation effect study and the favourable behavior of phosphonium based stationary phases is reported for the first time in SFC. It was not possible to always assign a retentivity order for the anion effect study, but wide variations in selectivity are noted for different anions showing the tunable nature of this class of stationary phases.

2.2 Introduction

Since the initiation of supercritical fluid chromatography (SFC) in 1961 by Klesper et al.,² it has developed in an interesting and somewhat sporadic manner. In the 1980s there were high expectations for capillary SFC (capSFC) while packed column SFC (pcSFC) was relatively neglected.^{8,9,56-58} However in the 1990s and more recently pcSFC has flourished and expanded into areas of analytical and preparative importance while capSFC, although rarer in extent, enjoys a niche field in petrochemical applications.^{59,60} The use of a polar organic modifier in pcSFC allowed the elution of more polar, strongly

retained molecules, thereby enhancing its usefulness while maintaining many of the advantages of a supercritical fluid mobile phase.⁶¹ Indeed SFC has emerged as a predominantly packed column technique somewhat analogous to normal phase liquid chromatography (NPLC).⁶² Accordingly many SFC stationary phases are polar⁶³⁻⁷² (diol, cyanopropyl, aminopropyl etc.) to retain and separate polar analytes. Yet non-polar, hydrophobic stationary phases are used in pcSFC as well.⁷³⁻⁷⁸ Typically columns made for HPLC are used in pcSFC. Often this results in separations where some analytes are excessively retained, others are not sufficiently retained and poor peak symmetry is not uncommon. However the attraction for SFC continues to grow, particularly in pharmaceutical applications, because scCO₂, with its low viscosity and high diffusivity, can accommodate higher flow rates with modest pressure drops.^{79,80} This makes it ideal for preparative scale separations and requires less organic or liquid solvent than conventional preparative HPLC separations. Despite this, there are few reports on the design and use of stationary phases specifically for SFC.

Ionic liquids (ILs) consist of large, phosphorous or nitrogen containing, organic cations with various kinds of organic and inorganic counter anions. Typically the melting point of an IL is less than ~100 °C. If the compound is a liquid at room temperature it is further designated a room temperature IL (or RTIL). Being ionic, ILs have negligible vapour pressure. Additionally they are characterized by high ionic conductivity, high thermal stability and varying degrees of viscosity.^{81,82} These properties have made ILs attractive as new solvents for organic synthesis.⁸³⁻⁸⁶ In analytical separation techniques,⁸⁷ ILs have found widespread use as coated stationary phases in gas chromatography (GC),⁸⁸ immobilized stationary phases in solid phase micro extraction (SPME) fibres,⁸⁹ LC⁹⁰⁻⁹⁵ and SFC⁹⁶ stationary phases, as ion-pairing agents in reversed phase LC^{97,98}

(RPLC), as wall-coating agents and as background electrolytes in capillary electrophoresis⁹⁹ (CE) to name but a few.

This paper endeavors to address the application of immobilized ionic liquids (IILs) as a class of stationary phases for SFC. Strictly speaking, the term “ionic liquid” in IIL is a misnomer. Upon immobilization the IL is bereft of its key property, that of being a liquid. And yet, by way of metonymy, the use of the term is not improper, but easily understood by those familiar with the field.

Technically IILs are really exotic strong anion exchangers (SAXs). SAX columns in LC are well known. However, there have only been a few of the IIL-type stationary phases reported and they were all imidazolium-based.⁹⁰⁻⁹⁶ The first SAX column used for a pcSFC study was a quaternary ammonium type used to evaluate the elution of cationic analytes from polar stationary phases with and without the use of an ion-pairing agent (ammonium acetate).⁶³ However the first imidazolium IIL stationary phase was reported in 2009. It used a 1-octyl-3-propylimidazolium group bonded to silica gel as a stationary phase (counter anion = chloride) to separate acetaminophen, metoprolol, fenoprofen, ibuprofen, naphthalene, and testosterone.⁹⁶ Aside from these two publications, the former being a SAX and the latter an IIL, the use of stationary phases bearing a permanent charge for pcSFC is not common.

In the aforementioned pcSFC studies, there were no systematic comparisons of different kinds of IILs or any investigation into the effect of varying the counter anion. Furthermore, there have been no chromatographic studies, other than anion exchange,¹⁰⁰ conducted on immobilized phosphonium substrates. Most immobilized phosphonium substrates, like some of the other IILs,^{101,102} have been used as catalysts¹⁰³ – mostly phase transfer,¹⁰⁴⁻¹⁰⁶ while a few have been used as Lewis acid catalysts¹⁰⁷ and catalysts for cyclic carbonate synthesis.¹⁰⁸

In this paper a twofold study is reported: 1) a cation effect study (conducted on six different IILs, tripropylphosphonium, tributylphosphonium, methyl-imidazolium, benzyl-imidazolium, triphenylphosphonium and 4,4'-bipyridyl, while keeping the counter anion constant) and 2) an anion effect study (conducted on immobilized tributylphosphonium with five different anions: acetate (CH_3COO), trifluoroacetate (TFA), chloride (Cl), perchlorate (ClO_4) and bis(trifluoromethanesulfonyl)imide anion (NTf_2)). The performance of phosphonium based stationary phases versus imidazolium ones is examined and the tunable nature of IILs is discussed.

2.3 Experimental

2.3.1 Equipment

The SFC instrumentation consisted of a Jasco 2000 series semi-prep SFC (SFC-2000-7) equipped with a PU-2086-CO₂ pump chilled to -10 °C using a Julabo chiller, a PU-2086 modifier pump, a PU-2080 makeup pump supplying additional methanol to the back pressure regulator (after the detector), an AS-2059-SFC autosampler, CO-2060 column oven heated to 40 °C, BP-2080 back pressure regulator with two heating controllers (primary and secondary) maintained at 60 °C, a high pressure flow cell unit and a UV-2075 UV/vis VWD. The SFC was controlled by computer and data was collected using the Jasco software, ChromNAV, and the LC-Net II/ ADC.

2.3.2 SFC Operation

CO₂ was used as the supercritical fluid (99.95 %) and HPLC grade methanol (EMD Chemicals) as the modifier with a total flow rate of 3 mL/min. Different additives were used in the modifier which will be discussed later. Care had to be taken not to operate too close to the lower precision limit of the PU-2086 pump flow rates which was 0.2 mL/min and thus mobile phase compositions were never lowered below 90/10 CO₂/MeOH. The back pressure regulator was maintained at 15 MPa and 60 °C at all

times. Four back pressure regulator failures were encountered (etching or scratching of the spindle/ needle) in less than one year of operation. The root cause of these failures could not be ascertained and the needle valve, seat and seal had to be replaced each time. It was decided to maintain the methanol makeup pump flow rate at 0.6 mL/min in the event that the damage was being caused by precipitation. The only possible sources of precipitation are the analyte salts and the salt additive in the modifier. Column oven temperature was maintained at 40 °C at all times and UV detection was achieved at 220 nm.

2.3.3 Reagents and chemicals

Triphenylphosphine (99 %), tributylphosphine (97 %), tripropylphosphine (97 %), 1-methylimidazole (99 %), 4,4'-Dipyridyl (98 %) , 1-benzylimidazole (99 %), ammonium trifluoroacetate (98 %), ammonium perchlorate (99.999 %), sodium perchlorate (> 98.0 %) ammonium acetate (> 99.0 %), ammonium chloride (> 99.5 %), lithium bis(trifluoromethanesulfonyl)imide (99.95 %), (3-chloropropyl)-trimethoxysilane (> 97 %), (3-iodopropyl)-trimethoxysilane (> 95 %), anhydrous dimethylformamide (99.8 %) were all purchased from Sigma-Aldrich. Daisogel silica gel (5 μm x 450 m² x 100 Å) was purchased from Supelco.

2.3.4 Samples

Acebutolol hydrochloride, alprenolol hydrochloride, atenolol, carvedilol, esmolol hydrochloride, labetalol hydrochloride, nadolol, pindolol, dl-propranolol hydrochloride, metoprolol tartrate, lidocaine, flunarizine dihydrochloride, ibuprofen, diltiazem hydrochloride, verapamil hydrochloride, imipramine hydrochloride, nifedipine, ketoprofen, terfenadine, procainamide hydrochloride, dipyridamole, niflumic acid, bumetanide and acetazolamide were all purchased from Sigma-Aldrich (see Figure 2-1).

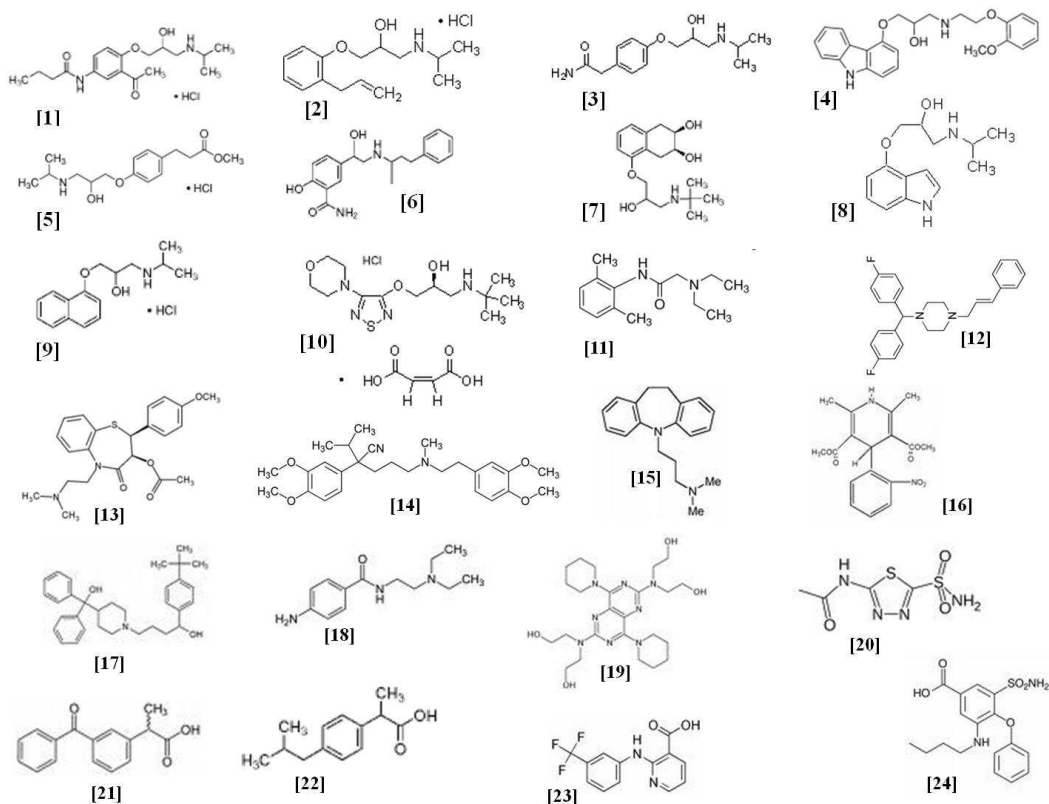


Figure 2-1 A list of basic and acidic drugs analyzed by SFC.

[1] acebutolol, [2] alprenolol, [3] atenolol, [4] carvedilol, [5] esmolol, [6] labetalol, [7] nadolol, [8] pindolol, [9] dl-propranolol, [10] metoprolol, [11] lidocaine, [12] flunarizine, [13] diltiazem, [14] verapamil, [15] imipramine, [16] nifedipine, [17] terfenadine, [18] procainamide, [19] dipyridamole, [20] acetazolamide, [21] ibuprofen, [22] ketoprofen, [23] niflumic acid and [24] bumetanide.

For ease of screening of compounds, the above analytes were grouped according to the following scheme: BB Mix 1 = alprenolol, esmolol, nadolol, labetalol, atenolol and carvedilol; BB Mix 2 = metoprolol, propranolol, acebutol and pindolol; BD Mix 1 = lidocaine, diltiazem, imipramine, terfenadine, procainamide and acetazolamide;

BD mix 2 = flunarizine, verapamil, nifedipine and dipyridamole; Acid mix = ibuprofen, ketoprofen, niflumic acid and bumetanide. All analytes are ionizable.

2.3.5 Synthesis of ionic-liquid-based stationary phases

Silica gel was dried in an oven at 175 °C for 2 days and then allowed to cool in a vacuum drier at 40 °C before use. Residual moisture was removed by azeotropic distillation of the adsorbed moisture using toluene as the refluxing solvent and a Dean-Stark trap to collect the azeotrope. All reactions were conducted under an argon atmosphere. All final products were dried over P₂O₅ in a vacuum drier (40 °C) for at least 24 hours. There was one of two basic reaction methods followed for each stationary phase (see Figure 2-2).

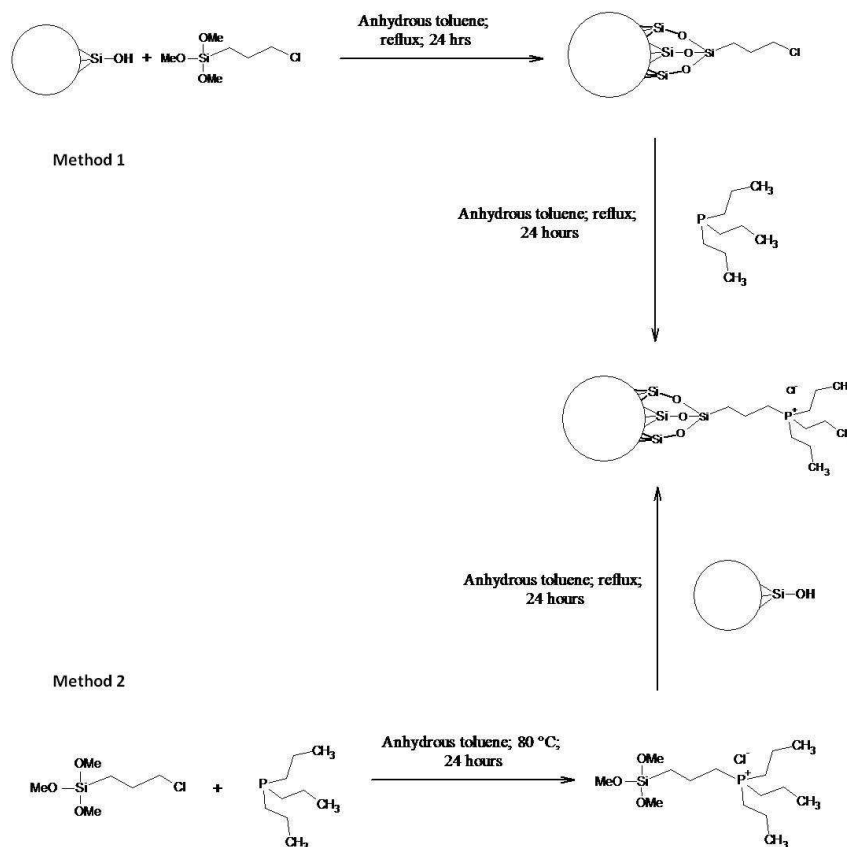


Figure 2-2 Outline of the two possible reaction schemes for the synthesis of IILs.

Method 1 involved first derivatizing the silica gel with the silane linker, and then reacting the resultant product with the selector of interest. Method 2 on the other hand allowed for reacting the silane linker with the selector of interest first, and then reacting the resultant ionic-liquid product with silica gel. In some cases stationary phases were prepared in bulk in order to perform many experiments from a single batch. Reaction details are briefly outlined in Table 2-1. Specific reaction details are as follows:

2.3.5.1 Tributylphosphonium stationary phase (PBU₃)

17.0 g of tributylphosphine was reacted with 21.0 g (3-iodopropyl)trimethoxysilane in 20 mL anhydrous toluene at 50°C for 24 hours to afford the ionic product (3-(tributylphosphonium)-propyl)trimethoxysilane chloride which was recovered by rotary evaporation. The crude product was washed with toluene (50 mL) and ether (50 mL) three times to remove unreacted starting materials. 18.35 g of the ionic product was added slowly over 1 hour to a slurry of 12.0 g dried silica gel in 200 mL anhydrous toluene and allowed to react for 24 hours under reflux conditions with sufficient stirring to observe the onset of a vortex. (Care had to be taken to avoid crushing silica gel particles by high stirring rates.) The final product (PBU₃) was recovered by filtration and washed with 400 mL toluene, CH₂Cl₂, acetone, methanol, water and then acetone again. The derivatized silica gel was dried in vacuo. Elemental analysis: %C = 14.01 %, %H = 2.78 %.

2.3.5.2 Tripropylphosphonium stationary phase (PPR₃)

5.0 g of tripropylphosphine was reacted with 8.3 g (3-chloropropyl)trimethoxysilane in 10 mL anhydrous toluene at 80°C for 24 hours to afford the ionic precipitate (3-(tripropylphosphonium)-propyl)trimethoxysilane chloride. The crude product was washed with toluene (50 mL) and ether (50 mL) three times to remove unreacted starting materials. 1.0 g of the ionic product was reacted with 2.0 g dried silica

Table 2-1 Summary of reaction conditions used for the synthesis of the six stationary phases

Silane linker	IL selector	Synthesis method	Reaction conditions	
			Formation of IL	Immobilization
(3-chloropropyl)-trimethoxysilane	Tributylphosphine	Method 2	Toluene, 50°C, 24 hrs	Toluene, reflux, 24 hrs
(3-chloropropyl)-trimethoxysilane	Tripropylphosphine	Method 2	Toluene, 80°C, 24 hrs	Toluene, reflux, 24 hrs
(3-iodopropyl)-trimethoxysilane	Triphenylphosphine	Method 1	Toluene, reflux, 4 days	Toluene, reflux, 24 hrs
(3-chloropropyl)-trimethoxysilane	1-methylimidazole	Method 2	Silane, 80°C, 24hrs	Toluene, reflux, 24 hrs
(3-chloropropyl)-trimethoxysilane	1-benzylimidazole	Method 2	Silane, 80°C, 24 hrs	Toluene, reflux, 24 hrs
(3-chloropropyl)-trimethoxysilane	4,4'-Bipyridyl	Method 1	Toluene, reflux, 24 hrs	Toluene, reflux, 24 hrs

gel in 25 mL anhydrous toluene for 24 hours under reflux conditions with sufficient stirring to observe the onset of a vortex. The final product (PPr₃) was removed by filtration and washed and dried as described for PBu₃. Elemental analysis: %C = 9.60 %, %H = 2.01 %.

2.3.5.3 Triphenylphosphonium stationary phase (PPh₃)

10 g of dried silica gel was slurried in anhydrous toluene (100 mL) and brought to reflux while being stirred with a mechanical, overhead stirrer. (3-Iodopropyl)-trimethoxysilane (35 mL) was then added dropwise to the mixture. The reaction continued under reflux conditions for one day. The resultant product (3-iodopropyl derivatized silica gel) was filtered and washed with diethyl ether and methanol to remove residual, unreacted silane. This product was then dried and submitted for elemental analysis (% C = 4.22 %).

The 3-iodopropyl derivatized silica gel was then re-slurried in toluene (100 mL) using mechanical stirring and reacted with 31.4 g triphenylphosphine which had been dissolved in toluene (100 mL). The reaction was conducted under an argon atmosphere and reflux conditions for 4 days. The resultant product (PPh₃) was washed and dried as for PBu₃. Elemental analysis: %C = 13.73 %, %H = 1.72 %.

2.3.5.4 Methyl-imidazolium stationary phase (Me-Im)

2.0 g of 1-methylimidazole was reacted with 20 mL of (3-chloropropyl)trimethoxysilane (excess and solvent) at 80 °C for 48 hours with stirring. Upon completion, the ionic product was precipitated out of solution by addition of ether. The crude product was washed with toluene and ether three times to remove unreacted starting material. The washed product, (3-(1-methylimidazolium)-propyl)trimethoxysilane chloride, was dried in vacuo. 1.0 g of this ionic product was reacted with 2.0 g of dried silica gel in 25 mL anhydrous toluene for 24 hours under reflux conditions. The final

product (Me-Im) was recovered by filtration and washed and dried as described above for PBU₃. Elemental analysis: %C = 8.57 %, %H = 0.95 %, %N = 1.94.

2.3.5.5 Benzyl-imidazolium stationary phase (Bz-Im)

2.0 g of benzyl imidazole was added to 20 mL (3-iodopropyl)-trimethoxy silane (excess and solvent) and allowed to react at 80 °C for 48 hours. The ionic product was precipitated upon addition of ether and washed in the same manner as is described for Me-Im. 1.0 g of this ionic product was reacted with 2.0 g of dried silica gel in 25 mL anhydrous toluene for 24 hours under reflux conditions. The final product (Bz-Im) was recovered by filtration and washed and dried as described above for PBU₃. Elemental analysis: %C = 12.09 %, %H = 0.97 %, %N = 1.76 %.

2.3.5.6 4,4'-Bipyridyl stationary phase (4,4'-BiPy)

2.90 g of 3-chloropropyl (prepared analogously to 3-iodopropyl derivatized silica gel in PPh₃) derivatized silica gel was slurried in a concentrated solution of 2 – 3 g of 4,4'-bipyridyl in toluene (20 – 30 mL) and allowed to react under reflux conditions for 24 hours. The final (4,4'-BiPy) product was collected by filtration and washed and dried as described for PBU₃. Elemental analysis: %C = 8.36 %, %H = 0.61 %, %N = 0.96.

2.3.6 Column packing

1.90 g of dried derivatized silica gel was suspended in 30 mL of 99/1 acetonitrile/water by sonication (5 – 10 mins). This slurry was then packed into a 15 cm x 4.6 mm stainless steel column using a pressurized (6000 psi) packing system with acetonitrile as the push solvent (300 mL). All stationary phases were packed with this method which proved to be inefficient as can be seen by the fronting peak shapes in the chromatograms. Efficient packing was an arduous and non-trivial task and was only realized at the end of our research (see Figure 2-3). The reader is directed to Bristow's

comments on slurry packing and flocculated vs. deflocculated systems.¹⁰⁹ Success was ultimately only found in deflocculated systems and that by trial and error.

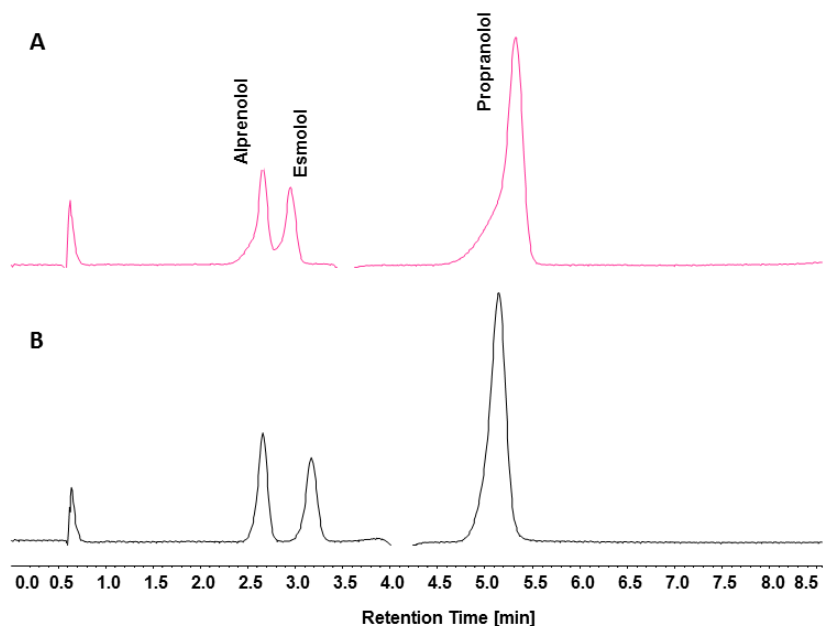


Figure 2-3 Improvement in peak shape through column packing.

A) PPh_3 stationary phase packed by slurring 1.95 g in 30 mL of 99/1 (v/v %) ACN/ H_2O and pushing with 300 mL ACN. B) The same stationary phase packed by slurring 1.94 g in 8 mL of CHCl_3 and pushing with 100 mL of 50/50 (v/v %) ACN/MeOH. Note the reduced peak asymmetry and improvement in resolution between alprenolol and esmolol.

2.3.7 Anion exchange

Since all stationary phases contained either chloride or iodide as the counter anion, they had to be exchanged for the anion of interest. There were two ways in which this was done.

Method 1: The stationary phase was placed in a sintered glass crucible (4.0 – 5.5 μm) and washed repeatedly, under vacuum filtration, with a concentrated (1 M) solution

(1:1 methanol:water) of a salt of the anion of interest. This was continued until the filtrate tested negative for the presence of halide using silver nitrate. This method was deemed less efficient and more wasteful than method 2.

Method 2: The stationary phase was slurry packed into the column in the halide form and then anion-exchange was carried out in the column by pumping a 0.1 M solution of the salt of the anion of interest at 0.2 – 0.5 mL/min through the column and testing the effluent for the presence of halide using silver nitrate. Usually the anion-exchange was complete after at most 200 – 300 mL of solution.

2.4 Results and Discussion

In initial studies diethylamine (DEA) at 0.1 % in the methanol modifier was used as an additive. This was based purely on SFC applications that have already been published as well as practical LC experience.^{61,64} However, problems were encountered with this additive such as systematic retention time variation (increasing or sometimes decreasing) as well as peak shape variation (single vs. splitting). It was as if the stationary phase was slowly being modified (Figure 2-4). Chou, et al.⁹⁶ also experienced problems with amine additives (TEA) on their 1-octyl-3-propylimidazolium chloride column such as increased retention and erratic baseline behavior. They attributed this to the role of the amine in deprotonating residual silanol groups although they did elaborate any further on this topic. Blümel, et al.¹¹⁰ have shown using ³¹P CP/MAS NMR spectroscopy that diphenylphosphines immobilized onto silica gel, when oxidized to a phosphonium species, can be and are stabilized by proximate siloxide groups on the stationary phase.

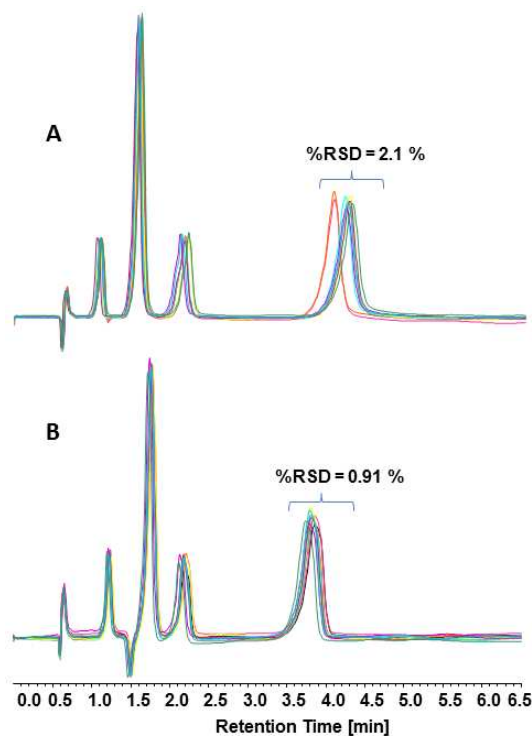


Figure 2-4 Retention time repeatability on the PBU₃ TFA stationary phase.

Repeatability was the result of 10 injections of BB Mix 2 overlaid. A) Modifier additive was 0.1 % DEA, B) 20 mM NH₄TFA

Notwithstanding the above arguments, since the examined stationary phases are permanently charged and thus always have some counter anion, one must consider the constancy of the counter anion. It is known that the amine additive can react with the abundant super-critical CO₂ (scCO₂) to form carbamic salts¹¹¹ and thus, by gradual mass action, displace the anion on the stationary phase. Alternatively, if moisture is present, the amine additive could also form hydroxide anions which react rapidly with the scCO₂ to form the bicarbonate anion, resulting in a similar effect. Regardless, it is certain that anionic or ionizable additives in the modifier other than the anion that was intended for

the stationary phase may result in an alteration of the stationary phase and affect the reproducibility of a separation. Figure 2-4 illustrates this observation. Clearly when an ammonium (or lithium in the case of NTf₂) salt of the counter anion was used as the additive, it maintained the anion of interest on the stationary phase and gave repeatable retention time results while amine additives did not.

2.4.1 Cation effect study

Six cationic stationary phases were evaluated using TFA as the counter anion and thus 5 mM ammonium trifluoroacetate was used as the additive in the methanol modifier. Table 2 shows the retention factor data for the separation of six beta-blockers (BB Mix 1) on each stationary phase using identical mobile phases (85/15 CO₂/MeOH) and instrumental conditions.

Table 2-2 Retention factors for six beta-blockers on six cationic stationary phases.

*Compound retained on column.

Analyte	PBu ₃	PPr ₃	Me-Im	Bz-Im	PPh ₃	4,4'-BiPy
Alprenolol	1.49	1.42	1.59	1.80	2.65	2.46
Esmolol	1.61	1.55	1.84	2.21	3.05	3.13
Nadolol	4.53	7.07	9.11	9.15	9.72	16.8
Labetalol	6.30	5.15	7.91	8.18	15.1	12.0
Atenolol	6.30	7.07	10.1	11.0	13.1	21.6
Carvedilol	19.5	27.7	28.2	35.7	45.1	*

It is evident, by monitoring carvedilol for instance, that the order of retentivity for the six stationary phases is 4,4'-BiPy > PPh₃ > Bz-Im > Me-Im > PPr₃ > PBu₃. An end-capped PPh₃ stationary phase (not shown) was compared to a conventional PPh₃ stationary phase to determine the effect of residual silanol groups on retention and it was

negligible. It seems likely that retention, in this group of stationary phases, is governed by at least two factors: 1) π - π interactions, i.e. the presence of aromaticity or double bonds in the selector, and 2) the presence of basicity, i.e. nitrogen groups which can undergo hydrogen bonding. The two trialkylphosphonium, PBU_3 and PPr_3 , have no double bonds (or aromaticity) and no hydrogen bonding ability in and of themselves. Accordingly, they have the lowest retention for the analytes. Regarding aromaticity, the order of increasing aromaticity, i.e. $\text{PPh}_3 > 4,4'\text{-BiPy} > \text{Bz-Im} > \text{Me-Im}$, almost matches the order of retentivity described above where the only exception is that of $4,4'\text{-BiPy}$ and PPh_3 which are switched. The presence of a neutral nitrogen group on $4,4'\text{-BiPy}$ imparts the additional hydrogen bonding ability to retain analytes. Considering the three nitrogen based stationary phases, $4,4'\text{-BiPy}$, Bz-Im and Me-Im , each contains one permanently charged nitrogen and one neutral nitrogen, the only other difference being the number of double bonds present. The order of retentivity matches the degree of unsaturation in the selectors. Also Bz-Im and Me-Im cannot hydrogen bond as easily as $4,4'\text{-BiPy}$.

In light of the above results, the question arises as to the nature of the retentive interactions for the trialkylphosphonium phases. These stationary phases, like all the others studied, are permanently charged and thus are very polar and will, according to Strubinger^{112,113} and Berger,⁶² have a methanol enriched layer, or at least a monolayer, on the stationary phase, somewhat analogous to the "enrichment property" of HILIC stationary phases which have an enriched water layer. This is by no means limited to polar stationary phases but is also observed in reversed phase (C18) applications. The enriched methanol monolayer can hydrogen bond with the analytes and effect retention. Lastly, the counter anion used, TFA, is also capable of hydrogen bonding. Indeed TFA can hydrogen bond both when it is electrostatically attracted to the stationary phase and when it is ion-paired with a basic analyte. Of course for the cation effect study, TFA ion-

pairs should be constant in each experiment and thus this is dealt with further in the anion effect study.

When optimizing the separation of the beta-blockers, the mobile phase strength (i.e. the methanol modifier content) was decreased until an acceptable separation between alprenolol and esmolol was achieved. This action was limited by the retention of carvedilol, the most retained analyte, in order to prevent the final run time from becoming prohibitively long.

Table 2-3 shows the retention factor data for all components analysed by using BB Mix 1, BB Mix 2, BD Mix 1, BD Mix 2 and Acid mix. For all the stationary phases, metoprolol and esmolol would have co-eluted had they been in the same sample. Some compounds were very well retained, e.g. acetazolamide on Me-Im and procainamide on 4,4'-BiPy, and could not be eluted without a gradient. 4,4'-BiPy also retained carvedilol very well (Table 2-3). It is interesting to note that none of the phosphonium stationary phases exhibited the strong retention that was characteristic of the imidazolium and pyridinium stationary phases. Bumetanide was not eluted on any of the nitrogen containing stationary phases whereas it could be eluted on phosphonium based stationary phases. Clearly the phosphonium-based stationary phases tend to produce the best separations with the least retention for the basic and acidic drugs under isocratic conditions.

Table 2-4 shows the selectivity factor (α) data for the separation of BB Mix 2 under optimal conditions for each stationary phase. Comparing the first three stationary phases, PBU_3 , PPr_3 and Me-Im, which have the same mobile phase strength, similar selectivities for propranolol over metoprolol (1.95, 2.13 and 1.93 respectively) and acebutolol over propranolol (2.65, 2.43 and 2.29 respectively) are exhibited. However the selectivity for pindolol over acebutolol differs greatly, 1.82, 2.56 and 3.02 respectively.

Table 2-3 Retention factor data for all analytes analyzed on the cationic stationary phases.

^{a,b}BB Mix 1 and BB Mix 2: PBU₃, PPr₃ and Me-Im) 90/10 CO₂/MeOH; Bz-Im, PPh₃ and 4,4'-BiPy) 85/15 CO₂/MeOH; ^{c,d}BD Mix 1 and BD Mix 2: PBU₃, PPr₃, Me-Im, Bz-Im and PPh₃) 90/10 CO₂/MeOH; 4,4'-BiPy) 85/15 CO₂/MeOH. ^eAcid Mix: PBU₃, PPr₃, Me-Im and Bz-Im) 90/10 CO₂/MeOH; PPh₃ and 4,4'-BiPy) 85/15 CO₂/MeOH. *Not eluted under stated conditions.

Analyte	PBU ₃	PPr ₃	Me-Im	Bz-Im	PPh ₃	4,4'-BiPy
Alprenolol ^a	2.8	2.69	3.04	1.80	2.65	2.46
Esmolol ^a	3.32	3.23	3.86	2.21	3.05	3.13
Nadolol ^a	11.6	16.9	25.8	9.15	9.7	16.8
Labetalol ^a	15.7	13.5	20.8	8.18	15.1	12.0
Atenolol ^a	18.3	22.9	30.3	11.0	13.1	21.6
Carvedilol ^a	58.8	82.1	88.7	35.7	45.1	*
Acebutolol ^b	16.1	15.4	15.7	6.98	10.8	11.1
Pindolol ^b	29.3	39.4	47.4	16.3	19.8	37.1
Propranolol ^b	6.07	6.34	6.85	3.70	5.81	6.64
Metoprolol ^b	3.12	2.97	3.55	2.02	2.90	3.00
Lidocaine ^c	1.31	1.31	1.41	1.64	1.93	1.61
Diltiazem ^c	2.25	2.07	2.06	3.47	4.80	3.00
Imipramine ^c	3.92	3.76	3.10	5.19	7.42	4.44
Terfenadine ^c	7.31	7.04	9.44	13.6	21.8	8.20
Procainamide ^c	15.5	19.3	13.6	20.5	28.0	*

Table 2 – 3 – Continued

Analyte	PBu ₃	PPr ₃	Me-Im	Bz-Im	PPh ₃	4,4'-BiPy
Acetazolamide ^c	25.3	35.9	*	63.9	42.1	27.8
Flunarizine ^d	2.08	1.75	1.72	2.60	4.44	1.55
Verapamil ^d	3.38	2.90	2.86	4.92	7.48	3.02
Nifedipine ^d	4.18	3.58	3.23	4.92	8.68	2.27
Dipyridamole ^d	10.3	9.9	10.8	18.8	22.9	13.8
Ibuprofen ^e	0.958	1.01	1.47	1.92	0.920	1.20
Ketoprofen ^e	2.94	3.23	4.80	7.03	2.95	4.14
Niflumic acid ^e	21.9	28.0	20.0	37.9	21.7	30.3
Bumetanide ^e	53.7	95.6	*	*	34.5	*

Table 2-4 Selectivity data for the separation of BB Mix 2.

Analyte	PBu ₃	PPr ₃	Me-Im	Bz-Im	PPh ₃	4,4'-BiPy
Metoprolol	-	-	-	-	-	-
Propranolol	1.95	2.13	1.93	1.83	2.00	2.21
Acebutolol	2.65	2.43	2.29	1.89	1.86	1.67
Pindolol	1.82	2.56	3.02	2.34	1.83	3.34

The increased selectivity of Me-Im can be explained by its different functionality, see above. The increased selectivity for PPr₃ vs. PBu₃ was unexpected. It is hard to imagine that a single carbon number change on each alkyl chain can make such a marked difference. Further it is noted that nadolol, labetalol and atenolol were retained differently on these two stationary phases (Table 2-2). For PBu₃, nadolol elutes first and

then labetalol and atenolol co-elute, whereas on PPr_3 , labetalol elutes first and nadolol and atenolol co-elute thereafter.

2.4.2 Anion effect study

In SFC, when introducing a salt, e.g. $\text{NH}_4\text{CF}_3\text{COO}$ (or NH_4TFA), into the mobile phase, it is known that ion-pairing takes place.^{63,64,66,70,71,114} TFA (in the case of $\text{NH}_4\text{CF}_3\text{COO}$) can also interact electrostatically with the IIL stationary phase since it bears a permanent positive charge. Once all the cationic sites are occupied (steady state conditions), ion-pairing will dominate. Basic analytes could ion-pair with the TFA anion whereas acidic analytes could ion-pair with the NH_4^+ cation.

In contrast to the cation effect study, where the counter anion was fixed and the cationic moiety on the stationary phase was varied, in this study the cationic moiety was tributylphosphonium, the least retentive stationary phase, and its counter anion was varied. Five anions were investigated: acetate (CH_3COO), trifluoroacetate (TFA), chloride (Cl), bis(trifluoromethanesulfonyl)imide anion (NTf_2) and perchlorate (ClO_4), which span the Hofmeister series.

Figure 2-5 shows the retention data for BB Mix 1 where the mobile phase conditions were identical, except for the additive which corresponded to the anion on the stationary phase. Assigning a retentivity order for the stationary phases based upon their counter anion is not as simple as it was in the cation study. Based upon the retention of alprenolol and esmolol the retentivity order is assigned as follows: $\text{ClO}_4 > \text{NTf}_2 > \text{Cl} > \text{CH}_3\text{COO} > \text{TFA}$. However, the retention for carvedilol, which was always the most retained compound in the cation study, gives the following order: $\text{ClO}_4 > \text{CH}_3\text{COO} > \text{Cl} > \text{NTf}_2 > \text{TFA}$. The elution order of the compounds are not the same. Carvedilol usually elutes last, but when NTf_2 is used as the counter anion it elutes before atenolol.

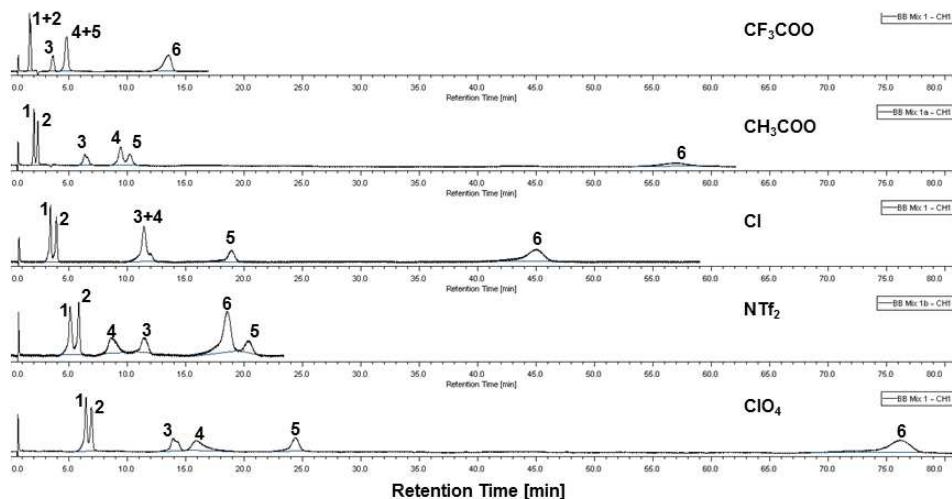


Figure 2-5 Anion effect for the separation of BB Mix 1 on PBu_3 .

SFC conditions: 85/15 CO_2 /MeOH with 5 mM of the ammonium salt of the counter anion (except for NTf_2 which is a lithium salt) in the methanol modifier. Analytes: 1) alprenolol; 2) esmolol; 3) nadolol; 4) labetalol; 5) atenolol; 6) carvedilol.

Another example of the changing elution order can be seen in Figure 2-6 (analysis of basic drugs; BD Mix 1 and 2). When the counter anion is TFA or acetate, acetazolamide elutes last and is well retained. However, when the counter anion is changed to Cl, ClO_4 or NTf_2 , it elutes much sooner. A similar trend is seen for nifedipine which has moderate retention with TFA and acetate, but is much less retained with the remaining anions. Likewise, lidocaine, flunarizine and diltiazem were poorly retained with TFA and acetate, but moderately well retained with the remaining three anions. Lastly, in Figure 2-7 (the separation of the Acid mix), ibuprofen and ketoprofen are always eluted first and are relatively weakly retained except when the stationary phase is in the acetate form. Then a more moderate retention of these compounds is observed even under the strongest mobile phase conditions used (20 % methanol).

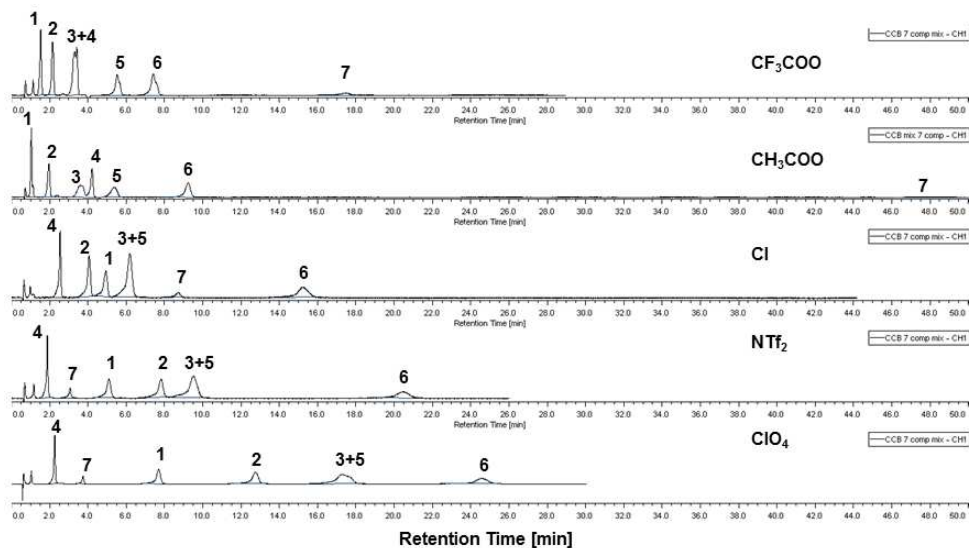


Figure 2-6 Anion effect for the separation of BD Mix 1 and 2 on PBu_3 .

SFC conditions: TFA and acetate) 90/10 CO_2/MeOH ; Cl, NTf_2 and ClO_4) 85/15 CO_2/MeOH . All have 5 mM of the counter anion ammonium salt as the additive in the methanol modifier (except NTf_2 which is a lithium salt). Analytes: 1) lidocaine; 2) diltiazem; 3) imipramine; 4) nifedipine 5) terfenadine; 6) dipyridamole; 7) acetazolamide.

Indeed, even under these strong mobile phases conditions, the acetate form of the stationary phase retained niflumic acid and bumetanide for more than 45 min whereas the ClO_4 , NTf_2 and Cl forms eluted these two compounds in less than ten minutes at 15 % methanol. When using DEA as an additive early on it was noted that niflumic acid and bumetanide were also very well retained, sometimes irreversibly. This shows the benefit of using the salt of the anion in the modifier since it can be used to separate both basic as well as acidic components provided their solubility is not compromised.

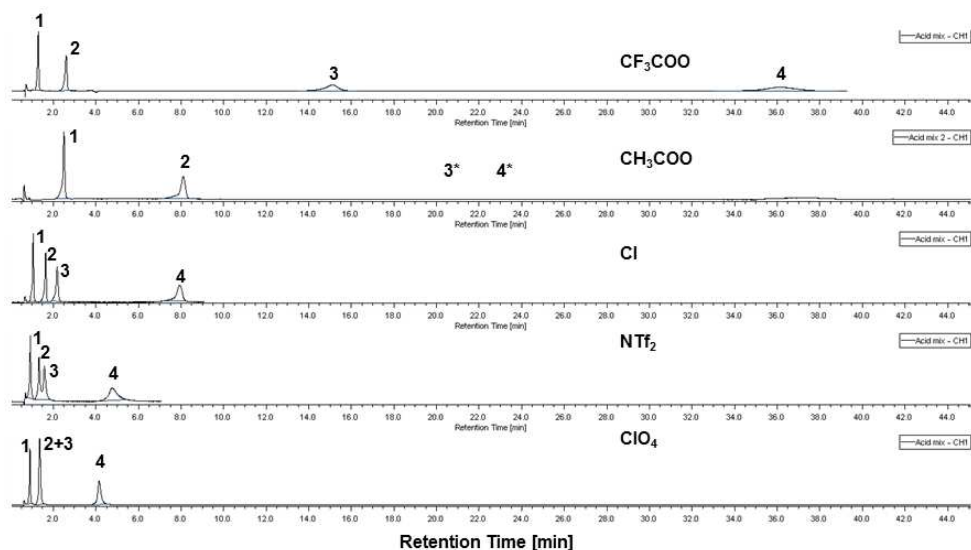


Figure 2-7 Anion effect for the separation of Acid Mix on PBu_3 .

SFC conditions: TFA) 90/10 CO_2/MeOH ; Acetate) 80/20 CO_2/MeOH ; Cl , NTf_2 and ClO_4) 85/15 CO_2/MeOH . All have 5 mM of the counter anion ammonium salt as the additive in the methanol modifier (except NTf_2 which is a lithium salt). Analytes: 1) ibuprofen; 2) ketoprofen; 3) niflumic acid; 4) bumetanide. *Not eluted under stated conditions.

The hydrogen bonding ability of the anion may play a role in the observed elution order and retention. Most of the selectivity and retention changes described above were between the relatively good hydrogen bonding anions (TFA and acetate) and the weak hydrogen bonding anions (the remaining three anions).

Table 2-5 shows the selectivity factor data for BB Mix 2 on each of the five different anion-bearing stationary phases. In each case the elution orders are the same, but selectivities are markedly different. Comparing the acetate, Cl , NTf_2 and ClO_4 forms of the stationary phase, the selectivity for propranolol over metoprolol and pindolol over acebutolol were least for the NTf_2 form. This anion seemed to induce poor selectivity – both the weakly and the strongly retained analytes becoming moderately retained.

Table 2-5 Effect of anion variation on the selectivity for BB Mix 2.

See Table 2-3 and footnote ^b for SFC conditions.

Analyte	TFA	Acetate	Cl	NTf ₂	ClO ₄
Metoprolol	-	-	-	-	-
Propranolol	1.95	2.24	1.99	1.22	1.89
Acebutolol	2.65	2.76	2.42	1.72	1.59
Pindolol	1.82	1.55	1.54	1.09	1.77

It is known that NTf₂ imparts a strong hydrophobic character to the cations it associates with. If metoprolol, propranolol, acebutolol and pindolol have comparable hydrophobicities, they should elute close to one another. In general the anion which afforded the fastest elution was TFA. The low retentivity of the TFA anion on the stationary phase makes it the counter anion of choice when quick analysis is required. It was the only anion, when coupled with the tributylphosphonium stationary phase, that consistently afforded elution of all the classes of compounds tested using 10 % methanol in the mobile phase.

This work also indicates the tunability of these stationary phases. A strongly retaining cationic moiety, PPh₃, coupled with a strongly retaining anion, ClO₄, gives an even stronger retaining total stationary phase. An experiment (not shown) was conducted in this regard which required conditions of 30 % methanol to elute the beta-blockers of interest (compare with Table 2-3 conditions). Notwithstanding this result, care must be exercised in making inferences from the tributylphosphonium anion study to other cation systems, e.g. imidazolium etc., which are significantly different.

2.5 Conclusion

As stated in the introduction, the weaker SFC mobile phase (compared to LC) can result in excessive retention and poor peak shape for some compounds. Hence stationary phase optimization for SFC should provide less retention and good peak shapes, while retaining adequate selectivity for a broad range of separations. In this regard the phosphonium based stationary phases performed better under isocratic conditions than the imidazolium and pyridinium ones. The least retentive stationary phase cation was tributylphosphonium and the least retentive anion was TFA. The anion which afforded the greatest retention for beta-blockers was ClO_4^- ; for acidic compounds it was acetate; for the remaining basic drugs there were mixed results. It was observed that the acetate anion exhibited the worst retention time repeatability and took the longest to reach baseline stability. NTf_2^- displayed poor efficiency in separations for tributylphosphonium based stationary phases.

The general order of retentivity for the cation study was $4,4'\text{-BiPy} > \text{PPh}_3 > \text{Bz-Im} > \text{Me-Im} > \text{PPr}_3 > \text{PBu}_3$. These stationary phases together with the counter anion can be tuned by combining strongly retentive cations and anions to afford a very strongly retaining stationary phase or by combining weakly retentive cations and anions to afford a very weakly retaining stationary phase. The best stationary phase in terms of low retention and good separation efficiency was the tributylphosphonium IIL with the TFA counter anion.

Chapter 3

Degradation study of carnosic acid, carnosol, rosmarinic acid, and rosemary extract (*Rosmarinus officinalis* L.) assessed using HPLC

3.1 Abstract

Rosemary, whose major caffeoyl-derived and diterpenoid ingredients are rosmarinic acid, carnosol, and carnosic acid, is an important source of natural antioxidants and is being recognized increasingly as a useful preservative, protectant, and even as a potential medicinal agent. Understanding the stability of these components and their mode of interaction in mixtures is important if they are to be utilized to greatest effect. A study of the degradation of rosmarinic acid, carnosol, carnosic acid, and a mixture of the three was conducted in ethanolic solutions at different temperatures and light exposure. As expected, degradation increased with temperature. Some unique degradation products were formed with exposure to light. Several degradation products were reported for the first time. The degradation products were identified by HPLC/MS/MS and UV. The degradation of rosemary extract in fish oil also was investigated, and much slower rates of degradation were observed for carnosic acid. In the mixture of the three antioxidants, carnosic acid serves to maintain levels of carnosol, though it does so at least in part at the cost of its own degradation.

3.2 Introduction

With increasing awareness of the health benefits of certain foods and the mounting awareness of health benefits from nutraceutical products, attention has been focused on natural antioxidants as potential replacements for artificial ones.^{115,116} Rosemary is a well-known perennial which has significant antioxidative activity.^{117,118} Its extracts have been added to lipids or lipid containing foods, such as fish oils,^{119,120} plant seed oils,¹²¹⁻¹²³ and meats,¹²⁴ to prevent oxidation and prolong their storage time. In

addition, in vivo rosemary or its extracts have been observed to protect biological tissues from oxidative stress.^{125,126} The antioxidative activity of rosemary appears to be due in significant part to its phenolic constituents.^{127,128} Carnosic acid (see Figure 3-1 for all compounds) and carnosol are the primary rosemary-derived phenolic diterpenes with greatest antioxidant effect.¹²⁷ Other phenolic compounds, such as rosmarinic acid, rosmanol, and epirosmanol, also contribute to the antioxidative properties of rosemary extract, albeit to a lesser degree.¹²⁹ Besides acting as antioxidants in food, rosemary extract and its constituents have also displayed useful physiological and medicinal properties.¹³⁰⁻¹³² For example, rosemary extract was reported to show inhibitory effects for human immunodeficiency virus (HIV) infection at very low concentrations.¹³² Carnosol was recently reported as a promising anticancer and anti-inflammatory agent.¹³¹

Quantitation of these phenolic compounds in rosemary extract is therefore of considerable interest. Two classical methods often have been used to determine the phenolic content of rosemary extracts. The Folin-Ciocalteu assay was used to measure the total amount of phenolic compounds.^{133,134} In this method the substance being tested, for example, rosemary or its components, is used to titrate the Folin-Ciocalteu reagent, and the total content of phenolic compounds is determined by the amount of the substance needed to inhibit the oxidation of the reagent. However, the Folin-Ciocalteu reagent is nonspecific. It is able to react with other reducing components that are not phenolic compounds. Thus the total content of phenolic compounds measured by this method can be inaccurate and potentially overestimated. Furthermore, the compositions of specific phenolic components of the rosemary extracts are not identified. The other approach is a chromatographic method which separates the phenolic and diterpenoid compounds. HPLC is the most frequently utilized chromatographic method for quantitative analysis of rosemary extract.^{135,136} However, most reported HPLC methods

require either long run times, during which the inherently unstable phenolic constituents may degrade, or baseline separation of the relevant compounds is not obtained, which compromise quantitation of the phenolic compounds in the extract. A few supercritical fluid chromatographic (SFC) methods also have been reported for the separation of antioxidative compounds in rosemary extracts. Since SFC was generally less effective analytically, it has been used primarily as a preparative method for isolating the major functional ingredients in rosemary.^{137,138} Capillary electrophoresis (CE) also was used for the analyses of rosemary extract.^{139,140} However, the electropherograms often display noisy baselines which made accurate quantitation difficult.

In this investigation, we present a new HPLC method for the study of the degradation of carnosic acid, carnosol, and rosmarinic acid in ethanol solution as well as for rosemary extract in fish oil. The relationship between the degradation processes of carnosic acid and carnosol also was investigated. Finally, a new oxidative pathway of carnosic acid was proposed.

3.3 Materials and methods

3.3.1 *Materials*

Carnosol, carnosic acid, and rosmarinic acid, which are primary standards for analysis (purity $\geq 96\%$), were purchased from ChromaDex (Irvine, CA, USA). Purity designated by the manufacture's certificate was supported by the absence of detectable levels of any degradants. Rosmanol was purchased from Avachem (San Antonio, TX, USA). Formic acid was purchased from Sigma-Aldrich (Milwaukee, WI, USA). HPLC grade methanol (MeOH), ethanol (EtOH), and acetonitrile (ACN) were obtained from EMD (Gibbstown, NJ, USA). Water was purified by a Milli-Q water purification system (Millipore, Billerica, MA, USA). Highly refined omega-3 rich fish oil in which the acid functionality has been replaced by ethyl esters (DSM Nutritional Products, Heerlen,

Netherlands) and the rosemary extract dissolved in fish oil (LycoRed, Orange, NJ, USA) were provided by Alcon Research, Ltd. (Fort Worth, TX, USA). The proportion of rosemary extract in fish oil was 5% (w/w). Rosemary powders (LycoRed, Orange, NJ, USA) was provided by Alcon Research, Ltd. (Fort Worth, TX, USA).

3.3.2 HPLC Methods

In the HPLC method, Agilent 1200 series autosampler, pump, diode array detector (DAD), and a Cyclobond I 2000 RSP column (25 cm × 4.6 mm) were used.⁴³ For the degradation study of the carnosol, carnosic acid, and rosmarinic acid standards, a gradient of binary solvents was used for elution. Solvent A consisted of 70% H₂O, 30% ACN, and 0.1% formic acid. Solvent B consisted of 40% H₂O, 60% ACN, and 0.1% formic acid. At a flow rate of 1 mL/min, the eluent consisted of 100% A for the initial 4 min, and then from 4 to 17 min the composition was ramped gradually to 100% solvent B. From 17 to 20 min, the eluent composition was returned to 100% solvent A. For the analysis of rosemary extract and the degradation study of the rosemary extract in fish oil, the procedure was modified to remove all the lipids remaining in the column after all the phenolic and diterpenoid compounds eluted by using 100% ACN as solvent C. Within the first 17 min, the procedure remained the same as described above. From 17 to 20 min, the eluent composition was ramped to 100% solvent C and then maintained at 100% solvent C from 20 to 22 min. From 22 to 25 min, the eluent composition was returned to 100% solvent A.

3.3.3 HPLC/MS/MS method

In the HPLC/MS/MS method, Thermo Finnigan Surveyor autosampler, MS pump, PDA detector, and Thermo LXQ linear ion trap mass spectrometer were used. The HPLC gradients were the same as described previously. The electrospray ionization (ESI) mass

spectra data were recorded in a negative ionization mode for the m/z range of 100–1000. Capillary voltage and spray voltage were set at -7 V and 4.7 kV, respectively. The normalized collision energy setting was 35 (arbitrary unit) while helium was used as the collision gas.

3.3.4 Calibrations

The stock solution of analyte was prepared by weighing the respective vials containing carnosol, carnosic acid, or rosmarinic acid, dissolving the contents in methanol, approximately 10 mg, and transferring them to a 10 mL volumetric flask, drying the vial in an oven at or above 110 °C and then reweighing the empty vial equilibrated to room temperature. Thus the transferred contents were accurately determined. The concentration of carnosol, carnosic acid, and rosmarinic acid in the stock solution was approximately 1000 mg/L for each of them.

Standard solutions of carnosol, carnosic acid, and rosmarinic acid were made up in the following approximate concentration ranges: 200, 400, 600, 800, and 1000 mg/L. The solvent system consisted of 150 mg/L butylated hydroxytoluene (BHT, European Union Code E321) in methanol. The addition of the antioxidant BHT, used only for the standard solutions for determination of the calibration curves, was purely precautionary to ensure the stability of carnosol, carnosic acid, and rosmarinic acid during the calibration study. The BHT eluted at 11.6 min and did not interfere with any of the compounds under investigation. All standards were stored at -10 °C in the dark. The linearity for the

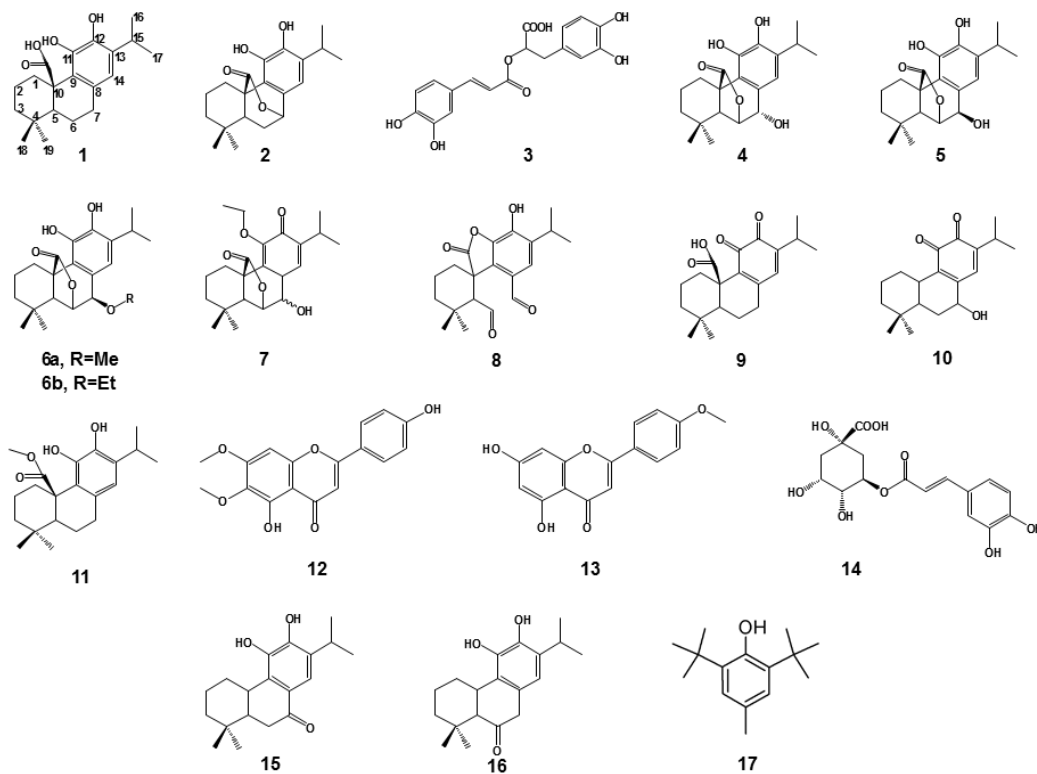


Figure 3-1 Structures of compounds for this study.

1, carnosic acid (C₂₀H₂₈O₄, MW 332.42); 2, carnosol (C₂₀H₂₆O₄, MW 330.44); 3, rosmarinic acid (C₁₈H₁₆O₈, MW 360.32); 4, rosmanol (C₂₀H₂₆O₅, MW 346.42); 5, epirosmanol (C₂₀H₂₆O₅, MW 346.42); 6a, epirosmanol methyl ether (C₂₁H₂₈O₅, MW 360.45); 6b, epirosmanol ethyl ether (C₂₂H₃₀O₅, MW 374.48); 7, 11-ethoxyrosmanol semiquinone (C₂₂H₃₀O₅, MW 374.48); 8, rosmadiol (C₂₀H₂₄O₅, MW 344.41); 9, carnosic acid quinone (C₂₀H₂₆O₄, MW 330.42); 10, 5,6,7,10-tetrahydro-7-hydroxyrosmariquinone (C₁₉H₂₆O₃, MW 302.40); 11, light induced degradation product of carnosic acid (structure unknown); 12, methyl carnosate (C₂₁H₃₀O₄, MW 346.47); 13, cirsimaritin (C₁₇H₁₄O₆, MW 314.29); 14, acacatin (C₁₆H₁₂O₅, MW 284.27); 15, chlorogenic acid (C₁₆H₁₈O₉, MW 354.31); 16a,b (C₁₉H₂₆O₃, MW 302.41), structures for products of carnosic acid degradation reported in reference¹⁴¹; 17, butylated hydroxytoluene (C₁₅H₂₄O, MW 220.35).

calibrations curves for carnosol, carnosic acid, and rosmarinic acid each had $r^2 \geq 0.999$, confirming the absence of any significant oxidation. The calibration curves, limit of detections (LOD), limit of quantitations (LOQ), intraday and interday precisions of the three standards are available in Table 3-1. The DAD detector was set at four different wavelengths, 230, 254, 280, and 330 nm. At 280 nm, the chromatograms had the flattest baseline. Consequently, the peak areas measured at 280 nm were used to calculate the concentrations of the analytes. The UV spectra of carnosol, carnosic acid, and rosmarinic acid are shown in Figure 3-2.

Table 3-1 Statistical figures of merit and calibration curve results

Standard	Regression line	r^2	% Precision		LOD	LOQ
			Intraday	Interday	(mg/L)	(mg/L)
Carnosol	$y = 1.8712x + 5.455$	> 0.99	1.0	1.3	2.0	6.8
Carnosic acid	$y = 1.3289x + 7.015$	> 0.99	0.8	1.0	3.1	10.3
Rosmarinic acid	$y = 2.4668x - 17.219$	> 0.99	1.0	1.4	3.8	12.8

3.3.5 Sample preparation and storage

Individual samples of carnosol, carnosic acid, and rosmarinic acid standards as well as a mixture of the three were prepared similarly to the stock solution in the calibration study except for a change in solvent to pure ethanol and exclusion of the BHT. The initial concentrations for each of these three antioxidants in either the 1-component or 3-component solutions were about 800–900 mg/L. These four standards were subjected to the following six conditions: (1) –10 °C in dark, (2) 4 °C in dark, (3) room temperature with light exposure, (4) room temperature in dark, (5) 40 °C with light exposure, (6) 40 °C in dark. The influence of temperature and light on degradation was observed for 13 days. The concentrations of the components in each sample were

analyzed every 24 h. The rosemary extract dissolved in fish oil was stored under five conditions: (1) 4 °C in dark; (2) room temperature in dark; (3) room temperature with light exposure; (4) 40 °C in dark; and (5) 40 °C with light exposure. This was monitored for 51 days. Prior to HPLC analysis, ~100 mg of the fish oil sample was added to a 15 mL screw-cap centrifuge tube and dissolved in 5 mL of methanol.

The injection volume for each HPLC analysis was 5 µL.

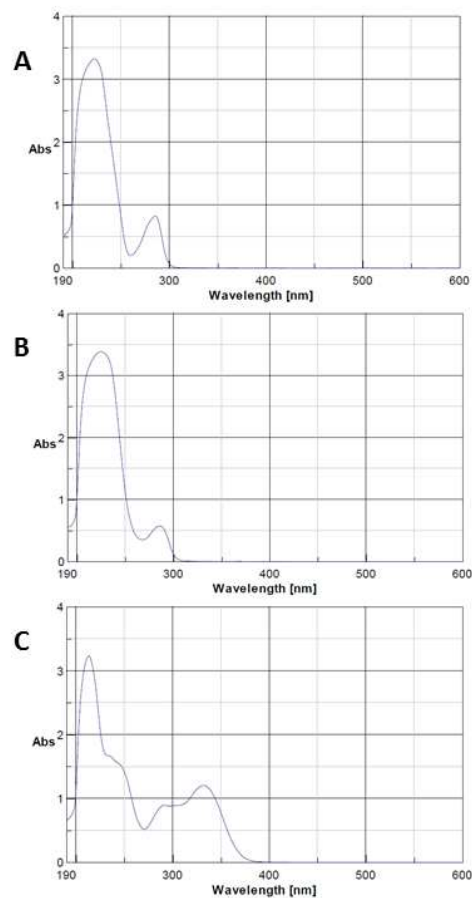


Figure 3-2 UV spectra of A) carnosol, B) carnosic acid and C) rosmarinic acid

3.3.6 Rosemary powder extraction

About 250 mg of rosemary powder was weighed and transferred to a 15 mL screw-top centrifuge tube. An aliquot of 2 mL of methanol was added to the centrifuge tube. The samples were allowed to incubate for 30 min at room temperature in the dark and then sonicated in an ultrasonication bath for 90 min while kept in the dark. The samples were then refrigerated at 4 °C overnight. Prior to LC analysis, samples were centrifuged for 5 min at 3000 rpm. 100 µL of the supernatant was diluted 10 times in an amber vial and then analyzed by HPLC. If completely extracted, the concentration of carnosic acid was expected to be about 2000 mg/L. The concentrations of carnosic acid and carnosol in the rosemary powder are 20.0 % and 2.3 % (dry weight), respectively.

3.4 Results and discussion

3.4.1 Analytical method

Cyclodextrin-based columns are widely used in HPLC enantiomeric separations.⁴³ However, used in the reversed phase mode they are also known to separate structural isomers and other closely related compounds better than other conventional reversed phase columns.^{37,39} This is due to their vastly greater shape selectivity for closely related compounds. In this study, a Cyclobond I 2000 RSP column provided better separations for the degradation products of carnosic acid and carnosol, and for other components in rosemary extract, many of which are structurally related.

3.4.2 Degradation of carnosic acid, carnosol, rosmarinic acid, and their mixture in ethanol solutions

Understanding the stability of antioxidants is important for improving use and efficacy, and for establishing proper storage conditions to extend shelf life. Rosemary extract and its constituents are well-known to protect a variety of foods and food supplements from oxidative degradation.^{118,127,142} However, the degradation of rosemary

extract and specifically its phenolic and diterpenoid components were examined only in a few instances.¹⁴³⁻¹⁴⁶ Schwarz and Ternes isolated carnosic acid and carnosol from rosemary extract and investigated their degradation in methanol over 9 days.¹⁴³ The same authors also reported the stability of the phenolic diterpenes from rosemary extract in lard under thermal stress of 170 °C.¹⁴⁴ Irmak et al. observed the stability of rosemary extract stored at 4 °C in the dark and at room temperature with light exposure for 14 weeks.¹⁴⁵ However, the effect of light and temperature on the degradation process could not be distinguished. Bano et al. investigated the oxidation of a single component, carnosic acid, in three different solvents under atmospheric conditions at 30 °C for 16 days.¹⁴⁶

In the present study, the degradation of rosmarinic acid, carnosol, carnosic acid, and the mixture of these three antioxidants under ambient air exposure and in ethanolic solution was followed under a series of different storage temperatures, with or without light exposure, over a 13 day period.

3.4.2.1 Degradation profiles of three primary phenolic antioxidants in rosemary

Rosmarinic acid, either by itself in the ethanolic solution or presented in the ethanolic solution of the mixture, did not degrade appreciably under any of the conditions during the 13 day study. Figure 3-3 A and B illustrated the degradation profiles of rosmarinic acid by itself and in the mixture respectively under different thermal and light exposure conditions.

On the other hand carnosol dissolved in ethanol degraded most rapidly of the three antioxidants. This was particularly noticeable at 40 °C with light exposure where the pure carnosol completely disappeared at day four (as shown in Figure 3-3 C). The rate of degradation of carnosol increased according to the following sequence: -10 °C in dark < 4 °C in dark < room temperature in dark < room temperature with light exposure < 40 °C

in dark < 40 °C with light exposure. Temperature was the major factor affecting the degradation of carnosol in solution, and light exposure further accelerated the degradation. In contrast to this, significantly slower apparent degradation was observed for carnosol in the solution of the mixture (see Figure 3-3 D). This could be attributed to protection by the other antioxidants present in the mixture or by the compensatory conversion of carnosic acid to carnosol. (See discussion in the Degradation of the mixture section 3.4.2.5 below.)

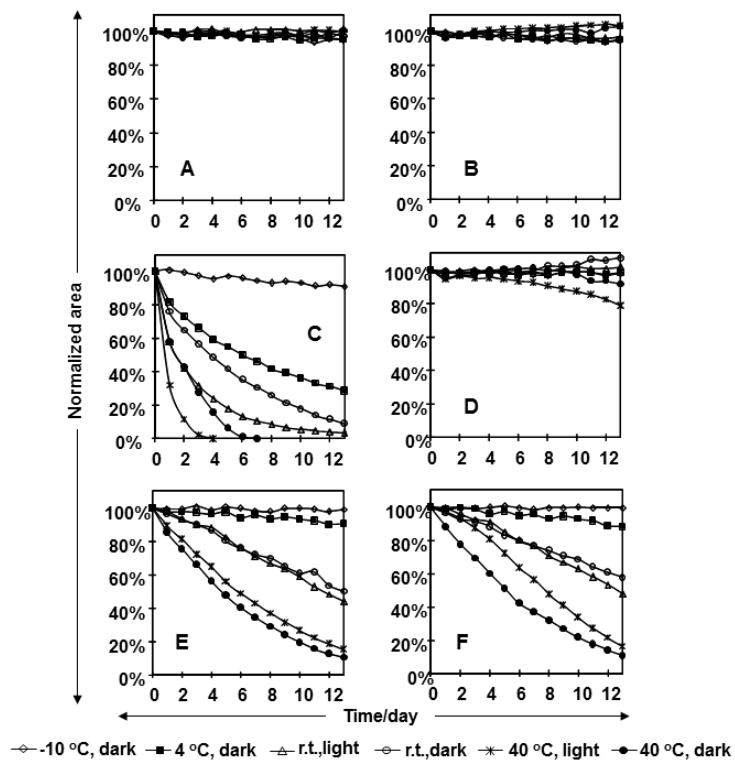


Figure 3-3 Degradation profiles of three primary phenolic antioxidants in rosemary. Ethanol solutions of (A) rosmarinic acid by itself, (B) rosmarinic acid in the mixture, (C) carnosol by itself, (D) carnosol in the mixture, (E) carnosic acid by itself, and (F) carnosic acid in mixture under different storage conditions.

Carnosic acid, by itself in ethanol solution and in the solution of the mixture, was fairly stable at -10 and 4 °C in dark (as shown in Figure 3-3 E and F). At higher temperatures and under light exposure conditions it degraded, but not so rapidly as did carnosol by itself in ethanol solution. Carnosic acid exhibited similar degradation in the mixture solution and in its own solution. It was noticed that the degradation of the carnosic acid stored in dark was higher than that of the carnosic acid exposed to light at the same temperature, especially when stored at 40 °C. This was in contrast to the results observed for carnosol.

3.4.2.2 Identification of degradation products and pathways of carnosol and carnosic acid. degradation products of carnosol

Rosmanol, epirosmanol and epirosmanol ethyl ether. Three major degradation products of carnosol were formed in the ethanol solutions and were labeled as compounds 4, 5, and 6b in Figure 3-4 A (structures shown in Figure 3-1). In negative mode of electrospray ionization (ESI), $[M - H]^-$ m/z values 345, 345, and 373 were observed for the compounds 4, 5, and 6b, respectively. When collision-induced dissociation (CID) energy was applied, compounds 4 and 5 had the same fragmentation pattern which gave two fragments at m/z 301 and 283, while compound 6b had two fragments at m/z 329 and 283. The λ_{max} values for compound 4, 5, and 6b were 289, 288, and 289 nm, respectively. These data were in good agreement with the literature values of rosmanol, epirosmanol, and epirosmanol ethyl ether.^{147,148} The compound 4 was also confirmed by comparing it to a rosmanol standard. It had the same retention time, molecular mass, MS fragmentation, and UV spectrum as the rosmanol standard. In the tandem mass spectra, decarboxylation ($[M - H - COO]^-$) of rosmanol (4), epirosmanol (5), and epirosmanol ethyl ether (6b) resulted in m/z values at 301, 301, and 329,

respectively. The m/z value at 283 was caused by the further loss of a H_2O molecule from rosmanol and epirosmanol or an ethanol molecule from epirosmanol ethyl ether.

It was observed that epirosmanol ethyl ether was not formed when carnosol was dissolved in an aprotic solvent, such as acetonitrile. However, when other protic solvents, such as methanol or isopropanol, were used, the corresponding ether of epirosmanol was formed. Also, it was noticed that the formation of these three degradation products was affected by temperature. Rosmanol was the most abundant among the three compounds when stored at $-10\text{ }^\circ\text{C}$. However, the peak area of rosmanol became relatively smaller than that of the epirosmanol ethyl ether when the temperature increased (see Figure 3-5). Apparently, high temperature is an important factor in the formation of epirosmanol ethyl ether, suggesting its energy barrier is higher than that for rosmanol, perhaps on the order of 1–2 kcal/mol.

11-Ethoxy-rosmanol semiquinone. The degradation compound 7 corresponding to peak 7 in Figure 3-4 A only appeared in the carnosol solution stored at $40\text{ }^\circ\text{C}$ with light exposure and after carnosol completely degraded. As seen in Figure 3-6, its peak area increased with a slow decrease of the peak areas of epirosmanol ethyl ether, rosmanol, and epirosmanol. Thus, this degradation product was inferred to arise indirectly from carnosol via other carnosol degradation products. It was slightly ionized in ESI negative ion mode and the $[M - H]^-$ m/z value was 373. When CID energy was applied, no fragments were observed. Even though the molecular m/z value of compound 7 was the same as epirosmanol ethyl ether, the difference in the ability to ionize indicated a significant difference in their structure. It is very likely that no phenol group or carboxylic group existed in the structure of compound 7. In the UV spectrum of compound 7, a maximum absorption peak at 261 nm with a shoulder at 296 nm and a second maximum

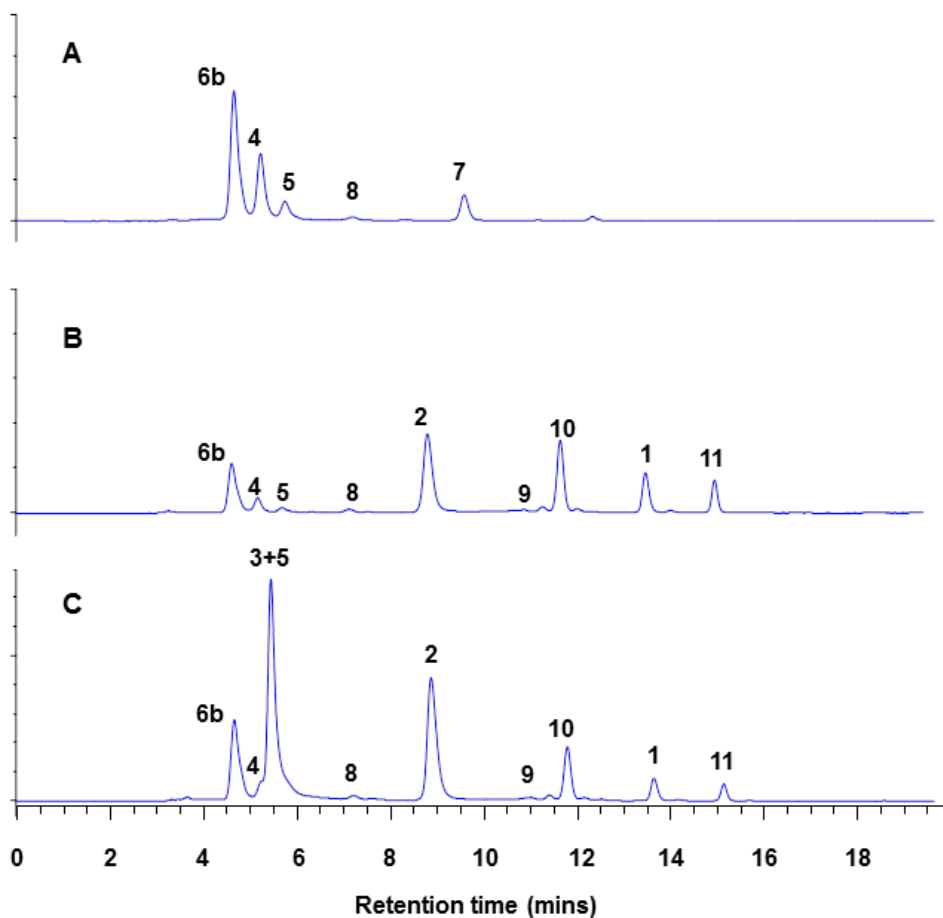


Figure 3-4 HPLC chromatograms of the degradation study.

(A) carnosol, (B) carnosic acid, and (C) a mixture of carnosol, carnosic acid, and rosmarinic acid in ethanol solutions stored at 40 °C with light exposure after 13 days. **1.** carnosic acid, **2.** carnosol, **3.** rosmarinic acid, **4.** rosmanol, **5.** epirosmanol, **6b.** epirosmanol ethyl ether, **7.** 11-ethoxy-rosmanol semiquinone, **8.** rosmadial, **9.** carnosic acid quinone, **10.** 5,6,7,10-tetrahydro-7-hydroxy-rosmariquinone and **11.** the light induced degradation product.

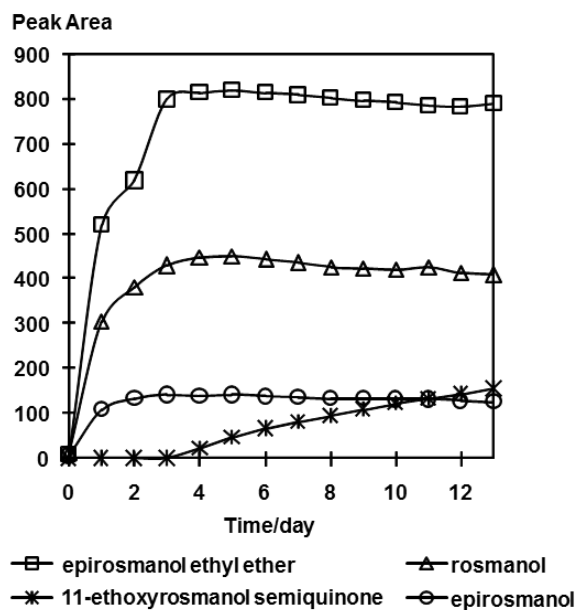


Figure 3-5 Degradation products of carnosol as a function of time at 40 °C with light exposure.

absorption peak at 322 nm with a shoulder at 335 nm also distinguished the functionalities of compound 7 from epirosmanol ethyl ether. It was reported that rosmanol and epirosmanol can be further oxidized to rosmanol o-quinone, which can be converted subsequently to another diterpene, galdosol, via a semiquinone intermediate when subject to heat. Under the conditions investigated, this semiquinone intermediate appeared to react with ethanol and form an ethyl ether adduct instead of converting to galdosol. The structure as shown in Figure 3-1 was proposed for compound 7. The UV absorbance maximum was computed from functional group contributions and found to be consistent with the observed values.¹⁴⁹⁻¹⁵¹

Rosmadiol. The small peak that eluted at 7.34 min in chromatogram Figure 3-4A was labeled as peak 8 and had a molecular $[M - H]^-$ m/z at 343 and two product ions

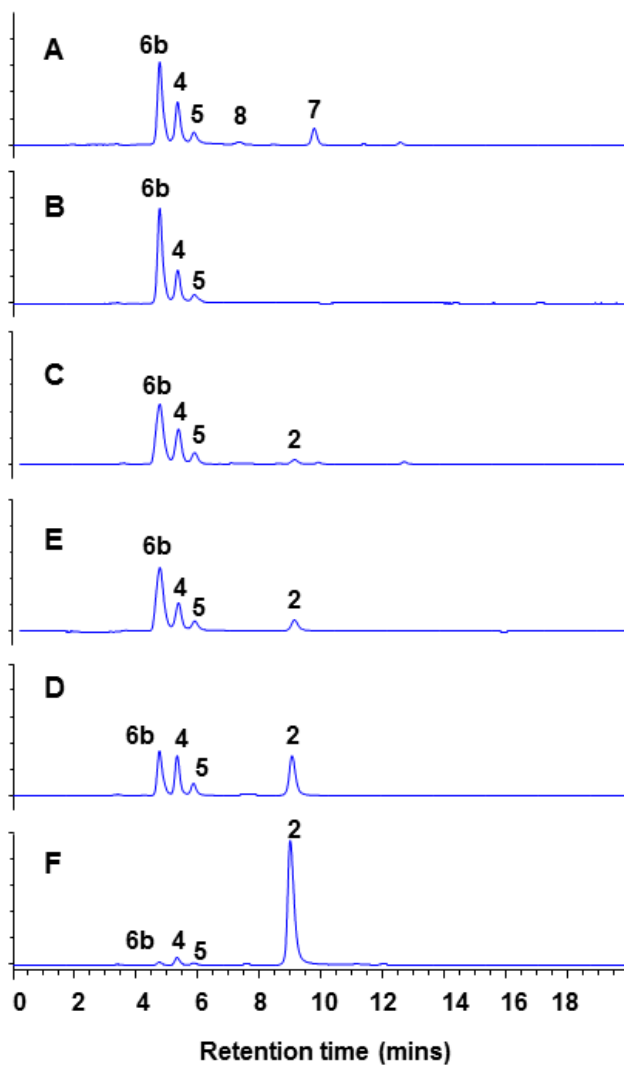


Figure 3-6 HPLC chromatograms of carnosol ethanol solutions stored under different conditions after 13 days.

A) 40 °C with light exposure, B) 40 °C in dark, C) room temperature with light exposure, D) room temperature in dark, E) 4 °C in dark, F) -10 °C in dark. The peaks are labeled as **2.** carnosol, **4.** rosmanol, **5.** epirosmanol, **6b.** epirosmanol ethyl ether, **7.** 11-ethoxyrosmanol semiquinone and **8.** rosmadial.

m/z at 315 and 299. The UV λ_{max} value was 286 nm. These data were in agreement with the literature values of rosmadial.^{147,148} The m/z at 315 suggested a loss of CO and the m/z at 299 may be caused by the cleavage of CO₂ from the molecular ion.

3.4.2.3 Degradation products of carnosic acid

Carnosic acid quinone. When carnosic acid was kept at -10 °C in dark for 13 days, carnosic acid quinone (Figure 3-1) was the only degradation product observed (see Figure 3-7). Under these conditions the degradation of carnosic acid was much slower as was the subsequent reaction of the intermediate quinone formed from it. Carnosic acid was completely converted to this compound after being stored at -10 °C in dark for 30 days. The completion of this conversion was confirmed by HPLC, UV and NMR. The chemical shift of catechol hydroxyls in carnosic acid at 7.74 ppm disappeared while the shift of carboxylic group at 12.31 ppm was retained. Also, the mass spectrum showed molecular [M - H]⁻ m/z at 329 and a fragment in the tandem mass spectrum at an m/z of 285, the result of a cleavage of a carboxylic group (CO₂) from the molecular ion. The compound had a UV maximum absorption at 428 nm which indicated the presence of an o-benzoquinone structure. These data were in agreement with that reported by others in the literature.^{152,153}

The peak area of carnosic acid quinone increased slightly when the storage temperature increased from -10 °C to room temperature but decreased afterward (see Figure 3-7). Carnosic acid quinone was postulated to be an intermediate in the oxidation pathway of carnosic acid to carnosol, rosmanol, etc.^{146,154-156} It was confirmed by Masuda et al. that carnosic acid quinone can convert to carnosol, rosmanol, and 7-methylrosmanol in methanol solution when subject to 60 °C for 2 h.¹⁵⁶ Also, the low temperature needed for the conversion of carnosic acid to carnosic acid quinone indicated a low energy barrier for this conversion. Therefore, carnosic acid quinone was

very likely to be the intermediate in the degradation pathway of carnosic acid, and its small peak area in Figure 3-4B at high temperatures is likely due to the conversion of carnosic acid quinone to other degradation products.

The essential role of this quinone as the primary initial degradant in the oxidation/light pathway analysis provided in Figure 3-8 is also supported by its elimination when carnosic acid is stored under an inert atmosphere¹⁴³ and by the analysis of the degradation kinetics provided below.

Carnosol and its degradation products. At 4 °C, a degradation product was eluted at 8.98 min (labeled as peak 2 in Figure 3-4B). It was confirmed to be carnosol. The peak area of carnosol increased with increasing temperature (see Figure 3-). After carnosol was formed in the solution, degradation products 4, 5, and 6b appeared in the solutions stored above 4 °C. These three degradation products were confirmed to be rosmanol, epirosmanol, and epirosmanol ethyl ether, respectively. This result indicated that these three compounds were generated from the carnosol that was produced via the degradation of carnosic acid. This agrees with the oxidation pathway of carnosic acid postulated by Wenkert et al.,¹⁵⁵ Bano et al.,¹⁴⁶ and Schwarz and Ternes.¹⁴³ Peak 8 eluted at 7.34 min in Figure 3-4B had a molecular [M –H]– at m/z 343 and two product ions at m/z 315 and 299. The UV λ_{max} value of 286 nm was observed. These data are consistent with the assignment of this compound to be rosmadial,^{147,148} as observed in the degradation of carnosol form which it was derived.

5,6,7,10-Tetrahydro-7-hydroxy-rosmariquinone. Another major degradation product derived from carnosic acid was eluted at 12.01 min and was labeled as peak 10 in Figure 3-4B. The formation of this degradation product was promoted by exposure to light. At the same storage temperature it had larger peak area in the solution exposed to light than in the one kept in the dark (as seen in Figure 3-7).

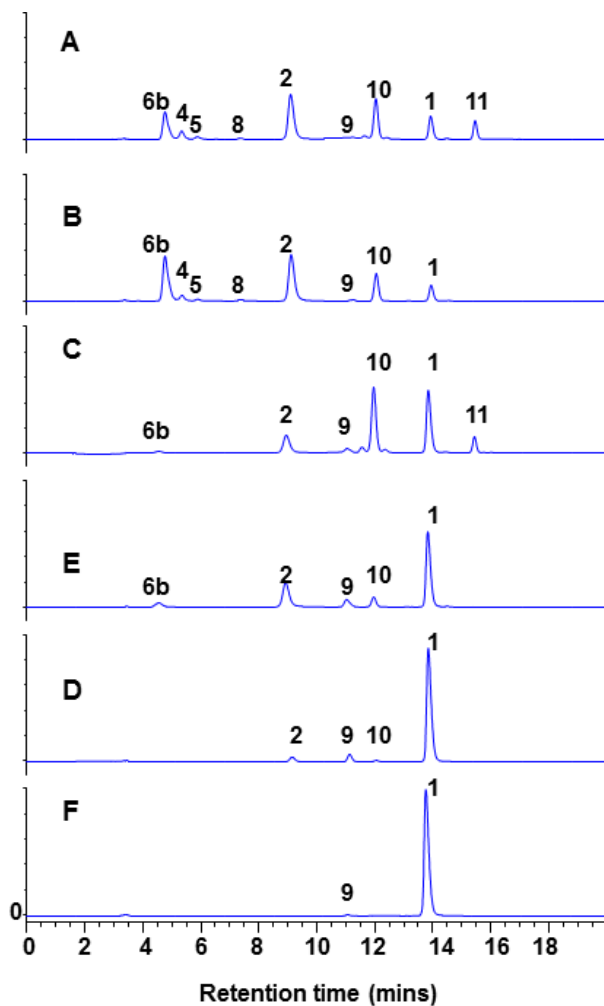


Figure 3-7 HPLC chromatograms of carnosic acid ethanol solutions stored under different conditions after 13 days.

A) 40 °C with light exposure, B) 40 °C in dark, C) room temperature with light exposure, D) room temperature in dark, E) 4 °C in dark, F) -10 °C in dark. **1.** carnosic acid, **2.** carnosol, **4.** rosmanol, **5.** epirosmanol, **6b.** epirosmanol ethyl ether, **8.** rosmadial, **9.** carnosic acid quinone **10.** 5,6,7,10-tetrahydro-7-hydroxy-rosmariquinone, **11.** the light induced degradation product.

Compound 10 was difficult to ionize, just barely ionizable in the negative mode of ESI. Therefore, the sample was concentrated by 10 times prior to LC-MS-MS analysis. A parent ion $[M - H]^-$ with m/z 301 was observed. The tandem mass spectrum gave fragments at m/z 283, 273, and 258, which suggested a loss of H_2O , CO, and an isopropyl group from the molecular ion, respectively. In the literature, two structures with m/z values of 301 were reported and are shown in Figure 3-1 (16a and 16b).¹⁴¹ However, the difficulty in ionization of compound 10 in ESI negative mode indicated the absence of phenol or carboxylic acid groups in the structure. The UV spectrum showed strong absorption at 279 and 409 nm. Thus, an *o*-benzoquinone structure was very likely to exist.¹⁵³ A structure for compound 10 was proposed as shown in Figure 3-1, and it was named as 5,6,7,10-tetrahydro-7-hydroxy-rosmariquinone. The common name of rosmariquinone for this base structure was proposed previously.¹⁵⁷

Degradation product generated by light exposure. As shown in Figure 3-4B, a compound was eluted after the carnosic acid and was labeled as peak 11. This compound only appeared in the solutions exposed to light and had strong UV absorption at 260 nm. Unfortunately, it could not be ionized in either negative or positive ion mode of ESI even at high concentrations and was labile when isolation from the solution was attempted. Insufficient amounts of this compound were collected from HPLC fractions for NMR analysis. Thus, no further information was obtained on the structure of this light induced degradation product, and it remains a topic for further investigation.

Minor degradation products. As seen in Figure 3-4B, there were three small peaks eluted at 11.52, 12.50, and 14.35 min, respectively. The first two peaks only appeared with light exposure. These compounds were not easily ionized, so given the small amounts present no further effort was made to identify their structures.

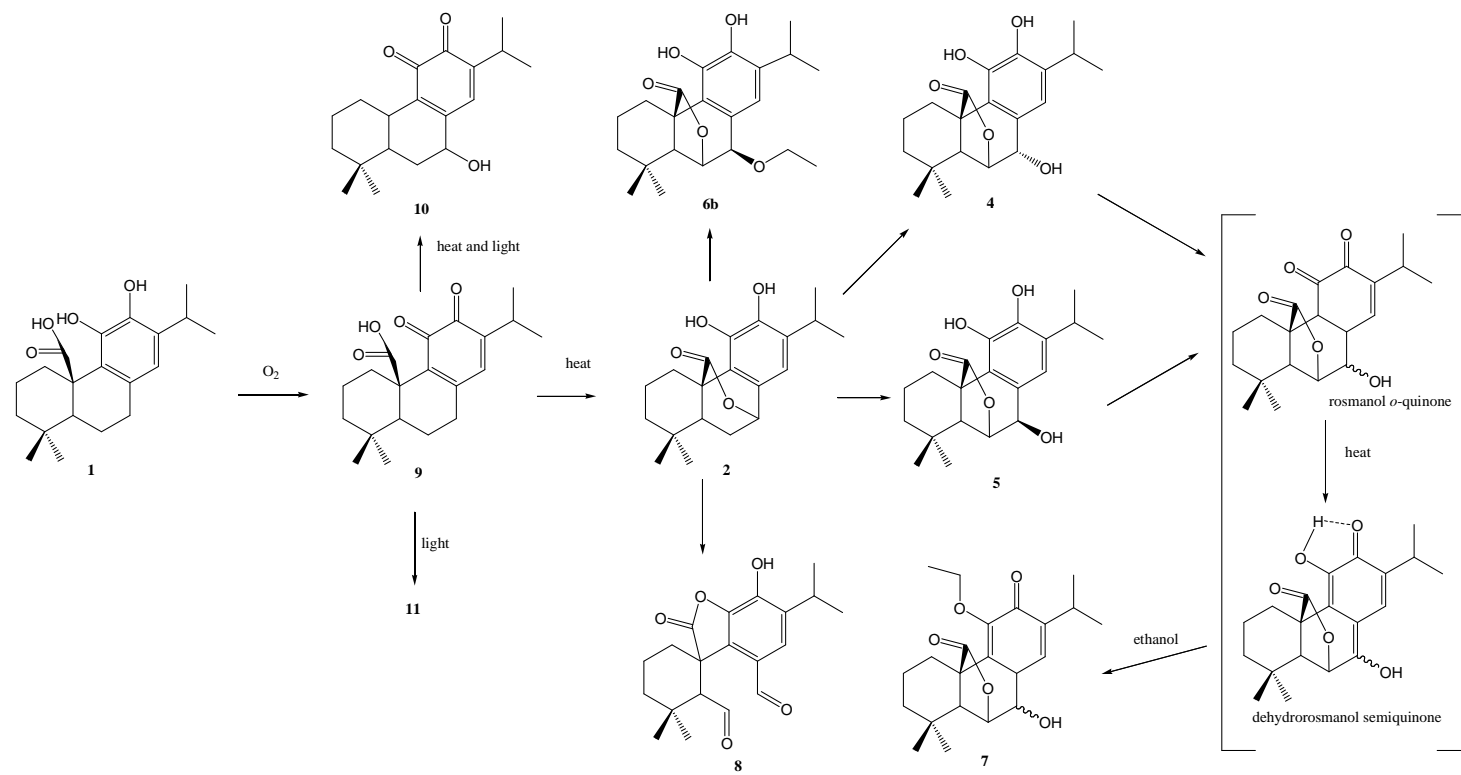


Figure 3-8 The proposed degradation pathway of carnosic acid in ethanol solution.

3.4.2.4 Degradation pathway of carnosic acid

On the basis of the discussion above, a degradation pathway of carnosic acid was postulated and is shown in Figure 3-8. Carnosic acid quinone was likely to be the intermediate in the pathway. It was confirmed that rosmanol, epirosmanol, and epirosmanol ethyl ether were generated from carnosol which is a degradation product of carnosic acid. Also, 5,6,7,10-tetrahydro-7-hydroxyrosmariquinone and the light induced degradation product, compound 11, were reported as degradation products of carnosic acid for the first time. A more detailed, though incomplete, analysis of the kinetics of degradation for carnosic acid and carnosol is provided in section 3.4.4.

3.4.2.5 Degradation of the mixture

When rosmarinic acid, carnosol, and carnosic acid were dissolved in the same solution, similar degradation products were generated as in the individual standard solutions of carnosol and carnosic acid (as shown in Figure 3-4C). Rosmarinic acid was stable in both ethanol solutions (see Figure 3-3A,B). Consequently, it is not considered in the following discussion regarding the degradation behavior of the antioxidants presented in the mixture solution. The rosmanol and epirosmanol peaks were observed to overlap the rosmarinic acid peak in Figure 3-4C. Their appearance as well as that of epirosmanol ethyl ether indicated the degradation of carnosol. However, the concentrations of carnosol in all the chromatograms in Figure 3-9 did not show significant change compared to their initial values.

A study of the concentrations of carnosol and epirosmanol ethyl ether in three solutions: carnosol ethanol solution (solution 1), carnosic acid ethanol solution (solution 2), and the ethanol solution of the three mixed antioxidants rosmarinic acid, carnosol, and carnosic acid (solution 3) was carried out. Epirosmanol ethyl ether was used as an

“indicator” for the rate of degradation of carnosol since it was the major degradation product of carnosol and the baseline resolution provided the most accurate quantitation.

The purpose of this study was to determine if carnosic acid had the ability to “protect” carnosol, or whether the loss of carnosol was simply compensated for by that which was produced from carnosic acid. The results at the 13th day were used for this assignment.

The initial concentrations of carnosol, carnosic acid, and epirosmanol ethyl ether in the three solutions were shown as below:

$$C_{C,1,initial} = C_{C,3,initial} \quad (3-1)$$

$$C_{CA,2,initial} = C_{CA,3,initial} \quad (3-2)$$

$$C_{E,1,initial} = C_{E,2,initial} = C_{E,3,initial} = 0 \quad (3-3)$$

where $C_{C,1,initial}$ and $C_{C,3,initial}$ were the initial concentrations of carnosol in solution 1 and solution 3, respectively; $C_{CA,2,initial}$ and $C_{CA,3,initial}$ were the initial concentrations of carnosic acid in solution 2 and solution 3, respectively. $C_{E,1,initial}$, $C_{E,2,initial}$, $C_{E,3,initial}$ were the initial concentrations of epirosmanol ethyl ether in solution 1, 2 and 3, respectively. The epirosmanol ethyl ether standard was not available and so its molar concentrations in the solutions were not calculable. Also the quantitative evaluation of this degradative pathway is unknown. However, the peak area of the epirosmanol ethyl ether in the chromatogram corresponds to its concentration since the injected volume for each HPLC analysis was the same. Thus the integrated peak area of epirosmanol ethyl ether instead of its concentration was used for this analysis/discussion. The peak area values are listed in Table 3-2.

If the degradation processes of carnosol and carnosic acid in the mix solution were independent of each other and occurred at the same rate as their degradation in the individual standard solutions, under each storage condition, then

$$P_{C,1,13\text{th-day}} + P_{C,2,13\text{th-day}} = P_{C,3,13\text{th-day}} \quad (3-4)$$

and

$$P_{E,1,13\text{th day}} + P_{E,2,13\text{th day}} = P_{E,3,13\text{th day}} \quad (3-5)$$

where $P_{C,1,13\text{th-day}}$ was the peak area of remained carnosol in solution 1 after 13 days storage, $P_{C,2,13\text{th-day}}$ was the peak area of remaining carnosol (which was first generated from degradation of carnosic acid) in solution 2 after 13 days storage, $P_{C,3,13\text{th-day}}$ was the concentration of carnosol in solution 3 after 13 days storage; $P_{E,1,13\text{th-day}}$, $P_{E,2,13\text{th-day}}$, and $P_{E,3,13\text{th-day}}$ were the peak areas of epirosmanol ethyl ether in solution 1, solution 2, and solution 3 after 13 days of storage, respectively. According to the peak area values listed in Table 3-2, the peak area of epirosmanol ethyl ether in solution 3 was much smaller than the sum of its peak areas in solutions 1 and 2 under the same storage conditions.

$$P_{E,1,13\text{th day}} + P_{E,2,13\text{th day}} > P_{E,3,13\text{th day}} \quad (3-5)$$

This indicated the total amount of carnosol degraded in solution 1 and solution 2 was larger than the amount of carnosol being degraded in the mixture solution. The degradation of carnosol in this simple mixture, even in the absence of the multiple ingredients from the refined fish oil (below), was less than that found for carnosol alone in solution. Interestingly, the peak area of carnosol in the mixture solution was significantly larger than the sum of that in found in solutions 1 and 2,

$$P_{C,1,13\text{th day}} + P_{C,2,13\text{th day}} < P_{C,3,13\text{th day}} \quad (3-6)$$

At room temperature, the peak area of carnosol in the mixture solution was even larger than its initial value. Therefore, a portion of carnosol in the mixture solution was inferred to arise from the degradation of carnosic acid. Thus the relatively small change in the carnosol concentration in the mixture solution with time was due in part to the

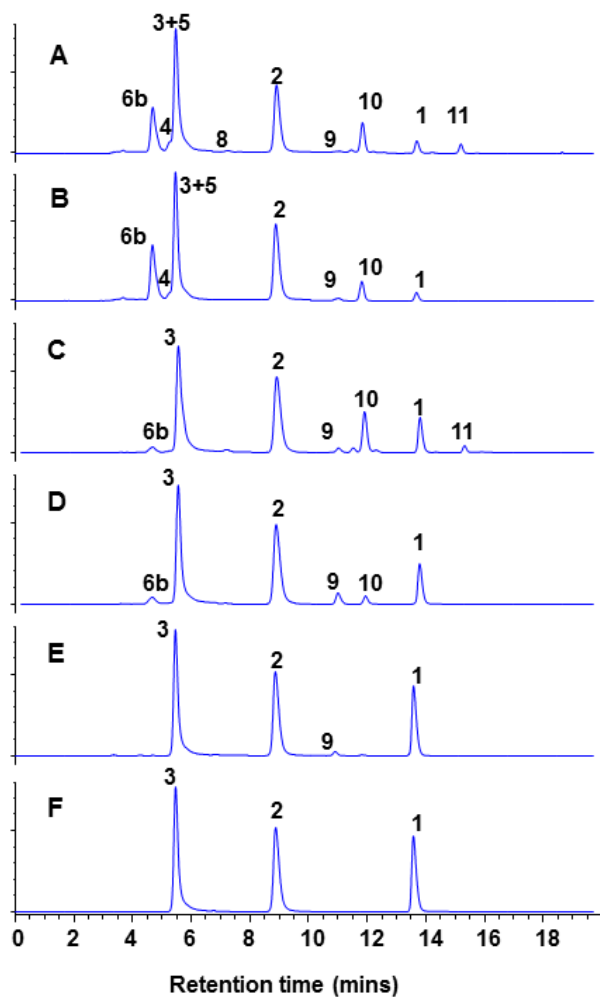


Figure 3-9 HPLC chromatograms of carnosic acid/carnosol mixture ethanol solutions stored under different conditions after 13 days.

A) 40 °C with light exposure, B) 40 °C in dark, C) room temperature with light exposure, D) room temperature in dark, E) 4 °C in dark, F) -10 °C in dark. 1. carnosic acid, 2. carnosol, 3. rosmarinic acid, 4. rosmanol, 5. epirosmanol, 6b. epirosmanol ethyl ether 8. rosmadial, 9. carnosic acid quinone 10. 5,6,7,10-tetrahydro-7-hydroxy-rosmariquinone, 11. the light induced degradation product of carnosic acid.

Table 3-2 Peak area data for epirosmanol ethyl ether and carnosol in solutions 1 – 3

Condition	Compound	Solution #		
		1	2	3
Initial	epirosmanol ethyl ether	0	0	0
	carnosol	1562.9	0	1556.3
40 °C with light ^a	epirosmanol ethyl ether	790.7	290.3	722.1
	carnosol	0	495.0	1222.5
40 °C in dark	epirosmanol ethyl ether	897.2	483.8	921.7
	carnosol	0	515.3	1423.0
r.t. with light ^a	epirosmanol ethyl ether	798.0	34.2	80.6
	carnosol	54.4	235.4	1586.2
r.t. in dark ^a	epirosmanol ethyl ether	852.0	54.2	136.1
	carnosol	140.7	316.4	1666.8
4 °C in dark	epirosmanol ethyl ether	435.3	0	0
	carnosol	446.7	36.8	1532.6
-10 °C in dark	epirosmanol ethyl ether	21.3	0	0
	carnosol	1418.3	0	1525.9

protective behavior of carnosic acid toward carnosol and also to the conversion of carnosic acid to carnosol.

3.4.3 Degradation of rosemary extract in fish oil

Rosemary extracts containing its major antioxidants are often added to polyunsaturated fatty acids (PUFAs) to prevent oxidation during processing and rancidification during storage.^{119,120} The focus of this portion of the study was to examine the stability of the two principal rosemary antioxidants, carnosic acid and carnosol, in fish oil. The specific value of the other extractables is yet to be determined.

The components in rosemary extract can be well separated by the HPLC method developed in this study (see section 3.3 for details). As shown in Figure 3-10A, besides carnosic acid and carnosol, cirsimaritin was another major component in the rosemary extract. The minor components included acacetin, chlorogenic acid as well as methyl carnosate, rosmanol, epirosmanol, rosmadial, and carnosic acid quinone, which may be derived from carnosic acid and carnosol (Figure 3-1). These compounds were confirmed by comparing the mass spectra and UV spectra (as shown in Table 3-3) with the values from the literature.^{147,148} The structures of the three small peaks eluted between chlorogenic acid and carnosic acid as well as the two small peaks eluted after methyl carnosate were not confirmed due to their low concentrations and difficulty in ionization.

When the sample of rosemary extract in fish oil was diluted with methanol and this solution was directly injected for HPLC analysis, a hump appeared at 11–15 min as shown in Figure 3-10B, C. This hump was due to the UV absorbance of the fish oil matrix. Consequently, the concentration of carnosic acid was quantitated by subtracting the raised baseline. The concentrations of carnosic acid and carnosol in the mixture of rosemary extract and fish oil were 4.2% and 0.60% (weight percent), respectively. Under all storage conditions, the carnosol in the processed fish oil was very stable. The fastest

degradation of carnosic acid was observed at 40 °C with light exposure. After 51 days at this condition, the concentration of carnosic acid was 3.7% indicating less than 12% of carnosic acid degraded. Compared to the rate of degradation observed for carnosic acid in ethanol solution, the stability of carnosic acid in the rosemary extract was greatly enhanced when it was dissolved in the processed omega-3 rich fish oil.

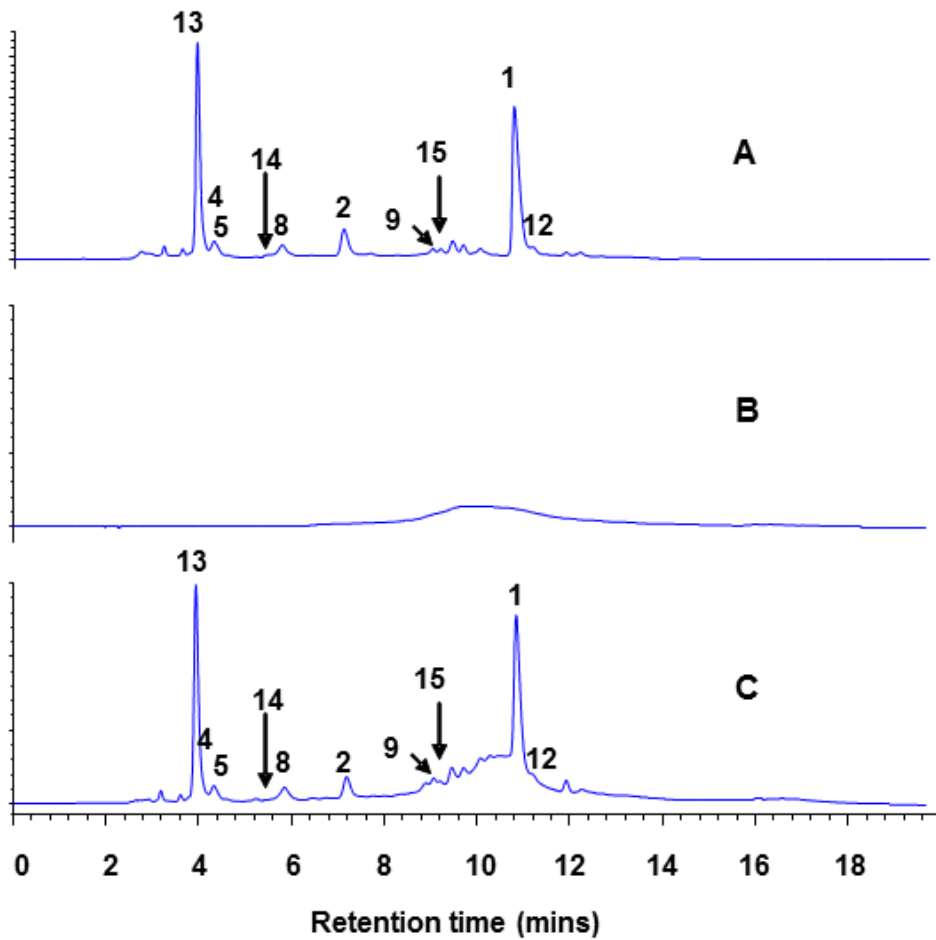


Figure 3-10 HPLC chromatograms of A) methanolic rosemary extract, B) fish oil and C) rosemary extract in fish oil

Table 3-3 MS and UV spectral data for rosemary compounds

No.	Compound name	t _R /min	[M-H] ⁻ m/z	Major fragments (intensity) m/z	λ _{max} /nm (ε)
1	carosic acid	13.75	331	287(100%), 244(2%)	284 (1655)
2	carosol	8.98	329	285(100%)	284 (2445)
3	Rosmarinic acid	5.50	359	315(15%), 223(12%), 197(27%), 179(19%), 161(100%)	330 (17021)
4	rosmanol	5.36	345	301(4%), 283(100%)	288 (2041)
5	epirosmanol	5.84	345	301(5%), 283(100%)	289
6	epirosmanol ethyl ether	4.70	373	329(40%), 283(100%)	289
7	11-ethoxy- rosmanol semiquinone	9.91	373	N/A	261, 296, 322, 335
8	rosmadial	7.34	343	315(34%), 299(100%)	286
9	carosic acid quinone	11.15	329	285(100%)	428
10	5,6,7,10-tetrahydro-7- hydroxy-rosmariquinone	12.01	301	283(42%), 273(15%), 258(100%)	279, 409
11	N/A	15.46	N/A	N/A	260
12	methyl carosate	13.97	345	301(100%), 286(6%)	289
13	cirsimaritin	4.92	313	298(100%), 283(5%)	333
14	acacetin	7.13	283	268(50%)	267, 334
15	chlorogenic acid	11.56	353	317(100%), 309(2%)	N/A

3.4.4 Kinetic data

The scheme for the degradation pathway of carnosic acid, shared with carnosol its major degradation product and described in the paper (Figure 3-8), can be represented by the diagram in Fig. 3-11. There the corresponding compounds and rate constants are assigned. The degradation products are all numbered and their correspondence with the compounds determined in the paper are provided in the caption. The pseudo first order rate constants have the format $R_{\text{from,to}}$, where the subscripts designate the (reactant, product) pair. These rate constants can be evaluated from loss of reactant or from an increase in product. Therefore, to be explicit the reactant or product monitored is designated as well; specifically, the rate constants are designated as $R_{\text{from,to}}(\text{compound monitored})$.

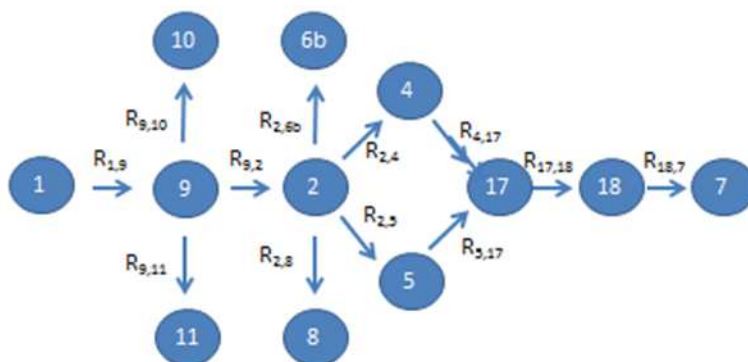


Figure 3-11 Rate constant diagram of Figure 3-8

1 carnosic acid, **2** carnosol, **4** rosmanol, **5** epirosmanol, **6b** epirosmanol ethyl ether, **7** 11-ethoxy rosmanol semiquinone, **8** rosmadial, **9** carnosic acid quinone, **10** 5,6,7, 10-tetrahydro-7-hydroxy-rosmariquinone, **11** unidentified, **17** rosmanol o-quinone, **18** dehydrorosmanol semiquinone

The dataset of greatest interest and concern is that which corresponds to conditions where degradation occurs most rapidly. This dataset is also the most complete, following degradation occurring at highest temperature, 40 °C, and with exposure to ambient light. The degradation rate constants were determined from the initial degradation of solutions of the pure standards, from pure carnosic acid in ethanol and from pure carnosol in ethanol. No more than 0.1% water was found in these solutions.

3.4.4.1 Analysis and discussion

The first step in understanding the complicated interdependence of stability of carnosic acid and carnosol in mixtures was to determine their behavior in more simple systems. The degradation of carnosol has at least four paths as indicated in Fig. 3-11. It is noted from Table 1 that at 40 °C and exposed to ambient light carnosol's degradation is characterized by the following approximate equality:

$$R_{(2,all)}(2) \sim R_{2,6b}(6b) + R_{2,4}(4) + R_{2,5}(5) \quad (3-7)$$

Note that while $R_{2,8}(8)$ was not tabulated because of its unquantifiably low value, this observation of its insignificance is supported by the near equality in Eq. 7, relegating rosmadial's contribution to degradation to relative insignificance, of importance considerably less than the alternate parallel paths. Another consequence of Eq. 7, is that $R_{(2,all)}(2)$ provides a useful characterization of the overall degradation of carnosol, one that can be compared with the degradation of carnosic acid, $R_{1,9}(1)$. In the ethanolic solutions of these pure standards, carnosic acid is observed to degrade much more slowly than carnosol and would appear not to be capable of sustaining the level of carnosic acid in a mixture of these ingredients. And in particular, it would not be expected that carnosic acid would deplete the solution of oxygen and by this mechanism serve to protect carnosol.

Table 3-4 Summary of rate constants for the degradation of carnosic acid and carnosol, and for the formation of their degradation products

Compound	Rate Constant	Regression line	r ²	Light/ dark	Value
Carnosic Acid	R _{1,all} (1)	y = -0.0539x + 6.7689	0.963	Light	0.05
Carnosic Acid	R _{1,all} (1)	y = -0.1265x + 6.7515	0.999	Dark	0.13
Carnosol	R _{2,all} (2)	y = -0.4146x + 6.6758	0.9887	Light	1.25
Carnosol	R _{2,all} (2)	y = -1.2536x + 6.8166	0.9881	Dark	0.41
Epirosmanol ethyl ether	R _{2,6b} (6b)	y = -0.7943x + 6.6398	0.956	Light	0.79
Rosmanol	R _{2,4} (4)	y = -0.2932x + 6.6752	0.9272	Light	0.29
Epirosmanol	R _{2,5} (5)	y = -0.0824x + 6.7068	0.9002	Light	0.08

Nonetheless, this expected rapid elimination of carnosol was not sufficient to justify the simplification of the kinetic scheme to that presented in Figure 3-12A since the experimental profile of carnosol, only a sum of two exponentials with an initial concentration of zero, cannot be adapted to provide the appropriate convexity of the experimental curve, illustrated in Figure 3-12A. That is, the kinetic analysis requires the intermediate discovered experimentally, in this case (at least) the carnosic acid quinone. Indistinguishably good fits of the model to the data, as shown above, can be obtained with either ($R_{1,9} = 0.04 \text{ day}^{-1}$, $R_{9,2} = 0.7 \text{ day}^{-1}$, $R_{2,all} = 0 \text{ day}^{-1}$) or ($R_{1,9} = 0.04 \text{ day}^{-1}$, $R_{9,2} = 0.37 \text{ day}^{-1}$, $R_{2,all} = 0.005 \text{ day}^{-1}$). The latter is the scheme represented in Figure 3-12B.

Before elaborating further on the complicated stability of carnosol, it is useful to consider and contrast the effect of light on the degradation profiles of both antioxidants. Light results in a three-fold increase in the rate of degradation of carnosol, however a two-fold decrease in the rate of degradation of carnosic acid. One realistic explanation of the latter effect is that oxygen and light generate an intermediate degradation product of

carnosic acid that stabilizes the carnosic acid quinone and slows its degradation to carnosol.

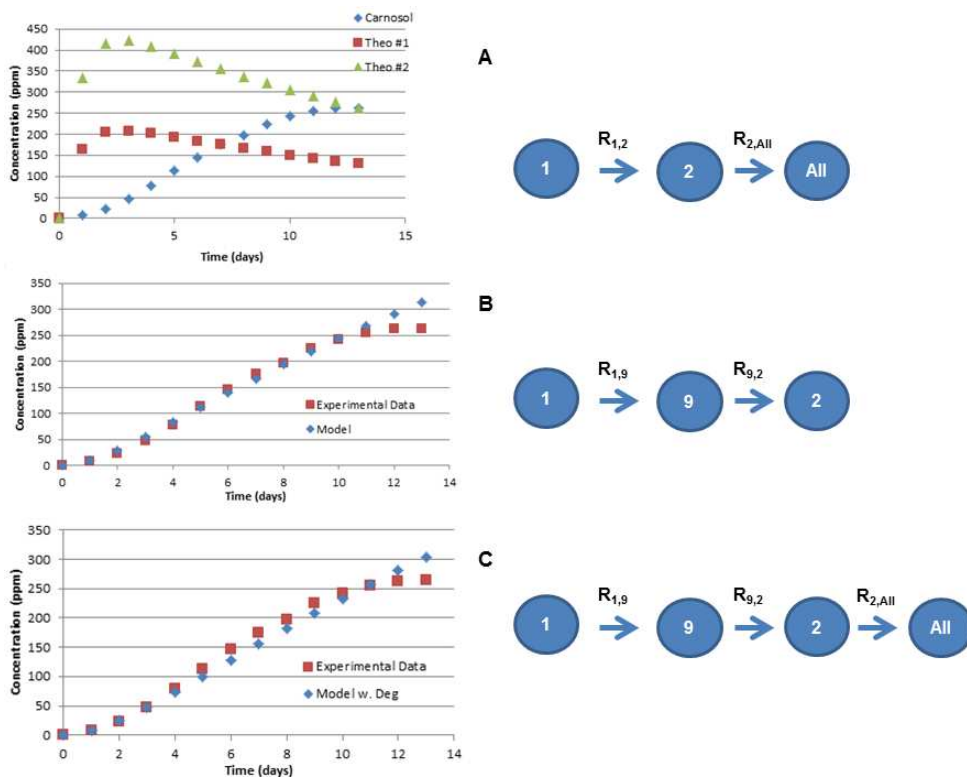


Figure 3-12 Carnosol kinetics for different simplifications of Figure 3-11.

The rationale for the effect of such a stabilizing intermediate is supported by the observation that carnosic acid not only by degrading to carnosol replenishes it, but appreciably retards carnosol's degradation. This is shown by the improved fitting of the model to the experimental curve in Figure 3-12B, and by the significantly reduced $R_{9,2}(2)$ in the mixture from that deduced from $R_{2,all}(2)$ observed for pure carnosol, 1.25 day^{-1} , a result deduced from the kinetic analysis and improved fit to the data. Note, also, that the curve assumes the corresponding convexity of the experimental profile. The result

inferred from this analysis is that $R_{2,\text{all}}(2)$ for the mixture will be no larger than 0.7 day^{-1} . The origin of this stabilizing effect and the associated stabilizing intermediate or alternatively a more reactive compound serving as an oxygen sink, are topics of ongoing research.

A somewhat non-intuitive observation from the model is that as $R_{2,\text{all}}(2)$ is allowed to increase, the consequence is that $R_{9,2}(2)$ actually must decrease in order to achieve a comparably good fit. The explanation of this anomaly is that the rate of increase of carnosol is driven by the increased concentration of the carnosic acid quinone more than the rate constant $R_{9,2}(2)$. The increased rate of production of carnosol then compensates for the increased loss engendered by the increase in $R_{9,2}(2)$.

Scrutiny of Figure 3-12B exposes the single remaining deficiency of the fit to the experimental data, the poor fit at the end of the study, from 10-13 days. While it is possible to select parameters that “improve” the fit ($R_{1,9} = 0.04 \text{ day}^{-1}$, $R_{9,2} = 0.5 \text{ day}^{-1}$, $R_{2,\text{all}} = 0 \text{ day}^{-1}$), as illustrated in Figure 3-12C and as determined by a least squares criterion for the entire dataset, it does not eliminate the absence of a good fit at the end of the run, it simply obscures the deficiency. It seems more likely that the good fits to the first 70% of the dataset, as shown in Figure 3-12B, accurately reflect the chemical kinetics of this mixture and the fidelity of the model to the chemistry. The inability of the model as it stands to produce the reduced rate of degradation at the end of the study indicates a new mechanism is becoming significant at about day 10. Perhaps the most likely explanation is the simple depletion of oxygen is slowing these pseudo first order reactions. With the total level of antioxidants increased in the mixture, this effect is more likely to occur for the mixture than for the individual primary antioxidants alone. Also, the effect of the collective reverse reactions each with small rate constants may ultimately be manifested.

3.5 Conclusion

Carnosic acid degraded in a cascade pathway in ethanol solution via an intermediate, carnosic acid quinone. 5,6,7,10-Tetrahydro-7-hydroxy-rosmariquinone was for the first time proposed as a degradation product of carnosic acid. A light induced degradation product compound was also reported. The degradation rates of carnosic acid and carnosol increased with temperature, while light exposure promoted the formation of unique degradation products. When carnosic acid and carnosol were present in the same ethanolic solution, carnosic acid exhibited a protection capability for carnosol. When rosemary extract was added to fish oil, the degradation of carnosic acid was greatly reduced.

Chapter 4

On the biosynthesis and optical activity of the flinderoles

4.1 Abstract

A proposed biosynthesis of the flinderoles described herein would produce racemic compounds through non-enzymatic dimerization of borrerine. However, an initial report of optical activity for natural flinderoles is inconsistent with that hypothesis as well as the racemic production of similar natural products. Herein, pure enantiomers of flinderole B were obtained and the specific rotations thereof were found to be significantly different from those in the original report, which were taken at low concentrations. These new data remove the inconsistency arising from the original data.

4.2 Introduction

Nature is adept at generating many complex structures from a few simple precursors.^{158,159} For example, a 2-isoprenylated indole building block (see 9, Figure 4-1) may be hypothesized for the biosynthesis of flinderoles A–C (1–3),¹⁶⁰⁻¹⁶² borreverine (4),¹⁶³ isoborreverine (6),¹⁶⁴ dimethylisoborreverine (7),¹⁶⁵ auricularine (5),¹⁶⁶ spermacoceine (10),¹⁶⁷ and their derivatives.^{165,168} Similarly, yuehchukene (12)¹⁶⁹ could be derived from a 3-isoprenylated indole as also proposed by the Dethe group.¹⁷⁰ Work in the 1970's not only defined the structure for the borreverines (4–7), but also validated a biosynthetic hypothesis wherein borrerine (8),¹⁷¹ a naturally occurring cyclized congener of 2-isoprenyl indole (9), served as a direct precursor to the more complex natural products. An enzyme-free dimerization was proposed for these natural products' in vivo synthesis (Figure 4-2), since acid was the only required reagent for their formation from borrerine and the compounds isolated from natural sources were not optically active.¹⁶⁴ Naturally occurring yuehchukene (12) is also isolated as a racemic mixture.¹⁶⁹ Biomimetic

synthetic studies for yuehchukene showed that it could be directly derived from 3-isoprenylindole (13) abiotically using acid-promoted dimerization.¹⁷²⁻¹⁷⁷

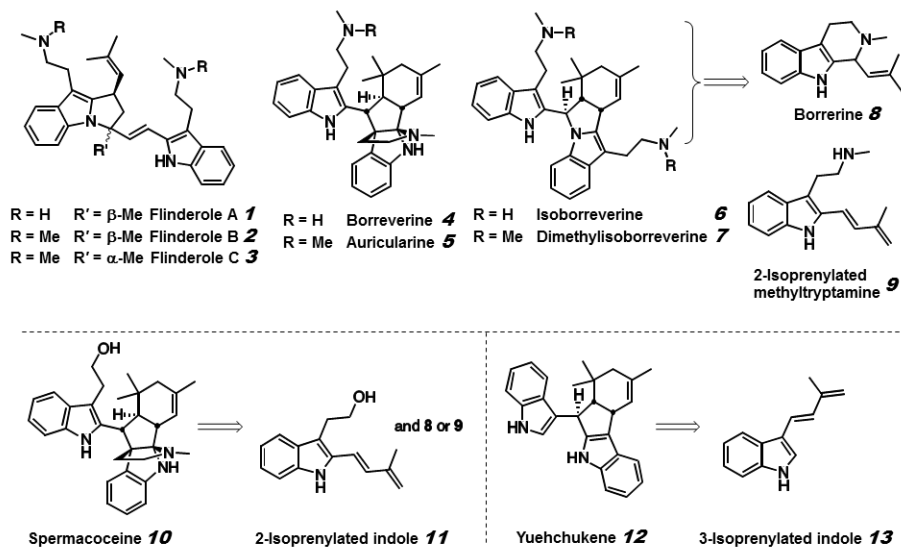


Figure 4-1 Isoprenylated indole natural products.

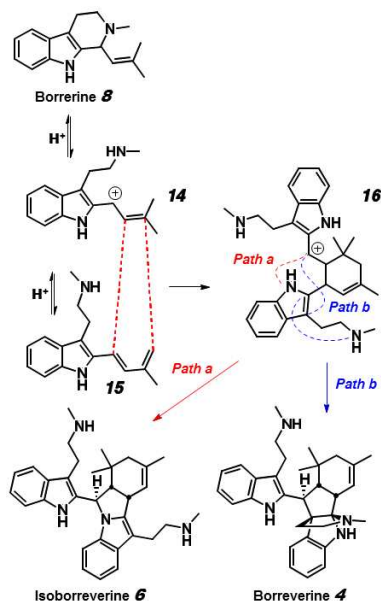


Figure 4-2 Biosynthesis of the borreverines.

Recently, constitutional isomers of the borreverines, the flinderoles (1–3), were structurally characterized.¹⁶¹ Interesting antimalarial activity was reported for these compounds and for isoborreverine (6) and dimethylisoborreverine (7).¹⁶² We have hypothesized a biosynthesis for the flinderoles stemming from borrerine (Figure 4-3).^{170,178,179} The pyrrolidine core of the flinderoles could be formed from intermediates 14 and 15, which are also found in the borreverine biosynthesis, via the stabilized cation 17. Experimental evidence from the use of borrerine as the starting material demonstrated that the flinderoles can indeed be formed as proposed.^{178,179} Furthermore, it was demonstrated that the dimethyl amine natural products can arise from initial methylation of borrerine, followed by acid-promoted dimerization. Additional total synthesis efforts of the flinderoles have also been reported.^{180,181}

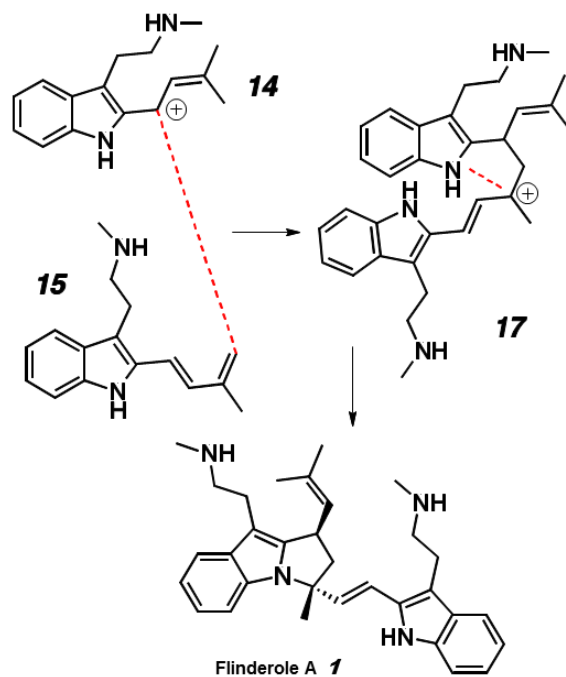


Figure 4-3 Biosynthesis of the flinderoles.

4.3 Experimental

4.3.1 Synthesis of flinderole B

The synthesis was carried by the May group using previously reported methodology.¹⁷⁸

4.3.2 Preparative HPLC

Preparative HPLC was performed on a Jasco 2000 series HPLC using a Chirobiotic V (Astec; 250mm x 21mm x 5 μ m) column. The pump (PU-2086) was set at 20mL/min with the mobile phase consisting of methanol with 0.5/0.5 v/v % acetic acid and triethylamine. Detection was monitored at 280nm with a high pressure UV/vis VWD (UV-2075). The enantiomeric fractions were collected using the Jasco SCF-Vch-Bp 6-valve change unit in the manual mode. Sample injection was performed using an autosampler (AS-2059-SFC) with a 1mL injection loop in the partial fill loop mode (injection volume=500 μ L). The resultant fractions were rotary evaporated and dried in a vacuum oven (40 °C over P₂O₅) over the weekend to afford the acetate salts.

4.3.3 Analytical HPLC

Analytical HPLC separations were performed on an Agilent 1200 series HPLC (Agilent Technologies, Palo Alto, CA, USA) equipped with a diode array detector and a temperature controlled column chamber, auto sampler and quaternary pump. All separations were carried out on a Chirobiotic V (Astec; 250mm x 4.6mm x 5 μ m) at room temperature (~22 °C) unless stated otherwise. For all HPLC experiments, the injection volume was 5 μ L and flow rate was 1.0 mL/min in isocratic mode. The following UV wavelengths were monitored for detection: 230, 254 and 280nm.

4.3.4 Mass spectrometry

Mass spectra (ESI) were acquired on a Thermo Finnigan LXQ (Thermo Electron Corp., San Jose, CA) operating in the positive mode by direct infusion.

4.3.5 Optical rotation determination

Optical rotations were measured on a Digipol 781 Automatic Polarimeter (Rudolph Instruments, Fairfield, NJ) at 589nm and calibrated with a double quartz control plate rotation standard (Rudolph Instruments). The sample cell was 50mm long and had a volume of 800 μ L. The polarimeter was zeroed with methanol prior to running samples. Each enantiomer was measured 10 times and the average and standard deviation reported in Table 4-1.

4.4 Results and discussion

One aspect of the original characterization data for the flinderoles is inconsistent with this biosynthetic hypothesis: flinderoles A–C were reported to have specific rotations ($[\alpha]_D^{22}$) of -6.5, -7.4, and -7.3, respectively.¹⁶¹ If the flinderoles are in actuality produced through an enzyme-free dimerization in the same manner as the *in vitro* experiments, then no optical activity would be expected. Thus the rotation data appeared to contradict our hypothesis and indicate that the flinderoles arise from different mechanisms than the borreverines and yuehchukene. However, the low absolute values of the rotations, the low concentrations used to obtain them, and the relative insensitivity of polarimetry at such low concentrations made these data seem questionable, especially in light of the accumulated evidence for the proposed biosynthesis. To resolve this discrepancy, a sample of each enantiomer of one of the flinderoles was sought to confirm or correct the optical activity in the original report. To this end, we prepared racemic samples of flinderole A–C that we planned to resolve into their component enantiomers. The conciseness of the May group's three-step biomimetic synthesis^{178,179} allowed the rapid formation of dozens of milligrams of flinderole B so that enough of the pure enantiomers would be available to obtain the optical rotation.

The expertise in chiral separation possessed by the Armstrong group was leveraged to obtain pure enantiomers of the flinderoles from the racemates produced in the biomimetic synthesis. Each was subjected to a variety of normal-phase, polar organic, and reverse-phase separation techniques. After extensive experimentation, a macrocyclic glycopeptide (vancomycin) based stationary phase (Chirobiotic V) was found to be suitable for the separation of enantiomers. Larger amounts (> 14 mg) of the pure enantiomers of flinderole B were secured through the use of a preparative-scale Chirobiotic V column. ¹H NMR spectra were in agreement with that published previously. Mass spectrometric data for each enantiomer were identical: [M+H]⁺ = 509.4, [M+Na]⁺ = 531.4, [M+2H]²⁺ = 255.2.

Table 4-1 Optical rotation data for (-)- and (+)-flinderole B.

Entry	Enantiomer	Concentration (g/100 mL)	α	Std. dev.	$[\alpha]_D^{22}$
1	Natural flinderole B	0.03	N/A	N/A	-7.4
2	1 st eluting	0.03	-0.006	0.008	ND
3	1 st eluting	1.40	-0.342	0.005	-48.9
4	2 nd eluting	0.33	0.079	0.002	48.6

Initially, the optical rotation for synthetic flinderole B was measured at the same concentration as was reported in the original characterization for the compound (see entry 1 and 2 of Table 4-1).¹⁶¹ It was observed, however, that the optical rotation was indistinguishable from the pure solvent and was close to the error of measurement (Table 4-1, entry 2). This observation suggests that the reported rotations likely do not accurately reflect the actual values of naturally isolated samples from *Flindersia*. The use

of higher concentrations of pure enantiomers allowed for the reproducible determination of $[\alpha]_D^{25}$ as -48.8 for the first eluting enantiomer (entry 3, $c = 1.4$ g/100 mL) and +48.6 for the more retained enantiomer (entry 4, $c = 0.325$ g/100 mL). Thus the rotation of enantiopure flinderole B is actually of a much greater magnitude than that originally reported. An example of the chromatographic separation of (-)- and (+)-flinderole B is shown in Figure 4-4.

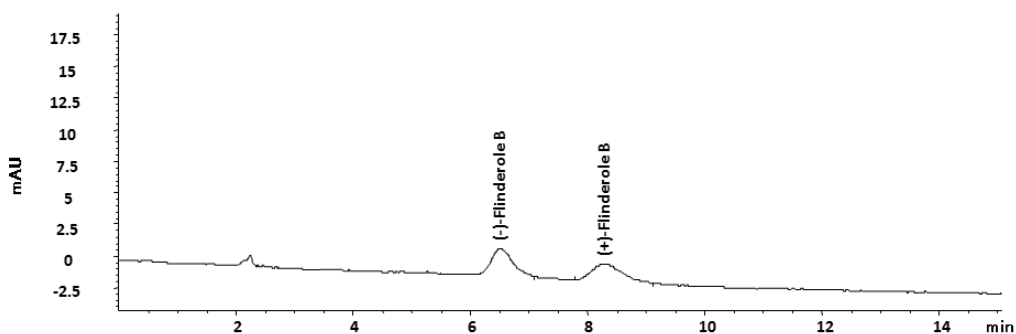


Figure 4-4 HPLC separation of (-)- and (+)-flinderole B on Chirobiotic V

Conditions: mobile phase=methanol (0.5/0.5 v % acetic acid/ triethylamine), detection at 280nm.

4.5 Conclusions

In light of the new data reported here, it appears that the original literature data are not reliable enough to preclude an enzyme-free biosynthesis of the flinderoles. The low concentrations used in the initial experiments lead to ambiguous results as evidenced by our control experiments. Thus, this study resolves a potential inconsistency in the literature related to a likely biosynthetic pathway for the flinderoles. To be clear, the data in Table 4-1 do not prove that the natural compounds are produced as racemates. The possibility remains that the natural samples are enantiopure or enantio-enriched to some degree.¹⁸² However, we predict that naturally occurring samples are likely to show no

optical activity, even at higher concentrations. This prediction is consistent with the lack of optical activity for the borreverines and yuehchukene and with the proposed biosynthesis. This study also demonstrates the power of modern HPLC techniques to resolve questions of enantiopurity. The analytical HPLC assay reported herein will enable rapid confirmation of the above hypothesis using a much smaller sample of compound than would be required for polarimetry. It is our hope that this report will encourage those with access to the source material to use the assay developed herein to determine the enantiomeric composition of the naturally occurring flinderoles.

Chapter 5

Enantioseparation of flinderoles and borreverines by HPLC on Chirobiotic V and V2 stationary phases and by CE using cyclodextrin selectors

5.1 Abstract

Racemic mixtures of the promising anti-malarial bisindole alkaloids, flinderole A – C, desmethyl flinderole C, borreverine and isoborreverine, are baseline separated for the first time by HPLC using vancomycin-based stationary phases and partially separated by capillary electrophoresis (CE) using cyclodextrin selectors. The HPLC results compare the performance of Chirobiotic V and V2 in the polar organic and reversed phase modes and their complementary selectivity is discussed. The performance of the cyclodextrin selectors in CE, while less effective, are discussed in terms of their selectivity in normal and reversed polarity modes.

5.2 Introduction

The treatment for malaria is an ongoing battle which is complicated by multidrug-resistant parasites of *Plasmodium falciparum* (*P. falciparum*). Recently Avery and co-workers screened a library of natural product extracts for anti-malarial activity against chloroquine-sensitive (3D7) and chloroquine-resistant (Dd2) *P. falciparum*.¹⁶⁰ The extract exhibiting the lowest IC₅₀ values for both strains with the lowest selectivity index (Dd2/3D7) corresponded to an extract taken from *Flindersia amboinensis* (*F. amboinensis*). In a subsequent publication, the same group isolated and identified flinderoles A – C (Figure 5-1), in addition to the already known borreverine, isoborreverine and dimethylisoborreverine, as being the key inhibitors.¹⁶¹ Flinderoles have also shown other antiparasitic properties.¹⁶² The identification of the structures of these alkaloids has been met with a series of publications addressing their total synthesis.^{170,178-180,183}

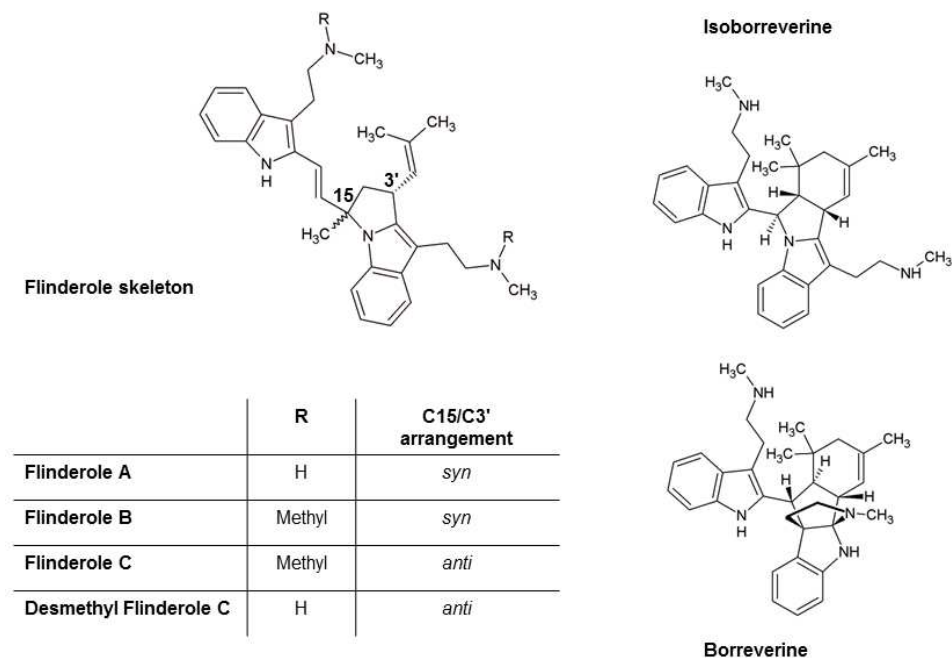


Figure 5-1 Structures of the flinderole and borreverine compounds.

Because of this work, the question arose concerning the enantiomeric purity of these alkaloids. Some alkaloids are known to be naturally racemic.¹⁷⁶ In the 1970s Tillequin, et al. showed that borreverine and isoborreverine, whether natural or synthetic, exhibited no optical activity.¹⁶⁴ They postulated that a non-enzymatic acid dimerization of borreverine was responsible. It has been shown elsewhere by Wang, et al. that the enantiomeric distribution of α -pinene in conifer resins varied widely, with values sometimes close to racemic proportions.¹⁸² Avery and co-workers reported specific rotations for flinderoles A – C of $[\alpha]_D^{25} = -6.5$, $[\alpha]_D^{25} = -7.4$ and $[\alpha]_D^{25} = -7.3$ respectively. Admittedly the concentrations they used, $c = 0.03$ g/100 mL, a consequence of the minute amounts isolated from the tree bark, were very low for optical rotation determination.¹⁶¹

It was clear that an analytical technique was necessary to determine the enantiopurity of these compounds. HPLC was the logical choice since it could also be conducted on a preparative scale. This was desirable in order to isolate the pure enantiomers to determine their optical rotation. In this publication we report, for the first time, the separation of six different flinderole and borreverine racemates, by chiral HPLC using vancomycin-based stationary phases (Chirobiotic V and V2) as well as by capillary electrophoresis (CE) using cyclodextrin selectors.

5.3 Experimental

5.3.1 Materials

Chirobiotic V and V2 columns (25 cm x 4.6 mm x 5 μ m) were purchased from Advanced Separation Technologies Inc. (Astec), now sold by Sigma-Aldrich. Acetic acid (HOAc; > 99%), triethylamine (TEA; > 99.5), ammonium acetate (NH₄OAc; > 98%) and ammonium trifluoroacetate (NH₄TFA; 98%) mobile phase additives were purchased from Sigma-Aldrich (St. Louis, MO). HPLC grade methanol (MeOH) was purchased from VWR (Sugarland, TX). Water was purified by a Milli-Q-water purification system (Millipore, Billerica, MA). Sodium phosphate monobasic (NaH₂PO₄), phosphoric acid (H₃PO₄) and sodium hydroxide (NaOH) were obtained from Fisher Scientific (Pittsburgh, PA, USA). Sulphated- α -cyclodextrin (s- α -CD), hydroxypropyl- β -cyclodextrin (HP- β -CD) and hydroxypropyl- γ -cyclodextrin (HP- γ -CD) were purchased from Sigma-Adrich (Milwaukee, WI, USA) and sulphated β -cyclodextrin (s- β -CD) was purchased from Fluka (Buchs, Switzerland). The untreated fused silica capillaries (50 μ m i.d.) for CE were purchased from Polymicro Technologies (Phoenix, AZ, USA). Flinderole B, C, borreverine and isoborreverine were supplied as purified products while flinderole A and desmethyl flinderole C were supplied as a diastereomeric mixture and designated as

diastereomer 1 and 2 in table 1 and 2. All flinderoles and borreverine compounds were synthesized by the May research group.¹⁷⁹

5.3.2 HPLC

The HPLC used in this publication was an Agilent 1200 HPLC (Agilent Technologies, Palo Alto, CA, USA) consisting of a diode array detector, a temperature controlled column chamber, auto sampler, quaternary pump and fraction collector. Data acquisition and analysis was controlled by ChemStation software (Rev. B.03.02[341], Agilent Technologies 2001-2008) in Microsoft Windows XP Professional OS. The extended performance reporting was used to calculate resolution with the tangent method, i.e. using the baseline width. Unless stated otherwise, all HPLC separations were carried out at room temperature (23 °C) with an injection volume of 5 μ L and a flow rate of 1.0 mL/min (isocratic). The following UV wavelengths were monitored: 230, 254, 280 and 310 nm.

Enantioseparations were evaluated and optimized in the polar organic mode and, when unsuccessful, in the reverse phase mode. The polar organic (PO) mode, sometimes referred to as the polar ionic mode, consisted of methanol with varying mixtures of acetic acid and triethylamine additives. The reverse phase (RP) mode consisted of a binary mixture of methanol (Solvent A) and buffer (Buffer A or B). Solvent A consisted of methanol containing 0.5% TEA and 0.5% HOAc. Buffer A and B consisted of aqueous 20 mM NH_4OAc and NH_4TFA respectively with no pH adjustment. The “hold-up time,” t_0 , was estimated by the solvent peak to be $t_0 = 3.0$ mins. All analytes were dissolved in methanol at ~1 – 2 mg/mL and stored in a freezer when not in use. All mobile phases were degassed by sonication under vacuum.

5.3.3 Preparative HPLC

Preparative HPLC was performed on a Jasco 2000 series HPLC using a Chirobiotic V (Astec; 250mm x 21mm x 5 μ m) column (software: Jasco ChromNav Ver. 1.17.01). The pump (PU-2086) was set at 20mL/min with the mobile phase consisting of methanol with 0.5% acetic acid and 0.5% triethylamine. Detection was monitored at 280nm with a high pressure UV/vis VWD (UV-2075). The enantiomeric fractions were collected using the Jasco SCF-Vch-Bp 6-valve change unit manually. Sample injection was performed using an autosampler (AS-2059-SFC) with a 1mL injection loop in the partial fill loop mode (injection volume=800 μ L).

5.3.4 Capillary electrophoresis (CE)

All CE experiments were carried out using a Beckman Coulter P/ACE MDQ (Fullerton, CA, USA) CE system equipped with an on-column UV-visible detector. Bare fused silica capillary (50 μ m ID x 358 μ m OD, 30 cm in length, 20 cm to the detector) was maintained at 20 °C during analysis. UV detection was accomplished at 214 nm. The capillary was conditioned by rinsing with 1M sodium hydroxide for 5 min, water for 5 min before its first use. Between each sample run, the capillary was flushed with 1 M sodium hydroxide for 2 min, water for 2 min and buffer solution for 2 min. Buffers were prepared by mixing equimolar solutions of H₃PO₄ and NaH₂PO₄ to afford pH = 2, sometimes adjusted to pH = 2.5. HP- β -CD and HP- γ -CD were used as chiral selectors in the 10 mM – 100 mM range while s- α -CD and s- β -CD was used at 0.5% and in the 1 – 5% (w/v) range respectively. Voltages were applied at either 10 kV or 15 kV across the capillary for normal and reverse polarity modes respectively. Samples were dissolved in methanol where unavoidable, but preferably prepared in buffer and injected hydrodynamically at 0.5 psi for 5 sec.

5.4 Results and discussion

The flinderoles (Figure 5-1) are bisindole alkaloids, both bearing aliphatic amine side chains analogous to tryptamine. The aliphatic amine side chains are either secondary amines (flinderole A and desmethyl flinderole C) or tertiary amines (flinderole A and B). Flinderoles have two stereogenic centers, C3' and C15, bearing an isoprenyl and methyl group respectively. The methyl group may either be syn (flinderole A and B) or anti (flinderole C and desmethyl flinderole C) to the isoprenyl group. The flinderole-derived borreverines also consist of two indole groups with aliphatic amine side chains, however in the case of borreverine, one of the indoles is rearranged in the form of an indoline moiety with its aliphatic side chain cyclized into an N-methylpyrrolidine moiety. Thus borreverine has three basic moieties whereas all the other analytes have only two. It also has five stereogenic centres one to two carbon atoms from the pyrrolidine group. Isoborreverine has three stereogenic centres, one adjacent to one of the indole nitrogens, the remaining two being one carbon atom away.

5.4.1 HPLC and preparative HPLC

Several columns from our research group were screened for enantioselectivity including the cyclodextrin line (Cyclobonds), the new cyclofructan line (LarihC) and lastly the macrocyclic glycopeptides (Chirobiotics). Only the vancomycin based stationary phase, Chirobiotic V and V2, from here referred to as V and V2 respectively, showed enantioselectivity. All efforts were thus focused on these two particular stationary phases. Vancomycin, thiostrepton and rifamycin B were introduced as a chiral stationary phases (CSPs) for the first time in 1994 by the Armstrong Research Group.⁴⁹ The commercial V column consists of vancomycin anchored through five linkers to silica gel. After nearly a decade of research into the nature of the linker used, its length and position on the macrocycle, a new vancomycin stationary phase, the V2, emerged.¹⁸⁴ This modified

phase, immobilized on 200 Å silica gel, exhibited a higher loading with greater retention and selectivity for basic compounds in the polar organic mode as well as increased sample capacity. There have been few publications comparing the two vancomycin stationary phases.^{185,186} Another example of this is now presented in this work. Table 5-1 shows the results for the separation of the flinderole and borreverine alkaloids on the V and V2 columns. When using methanol with 0.4% HOAc/ 0.4% TEA the V2 showed significantly greater selectivity and retention for all the analytes when compared to the V column. We thus sought to optimize all our polar organic mode separations using this column. Although the RP mode is statistically the most successful mode for Chirobiotic CSPs, we chose to start with the polar organic mode since we were interested in developing methods that were amenable to preparative HPLC.

The effect of the mobile phase additive ratio and concentration on retention, enantioselectivity and resolution was investigated (Table 5-1) for the V2. As TEA was increased from 0.4% to 0.8%, while keeping HOAc at 0.4%, retention for each analyte decreased. This may be explained by the masking of residual silanols, the degree of ionization of the analyte as well as of the stationary phase.¹⁸⁶ The highly basic nature of the flinderoles and borreverines may reasonably be assumed to have pK_a 's in the range of conventional secondary and tertiary aliphatic amines, i.e. between 10 and 11. The vancomycin molecule has six pK_a values, three phenolic (12.0, 10.40 and 9.59), one secondary amine (8.89), one primary amine (7.75) and one carboxylic acid (2.18).¹⁸⁷ It is not clear how many of these ionizable groups are blocked in the bonding to silica gel.¹⁸⁸ Furthermore, it is not clear how these pK_a values, which have been determined for aqueous systems, will be reflected in pure methanol. The volumetric ratios of HOAc to TEA, 0.4/0.4, 0.4/0.5 and 0.4/0.8, correspond to the following stoichiometric ratios, 2.44:1, 1.95:1 and 1.22:1 respectively. The highly acidic nature of the carboxylic acid

Table 5-1 Chromatographic parameters for the enantioseparation of flinderole and borreverine racemates on V and V2.

HOAc/ TEA (Vol. %)	Retention parameter	Compound					
		Flinderole B	Flinderole C	Borreverine	Isoborreverine	Diastereomer 1	Diastereomer 2
CHIROBIOTIC V							
0.4/0.4	k ₁	5.50	5.60	5.91	4.70	4.70	5.82
	α	1.35	-	1.13	1.08	-	1.44
	R _s	3.5	0.5	1.5	0.7	0.5	4.0
CHIROBIOTIC V2							
0.4/0.4	k ₁	7.71	9.11	9.78	10.06	13.26	25.30
	α	1.82	1.08	1.49	1.28	1.20	1.49
	R _s	6.0	0.7	3.7	2.2	1.4	3.0
0.4/0.5	k ₁	5.85	6.95	7.39	8.22	10.93	20.92
	α	1.80	1.08	1.48	1.28	1.20	1.47
	R _s	5.6	0.7	3.7	2.0	1.5	2.8
0.4/0.8	k ₁	2.44	2.95	3.06	4.71	6.5	12.52
	α	1.71	1.07	1.41	1.29	1.23	1.42
	R _s	4.1	0.4	2.8	1.9	1.7	2.6
1.0/1.0	k ₁	2.92	-	3.45	3.38	4.76	9.36
	α	1.73	-	1.48	1.30	1.25	1.40
	R _s	4.6	-	3.4	2.0	1.7	2.6

moiety on vancomycin and the highly basic nature of the analytes argue for a strong electrostatic interaction provided both remain ionized. With increasing TEA, while keeping HOAc constant, there remains less HOAc to protonate the analyte and thus electrostatic interactions are weakened and retention is lowered. The other modes of interaction that dominate in the polar organic mode and are necessary for chiral recognition are hydrogen bonding and π - π interactions both of which can occur with the indole moiety.

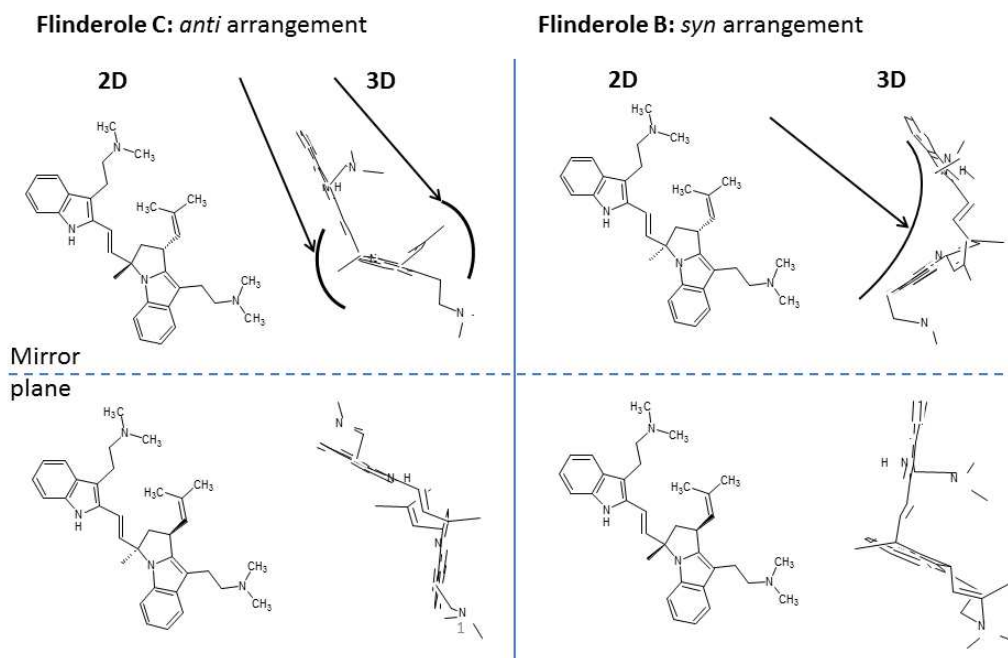


Figure 5-2 Comparison of the 2- and 3-dimensional representations of flinderole B and C.

Enantioselectivity, α , generally decreased (flinderole B, borreverine and diastereomer 2), or remained the same (flinderole C and isoborreverine), as the amount of TEA was increased from 0.4 – 0.8 % (HOAc = 0.4 %). Flinderole B exhibited a much larger enantioselectivity than flinderole C. This is believed to be due to the *syn* configuration of the methyl and isoprenyl groups (Figure 5-1). In the *anti* configuration both faces of the flinderole are blocked for π - π and hydrogen bonding interactions

whereas in the syn configuration one face is more accessible (Figure 5-2). Since diastereomer 1 and 2 are the demethylated analogues of flinderole B and C, we speculated that diastereomer 1, having the smaller enantioselectivity, corresponded to desmethyl flinderole C and vice versa. While desmethyl flinderole C could be baseline separated on the V2, flinderole C could not. A possible explanation for this result lies in the degree of substitution of the amine functional group. Secondary amines are more basic than tertiary amines and can act as hydrogen bond donors, providing an additional mode of interaction, whereas tertiary amines cannot. Since the vancomycin stationary phase is rich in hydrogen bond acceptor sites, it will retain hydrogen bond donors well and provide for different chiral recognition orientations. The remaining interactions governing chiral recognition arise from π - π interactions and steric effects or additional hydrogen bonding from other parts of the alkaloid molecule. Kosel et al. investigated the enantioseparation of citalopram and its desmethyl and didesmethyl metabolites on a V column in the polar organic mode.¹⁸⁹ They saw improved selectivities in the order desmethylcitalopram > didesmethylcitalopram > citalopram. The retention order was didesmethylcitalopram < desmethylcitalopram < citalopram. Clearly, for a given analyte, the change of amine group from primary to secondary to tertiary has a significant impact upon enantioselectivity and retention on vancomycin stationary phases and merits further study.

For enantioseparations to be successful in the polar organic mode there must be at least one ionizable group on or near the chiral centre. The term “near” is somewhat vague since beta blockers have their secondary amine one carbon away from the chiral centre,^{186,190} citalopram has its tertiary amine three carbons away¹⁸⁹ and flinderoles have their amine groups at least four carbons away from the nearest chiral centre and yet all these compounds are baseline separated on vancomycin stationary phases (see Figure

5-3 for structures of these compounds). Diastereomer 1 was abnormal in that its enantioselectivity actually increased from 1.20 – 1.23. Isoborreverine and borreverine are somewhat similar in structure and yet borreverine consistently displayed higher enantioselectivity. Borreverine has indoline and pyrrolidine moieties which are more rigid basic groups and are also in closer proximity to the chiral centres than the aliphatic amine side chain of isoborreverine. It is believed that rigidity affords fewer degrees of freedom and thus a stronger chiral recognition with better enantioselectivity.

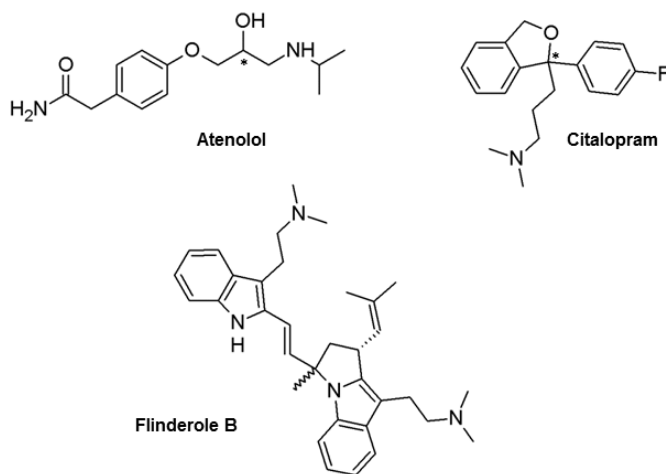


Figure 5-3 Structures of a beta-blocker (atenolol), citalopram and flinderole B

The use of greater volumetric ratios of HOAc with respect to TEA (not shown) only resulted in longer retention times which were undesirable. Having optimized the acid to base ratio for optimal selectivity and resolution, namely 0.4% HOAc/ 0.4% TEA, we then optimized the analysis time by increasing the concentration of this ratio to 1.0 % (see Table 5-1 and Figure 5-4).

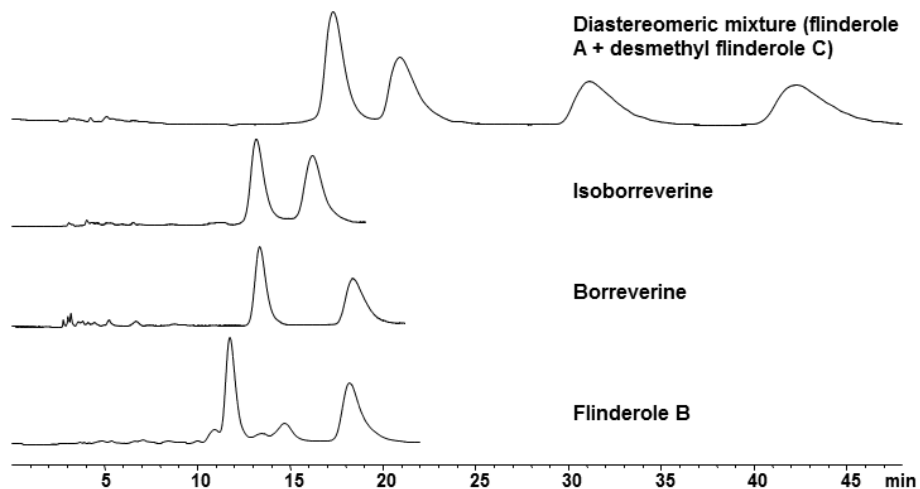


Figure 5-4 Enantioseparations of various flinderole and borreverine racemates on the V2 column in the polar organic mode

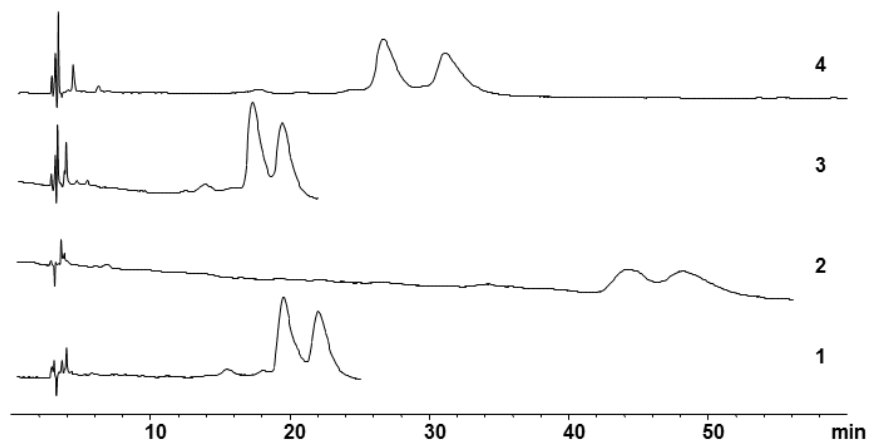


Figure 5-5 Flinderole C racemate on V2 (**2**) and V (**1**, **3** and **4**) columns.

Conditions: **1** and **2**) 60/40 (v/v %) Solution A/Buffer A; **3**) 60/40 (v/v %) Solution A/Buffer B; **4**) 50/50 (v/v %) Solution A/Buffer B

Next we optimized the enantioseparation of flinderole C in the RP mode. In this mode, conversely, the V showed better selectivity and peak shape than the V2 (Figure 5-

5). Under identical mobile phase conditions (60/40 Solution A/ Buffer A) flinderole C is retained twice as long on the V2 than on the V column with less than half the resolution (Table 5-2 and Figure 5-5 chromatograms 1 and 2). The separation was eventually optimized to greater than baseline on the V by using 50/50 Solution A/Buffer B (Figure 5-5 chromatogram 4). The modes of interaction governing chiral recognition in the RP mode are basically the same as in the polar organic mode, i.e. electrostatic, hydrogen bonding and π - π interactions, except that there is a weak inclusion complex that can occur only in the RP mode.^{49,191} The vancomycin macrocycle has three such hydrophobic pockets which are typically less hydrophobic than cyclodextrin cavities.¹⁹² We believe that inclusion complex formation accounts for the improved enantioselectivity of flinderole C on the V since the same result could not be achieved in the polar organic mode. Since the V and V2 have different binding chemistries, it seemed reasonable to suppose that the orientation of the macrocycle and hence the accessibility of the hydrophobic pockets would be different as well.

Finally we evaluated a preparative scale V column to separate flinderole B. Unfortunately due to low quantities of material we could not conduct a thorough loading study. Figure 5-6 shows a chromatogram for a baseline separation of ~12 mg of flinderole B racemate. The order of elution, for the racemate is (-)-flinderole B at 15.3 mins and (+)-flinderole B at 18.9 mins. We recently reported the specific rotations to be -48.8 and +48.6 (sodium D line) degrees respectively.¹⁹³

Table 5-2 Chromatographic parameters for the enantioseparation of flinderole C on V and

V2 columns in the reversed phase mode

Reversed phase mobile phase composition	Retention parameter	Flinderole C
CHIROBIOTIC V2		
	k_1	13.76
60/40 (v/v %) Solvent A/ Buffer A	α	1.10
	R_s	0.6
CHIROBIOTIC V		
	k_1	5.51
60/40 (v/v %) Solvent A/ Buffer A	α	1.15
	R_s	1.4
	k_1	4.78
60/40 (v/v %) Solvent A/ Buffer B	α	1.15
	R_s	1.2
	k_1	7.90
50/50 (v/v %) Solvent A/ Buffer B	α	1.19
	R_s	1.7

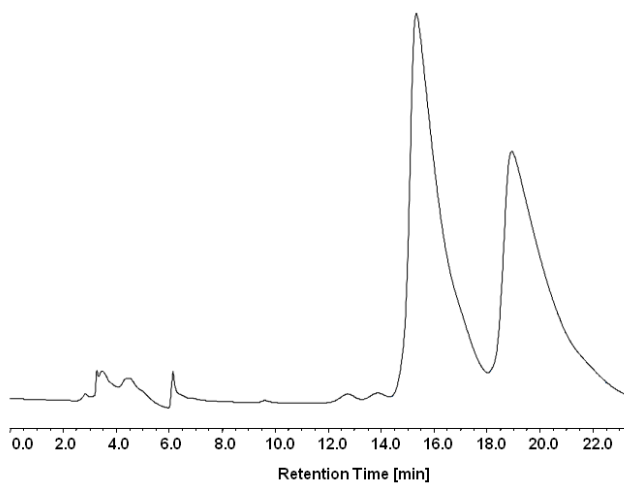


Figure 5-6 Preparative enantioseparation of flinderole B on V column

5.4.2 Capillary electrophoresis (CE) separations

The dominant interaction governing chiral recognition and retention with cyclodextrin (CD) chiral selectors in an aqueous system is inclusion in the hydrophobic cavity.¹⁹⁴ The remaining interactions arise from hydrogen bonding with hydroxyl groups on the rim or the hydroxypropyl groups of the CD and steric interactions. In the case of sulfated CDs, electrostatic interactions also are dominant. Table 5-3 shows a summary of the optimized enantiomeric recognitions for the compounds studied. Enantioselectivity values (α) ranged from 1.01 to as high as 1.27 while efficiency (N) ranged from 6000 (isoborreverine) to 64000 (borreverine).

Table 5-3 Optimized CE enantioseparations of flinderole and borreverine racemates.

Compounds	Chiral selectors	t_{m1}	α	R_s	N
Diastereomeric mixture	HP- β -CD (20 mM) diastereomer	6.2	1.03	1.4	17000
	HP- γ -CD (50 mM) diastereomer	7.0	1.03	1.4	29000
	HP- γ -CD (50 mM) enantiomer	7.0	1.01	0.6	22000
Flinderole B	HP- β -CD (20 mM)	6.5	1.04	1.2	8000
	HP- γ -CD (100 mM)	10.9	1.01	0.4	7000
Flinderole C	HP- β -CD (20 mM)	5.8	1.02	1.4	42000
Isoborreverine	HP- γ -CD (mM)	8.1	1.05	1.9	27300
	Sulfated- α -CD (%)	3.7	1.14	2.1	6000
	HP- β -CD (100 mM)	8.6	1.01	1.3	64000
Borreverine	Sulfated- α -CD (%)	4.8	1.27	4.8	15500
	Sulfated- β -CD (2%)	1.9	1.06	3.8	28000

The enantioseparations of flinderole B, C, the diastereomeric mixture of flinderole A and desmethyl flinderole C, and borreverine were investigated by CE with several CD chiral selectors. Preliminary studies using neutral chiral selectors revealed that at pH 7 the analytes were protonated and migrating ahead of the EOF but lacked sufficient enantioselectivity. At lower pH's, however, enantioselectivity improved. Accordingly we conducted all our separations at pH 2 with a phosphate buffer.

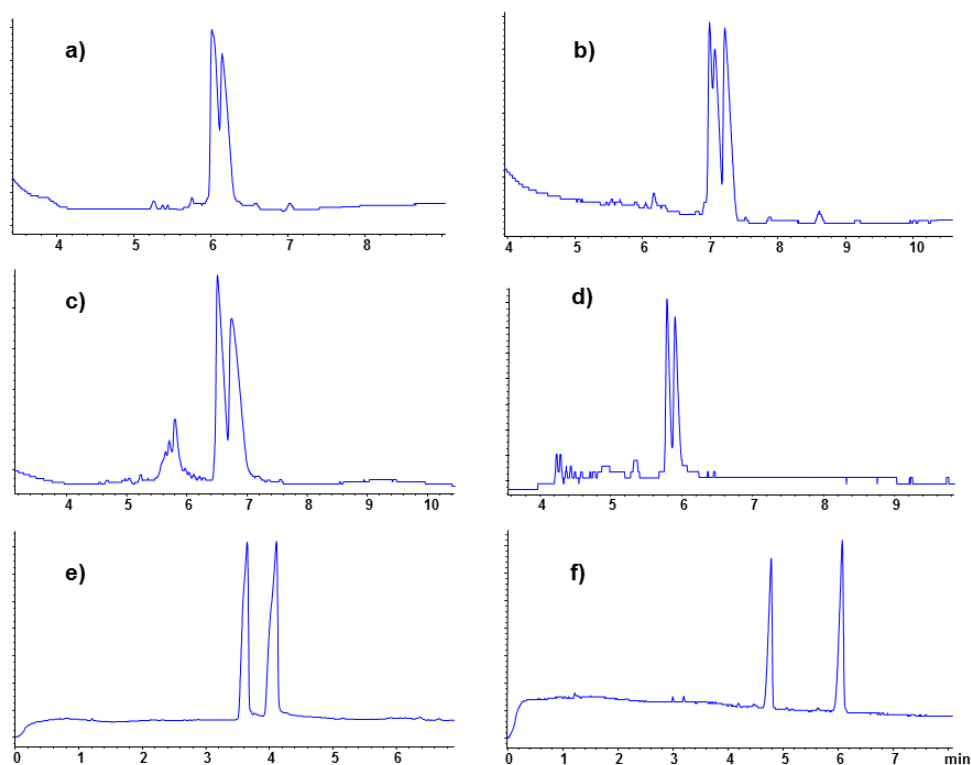


Figure 5-7 Electropherograms of the flinderole and borreverine racemates

The diastereomeric mixture of flinderole A and desmethyl flinderole C could be partially separated as diastereomers using 20 mM HP- β -CD and near baseline separated using 50 mM HP- γ -CD (Table 5-3 and Figure 5-7 a and b). A poor enantioseparation was

observed for only one of the diastereomers when using 50 mM HP- γ -CD ($R_s < 0.6$) while the other diastereomer showed no separation. These could not be improved with any of the other chiral selectors. We speculated that the diastereomer that showed enantioselectivity was flinderole A because the methylated analogue, flinderole B, also showed some selectivity under higher HP- γ -CD concentration (see Table 5-3), but flinderole C did not. Clearly a steric factor is involved since the flinderoles with the syn configuration show some selectivity, but the anti configuration does not.

Whereas HP- β -CD was unsuccessful in separating the enantiomers for the diastereomeric mixture, it was successful in partially separating the methylated analogues, flinderole B and C, with resolutions of 1.2 and 1.4 respectively (Table 5-3, Figure 5-7 c and d). Further increases in HP- β -CD concentration, however, only reduced resolution and efficiency (not shown). Here the ability for the flinderole to act as a hydrogen bond acceptor rather than donor seemed more important for chiral recognition and discrimination.

Borreverine also separated with HP- β -CD, but at higher concentrations. The resolutions ranged from 0.5 at 50 mM to 1.3 at 100 mM HP- β -CD (Table 5-3). No separation was observed when using HP- γ -CD selector. Sulfated α -CD, followed by sulfated β -CD, was by far the best chiral selector for borreverine giving baseline separation easily (Table 5-3 and Figure 5-7 f). Isoborreverine, however, was baseline separated only with sulfated α -CD and HP- γ -CD (Table 5-3 and Figure 5-7 e). Since sulfated β -CD was effective only for borreverine, it would appear that electrostatic interaction with the pyrrolidine or indoline moieties was more important than inclusion.

5.5 Conclusions

Racemic mixtures of a relatively new class of alkaloids, the flinderoles, and their more familiar constitutional isomers, the borreverines, were baseline separated for the

first time by HPLC. Five of the six alkaloids (flinderole A, B, desmethyl flinderole C, borreverine and isoborreverine) were baseline separated on the V2 column in the polar organic mode. The remaining alkaloid (flinderole C) was separated on the V column in the RP mode. The V and V2 columns were thus complementary in different chromatographic modes. Additionally we demonstrated the ability to conduct preparative scale separations of flinderole B on a V column.

In CE in the normal polarity mode, HP- β -CD was generally the most successful selector, followed by HP- γ -CD. Sulphated α -CD, in the reverse polarity mode, showed remarkable selectivity for both borreverine and isoborreverine.

Chapter 6

Enantiomeric separations of chiral sulfonic and phosphoric acids with barium-doped cyclofructan selectors via an ion interaction mechanism

6.1 Abstract

New cyclofructan 6-based chiral stationary phases (CSPs) bind barium cations. As a result the barium complexed CSPs exhibit enantioselectivity towards 16 chiral phosphoric and sulfonic acids in the polar organic mode (e.g. methanol or ethanol mobile phase containing a barium salt additive). Retention is predominantly governed by a strong ionic interaction between the analyte and the complexed barium cation as well as hydrogen bonding with the cyclofructan macrocycle. The $\log k$ vs. $\log [X]$, where $[X]$ = the concentration of the barium counter anion, plots for Larihc-CF6-P™ were linear with negative slopes demonstrating typical anion exchange behavior. The nature of the barium counter anion also was investigated (acetate, methanesulfonate, trifluoroacetate and perchlorate) and the apparent elution strength was found to be acetate > methanesulfonate > trifluoroacetate > perchlorate. A theory based upon a double layer model was proposed wherein kosmotropic anions are selectively adsorbed to the cyclofructan macrocycle and attenuate the effect of the barium cation. van't Hoff studies for two analytes were conducted on the LARIHC-CF6-P™ for three of the barium salts (acetate, trifluoroacetate and perchlorate) and the thermodynamic parameters governing retention and enantioselectivity are discussed. Interestingly, for the entropically driven separations, enantiomeric selectivity can increase at higher temperatures, even with decreasing retention.

6.2 Introduction

The separation of chiral phosphoric and sulfonic acids enantiomers is of great importance to synthetic and analytical chemists. The independent work of Akiyama¹⁹⁵

and Terada¹⁹⁶ in developing BINOL-phosphates to catalyze enantioselective C-C bond formation reactions in 2004 set the stage for asymmetric catalysis in a significant way.¹⁹⁷ Since then, great strides have been made in developing asymmetric catalysis for many reactions including, organocatalytic aryl-aryl bond formation,¹⁹⁸ spiroketalizations,¹⁹⁹ Mannich reactions,²⁰⁰ hydrocyanation of hydrazones,²⁰¹ reductive amination²⁰² and in crotylation reactions.^{203,204} Chiral sulfonic acids on the other hand, while also being strong Brønsted acids, have not enjoyed the same success in asymmetric synthesis but have rather been the focus of chiral resolving agents in the separation of basic compounds. Recently, Kellogg et al. broadened the concept of diastereomeric recrystallization from using a single chiral selector for purifying basic racemates to simultaneously using a family of enantiomers.²⁰⁵ This technique has been dubbed “Dutch resolution” and preferably requires three enantiomerically pure sulfonic acids from the same family (e.g., R-camphorsulfonic acid and R-bromocamphorsulfonic acid) to recrystallize basic compounds.²⁰⁵⁻²⁰⁷ Thus the synthesis and separation of sulfonic acid enantiomers is important to this field.

Cyclofructan 6 (CF6) is a cyclic oligosaccharide produced by the enzymatic digestion of inulin. It consists of an 18-crown-6 core, spiro-annulated with D-fructofuranose pendant groups. Since the discovery of cyclofructans in 1989 by Kawamura et al.,²⁰⁸ the interest in these macrocycles slowly increased. Research was primarily focused on assessing the ionophoric ability of CF6²⁰⁹⁻²¹² and nothing was conducted from a chromatographic perspective. In contrast to related cyclic oligosaccharides, the cyclodextrins, and even to synthetic crown ethers, cyclofructans have yet to reach the cusp of their research potential. In 2009, we published the first major chiral separations work with cyclofructans.⁵⁵ Subsequently this work has been further developed and greatly expanded.²¹³⁻²²¹ It was clear that native CF6 bonded to

silica gel was usually a poor chiral selector. However, upon derivitization with an isopropyl carbamate group, it exhibited pronounced and broad selectivity for primary amines in organic and supercritical fluid mobile phases.⁵⁵ However this selectivity did not extend to anionic or acidic compounds. It is known that the ionophoric proclivity of CF6 is particularly pronounced for barium and lead cations.²²² Thus the question arises as to whether this cation-affinity might be exploited somehow to induce a different kind of enantioselectivity. This question is interesting from both a mechanistic point of view and from the practical standpoint that these CSPs have excellent preparative capabilities. Herein we describe the first highly effective metal ion interaction approach for chiral separations since the classic ligand exchange work of Davankov.^{27,223} However, the nature of the metal ion, the mechanism and the selectivity in this work are shown to be unique. More specifically this transforms a neutral chiral selector into one with a great affinity for anionic (sulfonic and phosphoric acid) chiral compounds. It should be noted that the analytes in this work are retained either by: 1) ion-pairing with the barium cations in the mobile phase where the subsequent ion pair can partition to the stationary phase or 2) by dynamic anion exchange (i.e., where the cations, Ba²⁺ in this case, are so strongly bound that they can be considered an integral part of the stationary phase) or 3) a combination of both ion-pairing and dynamic anion exchange. Historically the terms ion interaction chromatography has been coined to encompass but not distinguish between all of the aforementioned possibilities particularly in reversed phase chromatography.²²⁴

In previous work Lindner et al. have shown using methanol mobile phases with acid/base additives that excellent separations of α , β and γ -aminophosphonic acids and chiral sulfonic acids (CSAs) can be attained on cinchona alkoid chiral stationary phases (CSPs).^{225,226} Thus far we know of no other enantioselective anion-exchange type CSPs commercially available which makes this an important area of research.

6.3 Experimental section

Barium acetate ($\text{Ba}(\text{OAc})_2$), barium hydroxide monohydrate, barium perchlorate ($\text{Ba}(\text{ClO}_4)_2$) (NOTE: all barium salts, with the exception of barium sulfate, are toxic and need to be handled with care), ammonium acetate (NH_4OAc), ammonium trifluoroacetate (NH_4TFA), triethylamine (TEA), trifluoroacetic acid (TFA), acetic acid (HOAc), methanesulfonic acid (MSA), ethylene diamine, (S)- and (R)-(-)-VAPOL hydrogenphosphate (CPA-1), (S)- and (R)-(-)-1,1'-binaphthyl-2,2'-diyl hydrogenphosphate (CPA-2), (S) and (R)-(-)-3,3'-Bis(triphenylsilyl)-1,1'-binaphthyl-2,2'-diyl hydrogenphosphate (CPA-3), (S)- and (R)-3,3'-bis[3,5-bis(trifluoromethyl)phenyl]-1,1'-binaphthyl-2,2'-diyl hydrogenphosphate (CPA-4), (S)- and (R)-(+)-2-hydroxy-4-(2-methoxyphenyl)-5,5-dimethyl-1,3,2-dioxaphosphorinane 2-oxide (CPA-5), (S)- and (R)-(+)-4-(2-chlorophenyl)-2-hydroxy-5,5-dimethyl-1,3,2-dioxaphosphorinane 2-oxide (CPA-6), camphor sulfonic acid (CSA-6), trans-chalcone, 4-chlorochalcone and 4-nitrochalcone were purchased from Sigma-Aldrich (Milwaukee, WI, USA). Compounds CSA-7 – CSA-9 were synthesized from the corresponding chalcones according to literature procedures.^{205,226}

The chiral sulfonic and phosphoric acids (see Figure 6-1) may be further subdivided as 1) chiral aryl sulfonic acids with either one (CSA-1 and CSA-4) or two (CSA-2, CSA-3 and CSA-5) chiral axes, 2) β -ketosulfonic acids (CSA-7 – 9) and 3) γ -ketosulfonic acid (CSA-6). The CPAs may also be further classified as 1) biaryl phosphoric acids (CPA-1 – 4), 2) cyclic phosphoric acids (CPA-5 and 6) and acyclic phosphoric acid (CPA-7). Barium trifluoroacetate ($\text{Ba}(\text{TFA})_2$) was prepared by neutralizing barium hydroxide monohydrate with an excess of trifluoroacetic acid and then allowed to evaporate to dryness. The resulting residue was further dried in a vacuum oven overnight and used without further purification. When not in use, the material was stored in a desiccator. Barium methanesulfonate was prepared in an analogous way using methanesulfonic acid and

barium hydroxide. HPLC grade methanol (MeOH), ethanol (EtOH), acetonitrile (ACN) and heptane (Hept) were purchased from VWR (Sugarland, TX). Water was purified by a Milli-Q-water purification system (Millipore, Billerica, MA).

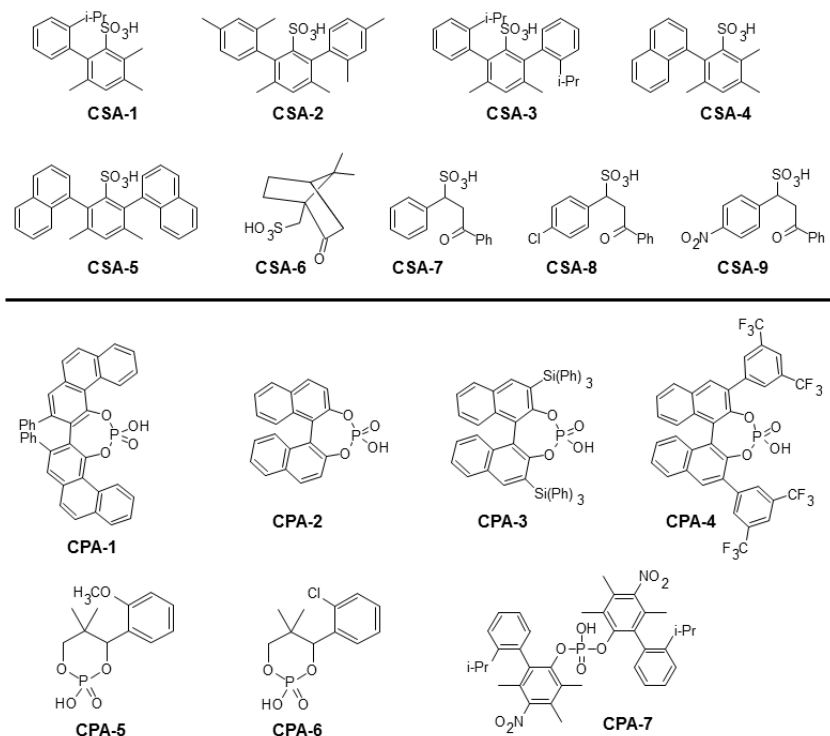


Figure 6-1 Structures of the chiral sulfonic and phosphoric acid analytes.

6.3.1 Synthesis of CSA-1 – 5 and CPA-7

See Figure 6-2.

6.3.1.1 CSA-1 – CSA-5

Sulfonic acids CSA-1 – 5 were synthesized starting from the cheap commercially available 3,5-dimethylphenol or 2,3,5-trimethylphenol, respectively, in a similar manner. Bis-ortho-arylation of 3,5-dimethylphenol or mono-ortho arylation of 2,3,5-trimethylphenol using the corresponding triarylbi-muth chloride reagents could afford the desired

phenols a1 – a5. The resulting highly substituted phenols were treated with NaH, then quenched with dimethylaminothiocabamoyl chloride to furnish the O-aryl thiocarbamates b1 – b5. Newman-Kwart rearrangement of O-aryl thiocarbamates b1 – b5 under microwave irradiation at 220 °C gave the corresponding S-aryl thiocarbamates c1 – c5. The mixtures of racemic and *meso* isomers of can be separated easily by column chromatography (Hexane: DCM = 10:1 to 2:1). The desired sulfonic acid CSA-1 – 5 can be obtained by oxidizing the racemic form of c1 – c5 using either hydrogen peroxide (H₂O₂) or chlorosuccinimide (NCS).

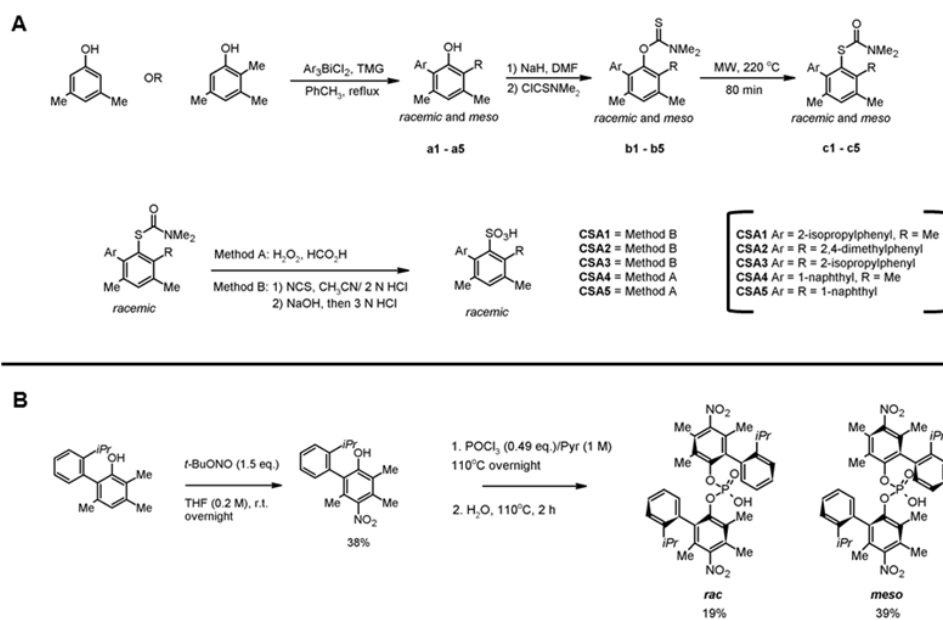


Figure 6-2 Synthetic schemes for: A) CSA-1 - 5 and B) CPA-7

6.3.1.2 CPA-7

A mixture of the nitrophenol (613.7 mg, 2.05 mmol) and phosphorus oxychloride (153.3 mg, 1 mmol) in pyridine (20 mL) was heated at 110 °C for 12 h. After being cooled to 0 °C, the reaction mixture was quenched by adding H₂O (5 mL). The resulting reaction

mixture was heated at 110 °C for another 4 h. The reaction mixture was extracted with DCM for three times and the combined organic phase was washed with brine and dried over Na₂SO₄ anhydrous. The organic solvent was removed and the residue was purified by column chromatography (SiO₂; DCM : MeOH, 50:1 to 20:1) to afford racemic and meso products, respectively [*rac*-9; yield: 128.3 mg (19%) and *meso*-9; yield: 206.9 mg (31%)].

6.3.2 HPLC

The HPLC used was an Agilent 1200 HPLC (Agilent Technologies, Palo Alto, CA, USA) consisting of a diode array detector, a temperature controlled column chamber, auto sampler, quaternary pump and fraction collector. Data acquisition and analysis was controlled by ChemStation software (Rev. B.03.02[341], Agilent Technologies 2001-2008) in Microsoft Windows XP Professional OS. Unless stated otherwise, all HPLC separations were carried out at 25 °C with an injection volume of 5 µL and a flow rate of 1.0 mL/min (isocratic). The following UV wavelengths were monitored: 230, 254, 265, 280 and 287 nm.

Enantiomeric separations were evaluated and optimized on barium doped LARIHC-CF6-P™ (isopropyl carbamate), LARIHC-CF6-RN™ (R-1-(1-naphthyl)ethylcarbamate) and FRULIC-N™ (native cyclofructan) chiral CSPs 250 mm x 4.6 mm x 5 µm (Azyp, LLC, Arlington, TX, USA) in the polar organic. The polar organic mode (sometimes referred to as the polar ionic mode) mobile phase consisted of methanol (or ethanol) containing a barium salt and when necessary, varying mixtures of acidic (HOAc, TFA or MSA) and basic (TEA, ethylene diamine) additives or ammonium salts. The void time, *t*₀, was measured by injecting 1,3,5-tri-*tert*-butylbenzene and monitored at 254 nm. All analytes were dissolved in methanol at ~1 – 2 mg/mL and stored in a freezer when not in use. CSA-6 however was prepared in the 8 – 10 mg/mL

range in water on account of its low UV absorbance and was monitored at 287 nm. All mobile phases were degassed by sonication under vacuum. Columns had to be conditioned by circulating the mobile phase overnight.

6.3.3 Preparative HPLC

Preparative HPLC was performed on a Jasco 2000 series HPLC using a FRULIC-N™ column (Azyz, LLC, Arlington, TX, USA; 250mm x 21mm x 5µm) treated with barium (software: Jasco ChromNav Ver. 1.17.01). The pump (PU-2086) was set at 20mL/min with the mobile phase consisting of methanol with 0.1% TFA and 0.1% TEA. Detection was monitored at 280nm with a high pressure UV/vis VWD (UV-2075) cell. The enantiomeric fractions were manually collected using the Jasco SCF-Vch-Bp 6-valve change unit. Sample injection was performed using an autosampler (AS-2059-SFC) with a 1mL injection loop in the partial fill loop mode (injection volume = 800µL).

6.3.4 van't Hoff plots

The van't Hoff experiments were conducted at 10, 20, 30, 40 and 50 °C in a thermostated column chamber equipped with Peltier cooler. Upon changing the temperature, the column was allowed to equilibrate for at least 30 mins before injecting the samples. The cyclofructan loading and phase ratio, ϕ , where $\phi = V_s/V_m$ (V_s = volume of the selector, V_m = volume of the mobile phase) was required for the determination of entropy from the $\ln k$ vs. $1000/T$ plot and was calculated as published in the literature.^{227,228} The values for the density of the LARIHC-CF6-P™ stationary phase and the unbonded chiral selector were measured by pycnometry (10 mL pycnometer) which was calibrated gravimetrically with DI water.

6.3.5 Barium loading and removal

Analytical columns were pre-conditioned with a 5 mM Ba(OAc)₂ or Ba(TFA)₂ solution containing 20 % methanol by volume for 30 minutes. The preparative FRULIC-

NTM column was pre-conditioned overnight with a 40 mM Ba(OAc)₂ solution containing 20 % methanol by volume. The columns were then either evaluated directly in the polar organic mode or stored in methanol.

The barium loading was estimated by the procedure described by Durmaz et al.²²⁹ Briefly, untreated columns were conditioned with water and then methanol, 10 column volumes each. An HPLC method was developed where the column was washed with methanol at 0.5 mL/min for 5 minutes and then switched to a 5 mM Ba(OAc)₂ solution in methanol at 5.01 minutes at 0.5 mL/min. The method was continued until the breakthrough point (monitored at 204 and 210 nm) was observed. To regenerate the column, barium cations were eluted from the stationary phase using a 100 mM NH₄OAc solution (pH = 4.1) for 30 minutes. Barium elution was monitored until the effluent showed no sign of turbidity upon addition of a few drops of concentrated sodium sulfate solution.

6.4 Results and discussion

While attempting to resolve enantiomers of CSA-5 by fractional recrystallization, simultaneous development of an HPLC method was undertaken to more accurately monitor the enantiomeric excess. Initially, a partial separation ($R_s = 1.2$) was obtained on the LARIHC-CF6-PTM in the reversed phase mode (see Figure 6-2A). This separation could not be optimized further though different acidic and basic additives as well as ammonium salts were explored (not shown). Finally, knowing that cyclofructans bind barium ions strongly, 5 mM Ba(OAc)₂ was added to the mobile phase with the hope that it might induce better enantioselectivity for CSA-5. However the presence of this additive in the reversed phase mode worsened the selectivity and efficiency (see Figure 6-2B). Upon returning to the normal phase, 80/20/0.1 heptane/EtOH/TEA (not shown), CSA-5 retained longer than before with strong peak tailing. Subsequently the polar organic mode

was used and an excellent separation was obtained ($R_s = 2.4$) with superior efficiency and peak shape compared to all other approaches (see Fig. 6-2C). The separation was easily scaled to preparative amounts on the FRULIC-N™ (see. Fig.6-4). When the barium is eluted from the stationary phase there is no retention or enantioselectivity for CSA-5 enantiomers in the polar organic mode. When the column was reconditioned with a barium solution, retention and enantioselectivity were restored.

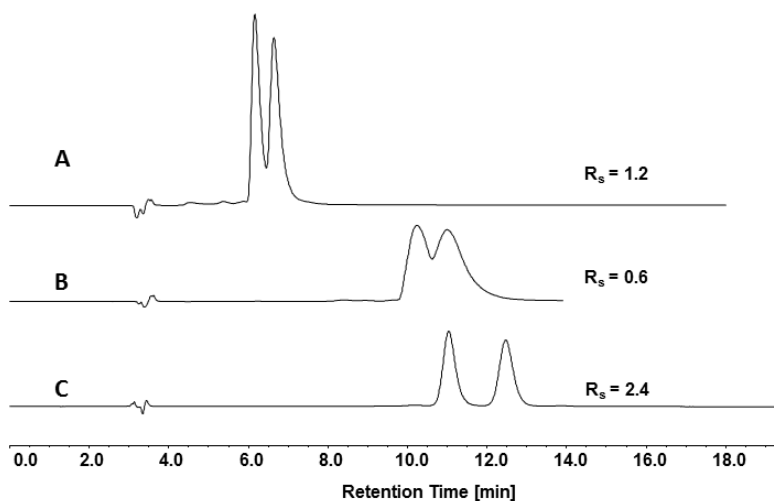


Figure 6-3 Original separation of CSA-5

Mobile phase: A) 80/20/0.1/0.1 (v/v %) water/MeOH/TEA/HOAc; B) 5 mM Ba(OAc)₂ in 80/20 (v/v %) water/MeOH; C) 50/50/0.1/0.1 ACN/MeOH/TEA/TFA; column: LARIHC-CF6-P™, flow rate: 1 mL/min; detector: UV at 254 nm.

Table 6-1 shows the clear effect of barium treatment on the cyclofructan CSPs for all of the analytes in Figure 6-1. The untreated column was evaluated in the polar organic mode using methanol containing 10 mM NH₄OAc. Under these conditions all analytes were eluted as sharp peaks close to the void volume with no enantioselectivity.

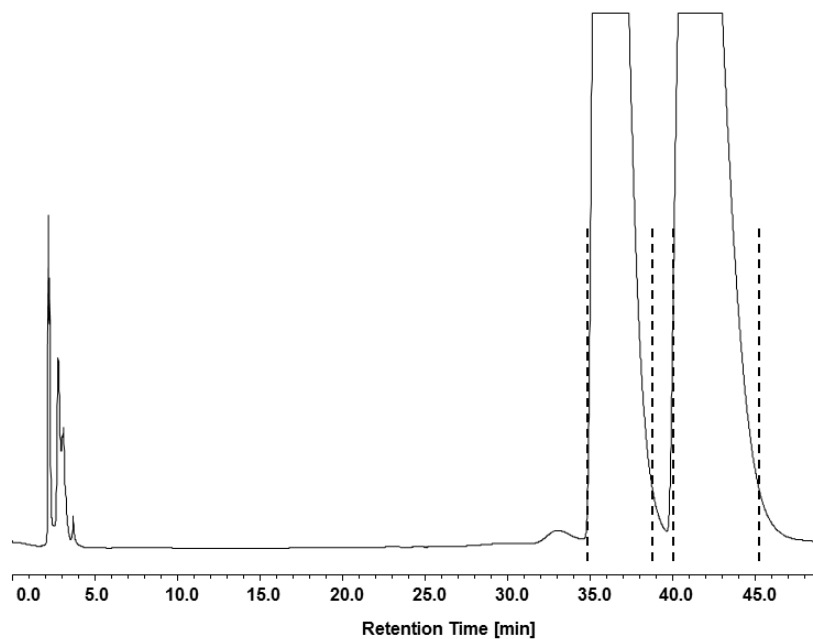


Figure 6-4 Preparative HPLC separation of racemic CSA-5 on Ba²⁺-doped FRULIC-N

If no additive was present in the mobile phase, analytes were still poorly retained but with poor peak efficiency. On a barium pretreated column and in the presence of a barium additive however, there was a significant increase in retention often accompanied by an increase in enantioselectivity. Addition of low levels of barium salt to the mobile phase was necessary to maintain a constant level of barium on the stationary phase and to afford highly reproducible elution volumes and good peak efficiency. The order of retention strength for the three Ba²⁺-doped columns, in this particular mobile phase, was FRULIC-NTM > LARIHC-CF6-RNTM > LARIHC-CF6-PTM. Retention is governed by 1) the loading of cyclofructan which also dictates the amount of barium that can be loaded, 2) the nature of the selector and 3) the nature of the analyte. The cyclofructan loading on the CSPs was determined to be 0.23, 0.12 and 0.18 mmol/g respectively. Thus even though the LARIHC-RNTM stationary phase had somewhat lower overall loading than the

Table 6-1 Effect of barium pretreatment on the retention and enantioselectivity of chiral

sulfonic and phosphoric acids on commercially available cyclofructan columns.

Mobile phase: No barium pretreatment: 10 mM NH₄OAc in MeOH, With barium

pretreatment: 5 mM Ba(OAc)₂ in MeOH, flow rate: 1 mL/min.

		RN	P	N	RN	P	N
		No barium pretreatment			With barium pretreatment		
CSA-1	α	1.00	1.00	1.00	1.00	1.00	1.00
	k ₁	0.12	0.00	0.74	1.93	0.82	8.40
CSA-2	α	1.00	1.00	1.00	1.00	1.00	1.04
	k ₁	0.12	0.00	0.65	2.02	0.84	8.12
CSA-3	α	1.00	1.00	1.00	1.04	1.00	1.00
	k ₁	0.11	0.00	0.58	1.95	0.81	7.91
CSA-4	α	1.00	1.00	1.00	1.01	1.00	1.02
	k ₁	0.17	0.01	0.96	2.27	0.94	10.49
CSA-5	α	1.00	1.00	1.00	1.12	1.12	1.12
	k ₁	0.23	0.01	1.03	2.62	0.98	11.03
CSA-6	α	1.14	1.00	1.00	1.12	1.09	1.07
	k ₁	0.27	0.08	1.27	1.82	0.99	9.67
CSA-7	α	1.00	1.00	1.00	1.00	1.00	1.03
	k ₁	0.21	0.02	1.16	2.94	1.03	12.43
CSA-8	α	1.00	1.00	1.00	1.00	1.00	1.04
	k ₁	0.18	0.02	1.08	2.45	0.96	12.44
CSA-9	α	1.00	1.00	1.00	1.01	1.00	1.04
	k ₁	0.20	0.02	1.19	2.56	0.95	14.03

Table 6-2 – Continued

		RN	P	N	RN	P	N
		No barium pretreatment			With barium pretreatment		
CPA-1	α	1.00	1.00	1.00	1.14	1.09	1.11
	k_1	0.29	0.01	0.99	2.38	0.81	9.77
CPA-2	α	1.00	1.00	1.00	1.00	1.00	1.03
	k_1	0.27	0.07	1.25	3.21	1.29	15.97
CPA-3	α	1.00	1.00	1.00	1.00	1.00	1.04
	k_1	0.26	0.00	0.43	2.16	0.62	4.93
CPA-4	α	1.00	1.00	1.00	1.00	1.00	1.00
	k_1	0.00	0.00	0.22	0.96	0.36	2.65
CPA-5	α	1.00	1.00	1.00	1.05	1.00	1.00
	k_1	0.23	0.09	1.24	4.13	1.83	19.50
CPA-6	α	1.00	1.00	1.00	1.04	1.00	1.00
	k_1	0.22	0.06	1.16	3.69	1.55	17.37
CPA-7	α	1.00	1.00	1.00	1.00	1.00	1.00
	k_1	0.06	0.00	0.37	3.56	0.47	10.02

LARIHC-CF6-PTM, its ability to utilize π - π interactions with aromatic analytes resulted in greater overall retention in many cases.

6.4.1 Effect of the counter anion of the Ba²⁺ salt

The barium-doped stationary phases in this study can be treated as anion-exchange phases. However to prevent slow leaching of the barium from the stationary phase and to maintain its level of saturation a small amount of a barium salt is put into the mobile phase. Since a small amount of barium salt is in the mobile phase the

question arises as to the effect, if any, of its counter anion. It is known that retention in ion-exchange systems is believed to be a combination of selective adsorption, ion-pairing and accumulation in the diffuse layer.²³⁰ As has already been shown (Table 6-1), in the absence of barium cations, analytes elute at the dead volume or are poorly retained on these stationary phases in the polar organic mode. However they are retained on the same stationary phases that have been doped with barium. The effect of three other barium salts (methanesulfonate, perchlorate and trifluoroacetate) on retention and enantioselectivity was explored using the LARIHC-CF6-P™ column (Table 6-2). It is clear that the order of elution strength for the four counter anions is: $\text{OAc}^- > \text{MSA}^- > \text{TFA}^- > \text{ClO}_4^-$. As retention increases, the number of analytes that show selectivity ($R_s > 0.4$) also increases as follows: 11 compounds for ClO_4^- , 8 compounds for TFA-, 4 compounds for MSA- and 3 compounds for OAc^- . However, the observed enantioselectivities are not simply a function of retention. Figure 6-5 shows the separation of CSA-5 and CPA-1 using the four different barium salts at concentrations that afford similar retention. ClO_4^- has a profound effect on the enantioselectivity for these two compounds that is clearly greater than TFA^- , MSA^- and OAc^- .

Moyer et al. used the phrase “Hofmeister effect or bias” in their research on cesium extraction by crown ethers.²³¹ The phrase was used to describe the observation that in liquid-liquid extraction systems, the partitioning of cesium improved when chaotropic counter anions were present. It appears that there are analogous effects or trends in these chromatographic results. The well-known Hofmeister series ranks the counter anions used in this publication as: $\text{OAc}^- > \text{MSA}^- > \text{TFA}^- > \text{ClO}_4^-$ with OAc^- being the most kosmotropic (water structure or hydrogen bond making) and ClO_4^- the most chaotropic (water structure or hydrogen bond breaking).^{231,232} While these terms, water structure making or breaking, may seem to have no direct bearing on the polar organic

mobile phase used here, other recent publications have indicated Hofmeister effects in non-aqueous solvents or aqueous organic mixtures.^{233,234} Indeed, the current trend for explaining the Hofmeister series for anions is not in terms of their effect on bulk water structure, but rather their direct interaction with the interface of the substrate.²³⁵

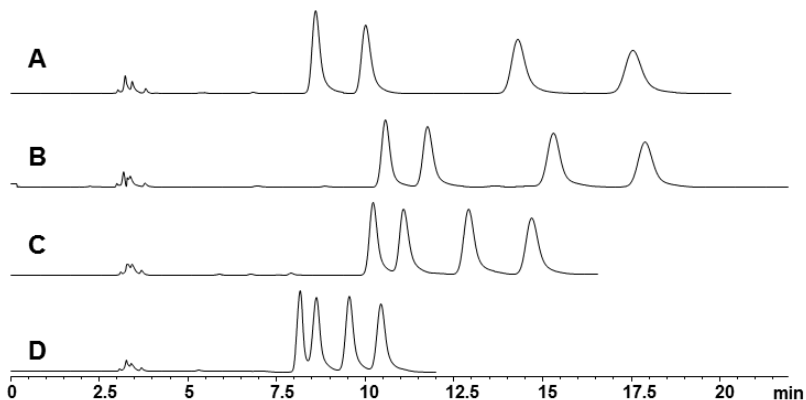


Figure 6-5 Barium counter anion effect on enantioselectivity.

First pair of enantiomers corresponds to CPA-1 and the latter to CSA-5; flow rate: 1 mL/min, UV = 230 nm. Mobile phase conditions and enantioselectivity: A) 5.11 mM $\text{Ba}(\text{ClO}_4)_2$ in methanol, $\alpha_{\text{CPA-1}} = 1.25$, $\alpha_{\text{CSA-5}} = 1.29$; B) 4.16 mM $\text{Ba}(\text{TFA})_2$ in methanol, $\alpha_{\text{CPA-1}} = 1.16$, $\alpha_{\text{CSA-5}} = 1.21$; C) 2.00 mM $\text{Ba}(\text{MSA})_2$ in methanol, $\alpha_{\text{CPA-1}} = 1.12$, $\alpha_{\text{CSA-5}} = 1.18$; D) 1.00 mM $\text{Ba}(\text{OAc})_2$ in methanol, $\alpha_{\text{CPA-1}} = 1.09$, $\alpha_{\text{CSA-5}} = 1.12$

We postulate that kosmotropic anions, such as acetate, will have a tendency to selectively adsorb to cyclofructan through its many hydroxyl groups. The effect of such a selective adsorption is illustrated in Figure 6-6. The original surface potential of the barium-complexed cyclofructan, ψ_0 , is lowered to a new surface potential, $\psi_{0,\text{Ads}}$, by the adsorption of acetate anions to the cyclofructan macrocycle resulting in decreased

retention of analytes. In extreme cases this selective adsorption can lead to a reversal of the surface potential.²³⁰ Interestingly, this behavior was observed when oxalic acid/ TEA

Table 6-3 Comparison of different barium salt additives (~ 5 mM in each mobile phase) on the retention (k), selectivity (α) and resolution (R_s) of chiral sulfonic/ phosphoric acids on LARIHC-CF6-P in the polar organic mode.

Analyte	Ba(OAc) ₂			Ba(ClO ₄) ₂			Ba(MSA) ₂			Ba(TFA) ₂			Ba(TFA) ₂		
	k	α	R_s	k	α	R_s	k	α	R_s	k	α	R_s	k	α	R_s
CSA-1	0.57	1.00	<0.2	4.48	1.04	0.6	1.92	1.00	<0.4	2.89	1.03	0.4	3.94	1.06	0.6
CSA-2	0.57	1.00	<0.2	4.10	1.02	<0.5	1.76	1.00	<0.2	2.73	1.03	0.4	2.35	1.10	0.7
CSA-3	0.54	1.00	<0.2	4.18	1.00	<0.2	1.86	1.00	<0.2	2.82	1.00	<0.2	2.92	1.00	<0.2
CSA-4	0.90	1.00	<0.2	5.29	1.04	0.7	2.15	1.00	<0.4	3.30	1.03	0.4	4.11	1.06	0.6
CSA-5	0.68	1.11	1.0	4.86	1.28	4.2	2.06	1.16	2.4	3.20	1.21	3.3	2.91	1.22	1.8
CSA-6	0.76	1.07	0.4	3.68	1.24	1.8	1.46	1.12	1.3	2.29	1.15	1.9	2.79	1.25	1.6
CSA-7	0.71	1.00	<0.2	6.12	1.00	<0.2	2.34	1.00	<0.2	3.66	1.00	<0.2	6.28	1.00	<0.2
CSA-8	0.67	1.00	<0.2	5.55	1.00	<0.2	2.26	1.00	<0.2	3.42	1.00	<0.2	6.13	1.00	<0.2
CSA-9	0.66	1.00	<0.2	5.42	1.03	0.5	2.35	1.00	0.4	3.37	1.02	0.4	6.91	1.04	0.5
CPA-1	0.58	1.09	0.7	2.35	1.24	3.4	1.56	1.11	1.5	1.95	1.16	2.3	2.16	1.37	3.1
CPA-2	0.91	1.00	<0.2	8.40	1.03	0.5	3.04	1.00	<0.2	4.84	1.00	<0.4	8.44	1.09	1.1
CPA-3	0.38	1.00	<0.2	1.69	1.00	<0.2	1.53	1.00	<0.2	1.70	1.00	<0.2	2.23	1.18	2.0
CPA-4	0.20	1.00	<0.2	1.00	1.05	0.6	0.92	1.00	<0.2	1.02	1.00	<0.4	2.25	1.19	2.8
CPA-5	1.21	1.00	<0.2	15.95	1.03	<0.4	3.96	1.03	0.5	7.18	1.04	0.6	11.64	1.08	0.6
CPA-6	1.08	1.00	<0.2	12.93	1.02	<0.4	3.59	1.00	<0.2	6.32	1.00	<0.2	10.83	1.00	<0.2
CPA-7	0.28	1.00	<0.2	1.65	1.00	<0.2	1.27	1.00	<0.2	1.47	1.00	<0.2	2.83	1.10	1.4

or phosphoric acid/TEA were evaluated as mobile phase additives with no barium present in the mobile phase. The result (data not shown) was that chiral phosphoric and sulfonic acids eluted at the void volume (exclusion) and racemic 1-(1-naphthyl)ethylamine was retained and separated! Selective adsorption to the stationary phase particle will lessen as the nature of the anion becomes more chaotropic as with perchlorate.

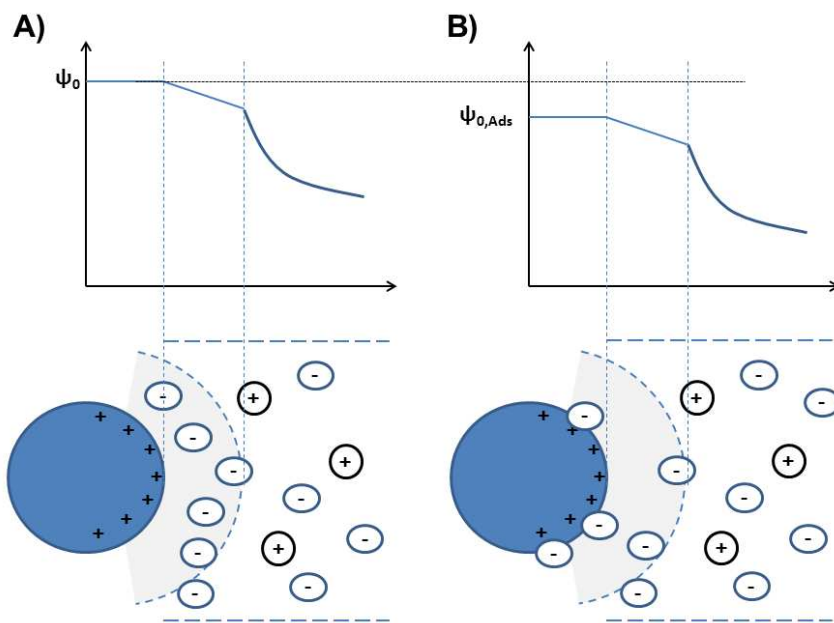


Figure 6-6 Effect of selective adsorption of eluent anions on the potential curve of a charged surface.

Solid sphere represents a charged particle; shaded, hemispherical area with dashed boundary is the Stern layer; the ovoid shapes with a negative charge indicate eluent anions, the spheres containing positive a charge indicate cations; the boundary to the diffuse layer is not shown. A) No selective adsorption of anions to the charged surface, potential is ψ_0 . B) Selective adsorption of anion to the charged surface, $\psi_0 > \psi_{0,Ads}$.

6.4.2 Effect of the mobile phase dielectric constant

Also in Table 6-2 we note the important role that the dielectric constant of the solvent plays. Methanol has a dielectric constant of 32.7 and ethanol has 24.5. The replacement of methanol for ethanol in Table 1, while using the same additive, 5.2 mM Ba(TFA)₂, shows, i) an increase in retention for every compound except CSA-2 and CSA-5, ii) an improvement in the enantioselectivity and iii) additional enantioselectivity that did not occur in methanol mobile phase (CPA-2 – 4 and 7). The number of compounds exhibiting enantioselectivity when changing from methanol to ethanol is improved from 8 to 12 respectively. The rationale for these improvements is that a lower solvent dielectric constant affords tighter ion pairing with the barium cation and therefore longer retention. Tighter ion pairing necessitates being closer to the chiral macrocycle thus enhancing enantioselectivity as well. Although ethanol was the preferable polar organic solvent, the kosmotropic barium salts (OAc⁻ and MSA⁻) were insoluble in it. The use of even lower dielectric constant systems was investigated for poorly retained compounds such as CPA-3 and CPA-4 by using heptane-ethanol mobile phases. This improved both the retention and the enantioselectivity, however it caused excessive retention of the other analytes.

6.4.3 Retention order

In methanol mobile phases containing MSA⁻, TFA⁻ and ClO₄⁻ (Table 6-3), the retention order on Larihc-CF6-P appeared to follow the geometry and accessibility of the anionic moiety. The more sterically hindered the ionizable group of the analyte was, the less it was retained. The most retained compounds, CPA-2, CPA-5 and CPA-6, are amongst the smallest and least sterically hindered of the CPAs and they are retained the longest. Conversely the largest analytes (CPA-3, CPA-4 and CPA-7) are the least retained, presumably because of the steric hindrance of the phosphate group.

6.4.4 Effect of varying concentration of the Ba²⁺ salt in the mobile phase

The retention of CPA-1 and CSA-5 was studied as a function of the barium salt concentration by systematically changing it from 1 – 5 mM for each of the barium salts (~1.0, 2.0, 3.0, 4.0 and 5.0 mM). Plots of the logarithm of the retention factor for the first eluting enantiomer (log k) versus the logarithm of the concentration of the counter anion of the barium salt (log [X], where X = OAc⁻, MSA⁻, TFA⁻ and ClO₄⁻) were all linear (r² > 0.99) according to the equation

$$\log k = -s \log [X] + \text{constant}$$

where k is the retention factor, s is the slope which usually found to be approximately equal to z_A/z_X, where z_A is the charge of the analyte anion and z_X is the charge of the barium counter anion. The negative slopes (see Table 6-4) indicated a decreasing retention time with increasing barium salt concentration typical of that found in ion exchange chromatography.^{226,230,236}

Table 6-4 Linear regression of the log k vs. log [X] plots for CPA-1 and CSA-5 for different Ba²⁺ salts.

Ba ²⁺ salt	CPA-1				CSA-5			
	Range ^a (mM)	slope	intercept	r ²	Range (mM)	slope	intercept	r ²
OAc ⁻	1 – 10	-0.66	0.42	0.999	1 – 10	-0.70	0.53	0.999
MSA ⁻	2 – 10	-0.85	0.88	0.999	2 – 10	-0.88	1.04	0.999
TFA ⁻	2 – 10	-0.93	1.25	0.999	2 – 10	-0.93	1.46	0.999
ClO ₄ ⁻	2 – 10	-1.02	1.31	0.998	2 – 10	-1.02	1.61	0.998

In classical ion-pairing techniques, analyte retention initially increases with increasing concentration of ion-pairing reagent up to a maximum and thereafter

decreases. Assuming linear behavior, a positive slope for $\log k$ vs. $\log [X]$ should be seen for the former case and a negative one for the latter. At greater barium salt concentrations, where solubility permitted, e.g. 100 mM $\text{Ba}(\text{ClO}_4)_2$, retention continued to decrease. When the concentration of the barium salt in the mobile phase is much greater than that on the stationary phase, the analytes predominantly ion-pair in the mobile phase and are not retained. Retention can then be increased by decreasing the barium salt concentration to afford separation.

Lamb et al. have shown in their work on C18 reversed phase columns coated with a lipophilic crown ether/ cryptand using a KOH hydro-organic mobile phase that below ~ 0.8 mM KOH retention increased with increasing KOH concentration but thereafter it decreased linearly.²³⁷ Such a turning point must exist for our stationary phase as well but we did not observe it. Fritz has observed that some ion pairing agents can be attached so strongly to the stationary phase that they may be considered as permanently coated.²³⁸ In our case this seems to have some merit since the binding of Ba^{2+} to cyclofructan is stronger in a pure organic solvent as is also common for crown ethers in general.^{222,239}

6.4.5 *van't Hoff plots*

Before delving into the thermodynamics of the chromatography, the thermodynamics of the barium-cyclofructan complex must be addressed. As with the binding of alkali and alkaline earth metals to synthetic crown ethers and cryptands, the binding of barium to cyclofructan is an exothermic process.²³⁹⁻²⁴² Although there is no quantitative thermodynamic data on the binding of barium to cyclofructan, it is nevertheless undisputed that it binds strongest to cyclofructan compared to the rest of the Group I and II metal cations.²²² Takai and Sewada have generated thermodynamic data for the binding of potassium, rubidium and cesium cations to permethylated cyclofructan

and have shown that $\Delta H_{\text{binding}}$ becomes increasingly exothermic.²⁰⁹ We therefore infer that an analogous enthalpy will be exhibited for barium binding to cyclofructan derivatives. A question arises as to how much barium will be decomplexed from the cyclofructan as the equilibrium shifts to dissociation with increasing temperature. The van't Hoff equation expresses the changing equilibrium constant as a function of temperature as follows²⁴¹

$$\ln\left(\frac{K_2}{K_1}\right) = \frac{-\Delta H}{R}\left(\frac{1}{T_2} - \frac{1}{T_1}\right)$$

where K_1 and K_2 represent the equilibrium constants at absolute temperatures T_1 and T_2 respectively, ΔH is the change in enthalpy (in $\text{J}\cdot\text{mol}^{-1}$) and R is the gas constant ($8.314 \text{ J}\cdot\text{K}^{-1}\cdot\text{mol}^{-1}$). Thus, if ΔH , K_1 and T_1 is known, the equilibrium constant, K_2 , at some other temperature, T_2 , can be readily calculated. Furthermore, the ratio of Ba^{2+} -CF6 complex on the stationary phase to uncomplexed CF6 on the stationary phase may be expressed as follows²³⁷

$$\frac{[\text{Ba}^{2+} \dots \text{CF6}]_{S.P.}}{[\text{CF6}]_{S.P.}} = K[\text{Ba}^{2+}]_{M.P.}$$

where K is the equilibrium constant and $[\text{Ba}^{2+}]_{M.P.}$ represents the concentration of barium in the mobile phase, $[\text{Ba}^{2+} \dots \text{CF6}]_{S.P.}$ represents the concentration of barium-CF6 complex on the stationary phase and $[\text{CF6}]_{S.P.}$ represents the concentration of CF6 on the stationary phase. We chose a K value for Ba^{2+} -CF6 of $19,000 \text{ M}^{-1}$ taken from Takai and Sewada, et al.^{209,210} which is in agreement with research done by Na and Padivitage.²²² For ΔH we used the value reported by Takai and Sewada for cesium complexed to permethylated CF6,²⁰⁹ i.e. $\Delta H = -38 \text{ kJ}\cdot\text{mol}^{-1}$. These calculations are represented graphically in Figure 6-7. The net decrease in the amount of barium on the CSP over the temperature range studied is estimated to be $\sim 3.5 \%$ or in other words, 96.5 % of the

barium remains on the CSP. This very small change in the Ba^{2+} concentration with increasing temperature is not expected to have a significant impact on retention.

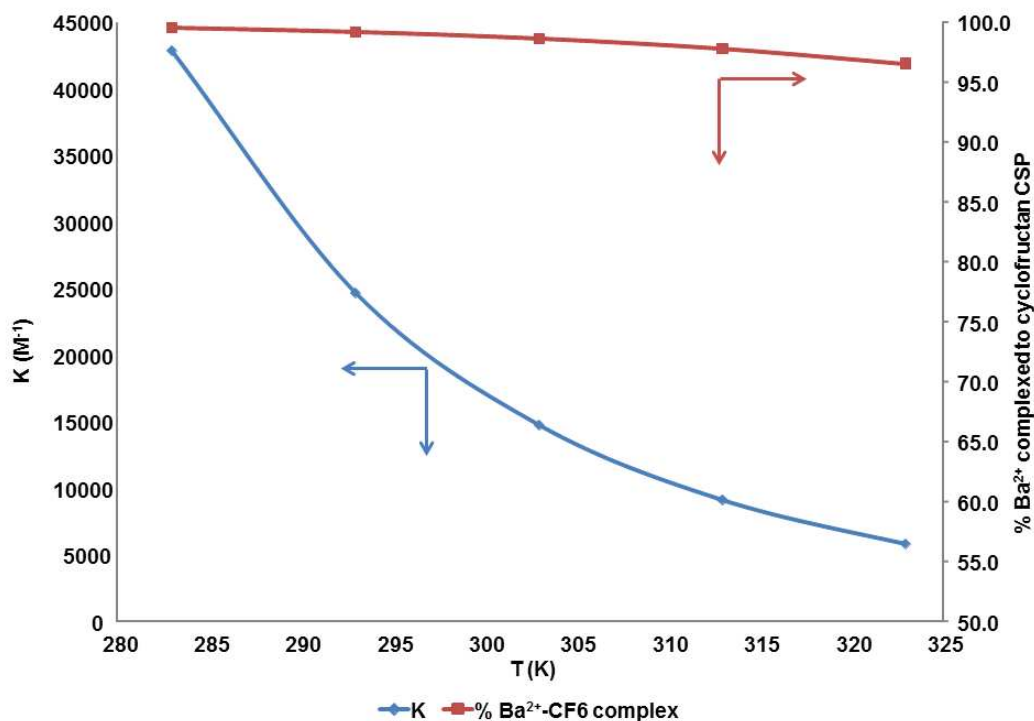
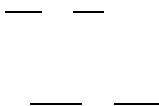


Figure 6-7 Change of K (blue diamond) and complexed Ba^{2+} (red square) as a function of temperature

6.4.5.1 $\ln k$ vs. $1000/T$

The retention and enantioselectivity of CPA-1 and CSA-5 on LARIHC-CF6-P™ were monitored as a function of mobile phase temperature according to the well-known van't Hoff expressions for chromatography



where k is the retention factor, ΔH is the change in enthalpy, ΔS is the change in entropy, $\Delta\Delta H$ is the change in ΔH , $\Delta\Delta S$ is the change in ΔS , R is the gas constant ($8.314 \text{ J}\cdot\text{K}^{-1}\cdot\text{mol}^{-1}$), T is the absolute temperature, ϕ is the phase ratio (V_s/V_m where V_s is the volume of the selector (i.e., excluding the silica support material) and V_m is the volume of the mobile phase) and α is enantioselectivity. The thermodynamic parameters calculated from the van't Hoff plots (see Figures 6-8 – 6-11) of CPA-1 and CSA-5 are shown in in Table 6-4. The $\ln k$ vs. $1000/T$ van't Hoff plot governs the thermodynamics of retention as the analyte moves from the mobile phase to the stationary phase. Here we observed two extremes: $\text{Ba}(\text{ClO}_4)_2$ was an enthalpy driven system ($\Delta H < 0$ and $\Delta H < T\Delta S$) while $\text{Ba}(\text{OAc})_2$ was purely entropy driven ($\Delta H > 0$ and $\Delta H < T\Delta S$). $\text{Ba}(\text{TFA})_2$ was intermediate between these two extremes in that although $\Delta H < 0$, the ΔG was dominated by the $T\Delta S$ contribution.

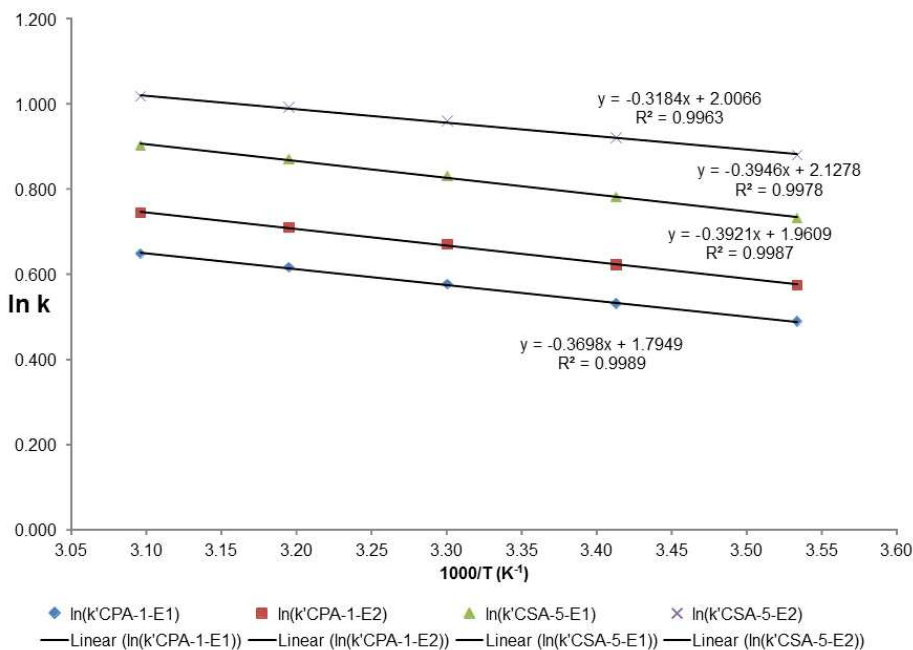


Figure 6-8 van't Hoff plot ($\ln k$ vs. $1000/T$) for CPA-1 and CSA-5 using $\text{Ba}(\text{OAc})_2$ additive

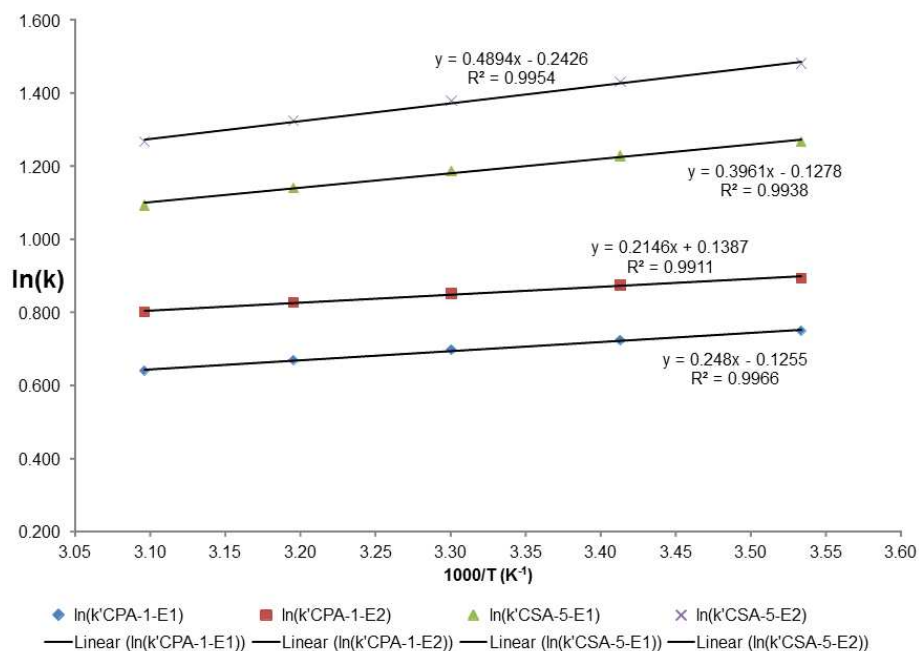


Figure 6-9 van't Hoff plot ($\ln k$ vs. $1000/T$) for CPA-1 and CSA-5 using $Ba(TFA)_2$ additive

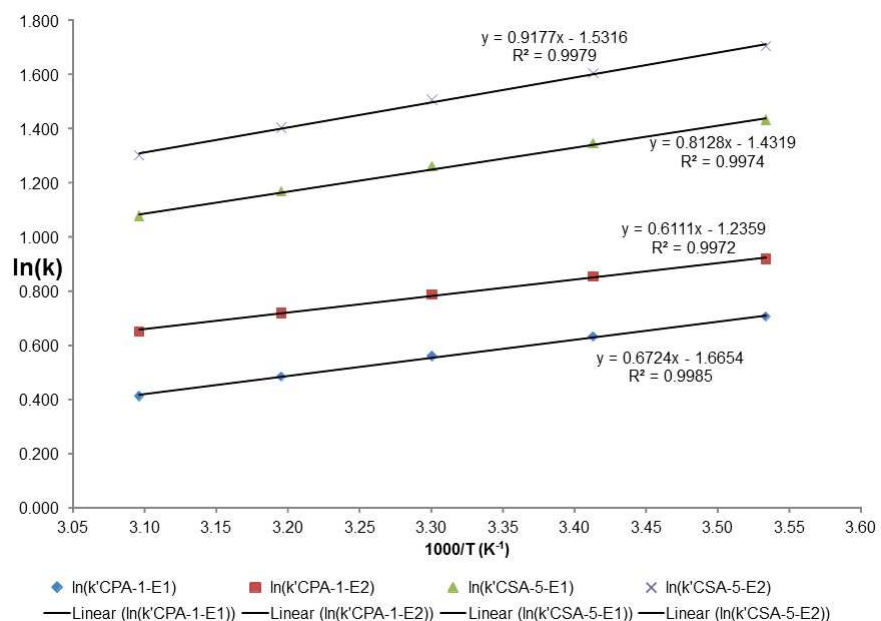


Figure 6-10 van't Hoff plot ($\ln k$ vs. $1000/T$) for CPA-1 and CSA-5 using $Ba(ClO_4)_2$ additive

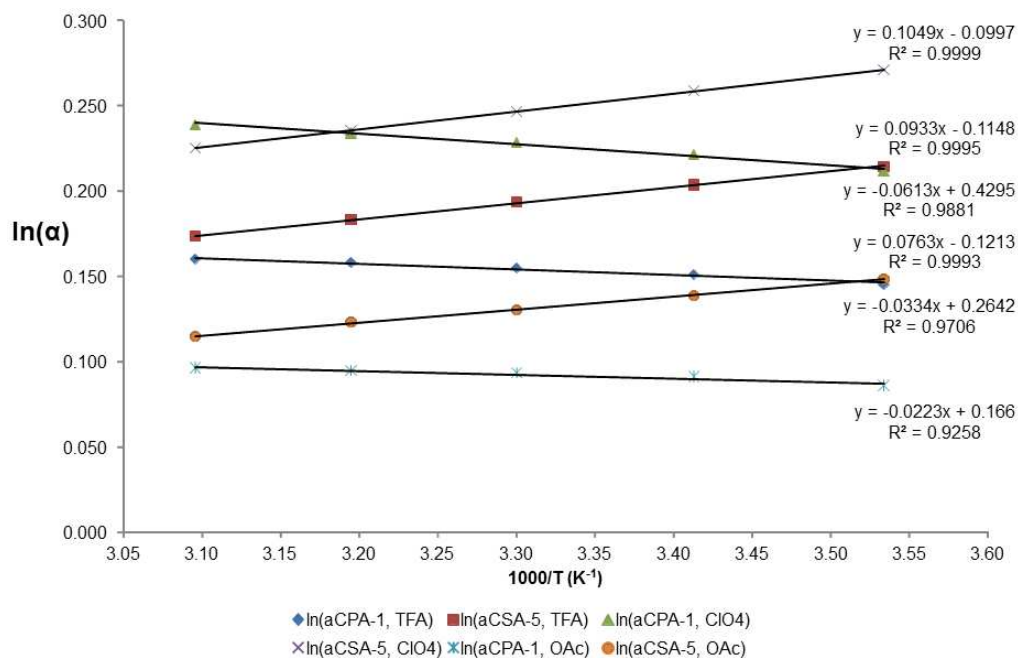


Figure 6-11 van't Hoff plot ($\ln\alpha$ vs. $1000/T$) for CPA-1 and CSA-5 using three different Ba^{2+} -salt additives

The solvation of the cyclodextran macrocycle, the barium cation and the analyte should be more or less constant in each mobile phase system. Furthermore the number of barium counter anions that undergo ionic interactions with the complexed barium should also be constant. The remaining variable is the nature of the anion and its ability to associate with the stationary phase via hydrogen bonding. We postulate that analyte retention is governed both by ionic interaction as well as hydrogen bonding. The former interaction will be present in both OAc^- and ClO_4^- mobile phase systems, however the latter interaction will be unfavorable for the strongly hydrogen bonded OAc^- system and absent in the ClO_4^- system. The removal of tightly hydrogen bonded OAc^- anions from the stationary phase to the mobile phase affords an increase in its degrees of freedom and a consequent increase in entropy.

Table 6-5 Thermodynamic parameters calculated from the van't Hoff plots in Figures 6-8

– 6-11.

		ln k vs. 1000/T			ln α vs. 1000/T		
		ΔH (kJ.mol ⁻¹)	ΔS (J.K ⁻¹ .mol ⁻¹)	ΔG _{298 K} (kJ.mol ⁻¹)	ΔΔH (kJ.mol ⁻¹)	ΔΔS (J.K ⁻¹ .mol ⁻¹)	ΔΔG _{298 K} (kJ.mol ⁻¹)
5.2 mM Ba(TFA)₂							
CPA-1	E 1	-2.06	15.30	-6.62	0.28	2.20	-0.38
	E 2	-1.78	17.50	-7.00			
CSA-5	E 1	-3.29	15.28	-7.85	-0.78	-0.95	-0.49
	E 2	-4.07	14.33	-8.34			
5.11 mM Ba(ClO₄)₂							
CPA-1	E 1	-5.59	2.50	-6.34	0.51	3.57	-0.55
	E 2	-5.08	6.07	-6.89			
CSA-5	E 1	-6.76	4.44	-8.08	-0.87	-0.83	-0.63
	E 2	-7.63	3.61	-8.71			
1.01 mM Ba(OAc)₂							
CPA-1	E 1	3.07	31.27	-6.86	0.19	1.38	-0.23
	E 2	3.26	32.65	-7.20			
CSA-5	E 1	3.28	34.04	-6.24	-0.63	-1.01	-0.33
	E 2	2.65	33.03	-6.47			

6.4.5.2 $\ln \alpha$ vs. $1000/T$

Regarding the Gibbs free energy (Table 6-4) for the enantioselectivity, we once again observed two extreme cases: $\text{Ba}(\text{ClO}_4)_2$ exhibits the most favorable $\Delta\Delta G$ (-0.55 and -0.63 $\text{kJ}\cdot\text{mol}^{-1}$ for CPA-1 and CSA-5 respectively) while $\text{Ba}(\text{OAc})_2$, though still favorable, exhibits the smallest $\Delta\Delta G$ (-0.23 and -0.33 $\text{kJ}\cdot\text{mol}^{-1}$ for CPA-1 and CSA-5 respectively). $\text{Ba}(\text{TFA})_2$ is once again intermediate between the two extremes (-0.38 and -0.49 $\text{kJ}\cdot\text{mol}^{-1}$ for CPA-1 and CSA-5 respectively). A possible explanation for the poor enantioselectivity observed in the $\text{Ba}(\text{OAc})_2$ system is that adsorbed acetate anions would impede hydrogen bonding interactions between the analyte and the chiral selector. Three points of interaction are required for chiral recognition²⁶ and one of these is ionic. The remaining interactions can be hydrogen bonding, dipole-dipole and/or steric interactions. In the case of $\text{Ba}(\text{ClO}_4)_2$ though, the analyte would be free to hydrogen bond and would therefore exhibit better chiral recognition which was observed.

The data in Table 6-4 demonstrates that the enantiomeric separation of CPA-1 is entropically driven while CSA-5 is enthalpically driven for each mobile phase system. This means, in the case of $\text{Ba}(\text{ClO}_4)_2$ and $\text{Ba}(\text{TFA})_2$ systems, that as temperature is increased enantioselectivity for CPA-1 improves even while retention is decreasing (see Figure 6-12). Such remarkable enantioselective behavior is rarely observed. Since it is unlikely that the cyclofructan macrocycle is changing and since the thermodynamic behavior for each analyte is consistent regardless of the barium additive used, the observed behavior must be related to the analyte structure. Both CPA-1 and CSA-5 are sterically hindered molecules however the sulfonate group has some rotational degree of freedom whereas the phosphate group does not.

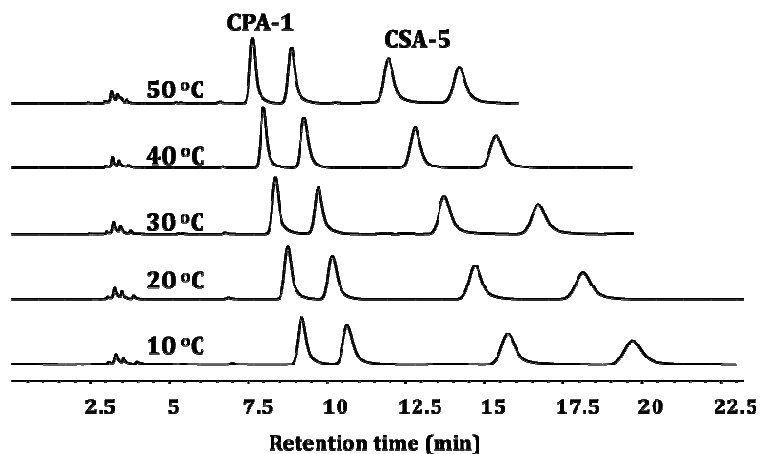


Figure 6-12 Effect of temperature on enantioselectivity for CPA-1 (entropy driven) and CSA-5 (enthalpy driven) in a methanol mobile phase containing 5 mM Ba(ClO₄)₂.

6.4.6 Optimized separations

Table 6-5 shows the optimized separations for all the analytes in Figure 6-1. For the β -ketosulfonic acids (CSA-7 – 9) the LARIHC-CF6-RNTM and the FRULIC-NTM showed complementary behavior. CSA-7, chalcone sulfonic acid containing no aromatic substituents, displayed enantioselectivity on the LARIHC-CF6-RNTM column whereas the para- substituted CSA-8 and 9 showed no selectivity. Evidently the presence of a para substituent was unfavorable for enantioselectivity. The FRULIC-NTM showed reasonable enantioselectivity for CSA-8 and 9, but only slight enantioselectivity for CSA-7. In fact the FRULIC-NTM was the only CSP to show appreciable selectivity for these two compounds. Single chiral axis sulfonic acids (CSA-1 and CSA-4) displayed longer retention but smaller enantioselectivity than the two chiral axes analogues (CSA-3 and CSA-5). Fig. 6-13 shows the overall performance of the three CSPs in separating chiral sulfonic and phosphoric acids (Figure 6-1). The LARIHC-CF6-RNTM was clearly the most successful in

terms of the number of baseline separations. It displayed enantioselectivity for every analyte except CSA-9 which was best separated on the FRULIC-N™.

Table 6-5 Optimized separations of chiral sulfonic/ phosphoric acids on cyclofructan columns. Flow rate = 1 mL/min (or 0.5 mL/min*).

Analyte	Column	Mobile phase	k ₁	α	R _s
CSA-1	Larihc-CF6-RN™	EtOH with 0.05/0.05 (v/v %) TEA/TFA and 0.5 mM Ba(TFA) ₂	17.49	1.04	0.7
CSA-2	Larihc-CF6-RN™	EtOH with 0.05/0.05 (v/v %) TEA/TFA and 0.5 mM Ba(TFA) ₂	11.86	1.09	1.5
CSA-3	Larihc-CF6-RN™	EtOH with 0.08/0.02 (v/v %) TEA/TFA and 1.0 mM Ba(TFA) ₂	7.22	1.12	1.9
CSA-4	Larihc-CF6-RN™	EtOH with 0.05/0.05 (v/v %) TEA/TFA and 0.5 mM Ba(TFA) ₂	19.59	1.06	1.1
CSA-5	Larihc-CF6-PT™	MeOH with 5 mM Ba(ClO ₄) ₂	4.86	1.28	4.2
CSA-6	Larihc-CF6-RN™	MeOH with 5 mM Ba(ClO ₄) ₂	3.68	1.24	1.8
CSA-7	Larihc-CF6-RN™	EtOH with 0.1/0.1 (v/v %) TEA/TFA and 1 mM Ba(TFA) ₂	13.88	1.05	1.0
CSA-8	FRULIC-N™	MeOH with 5 mM Ba(TFA) ₂	26.49	1.04	1.0
CSA-9	FRULIC-N™	MeOH with 5 mM Ba(TFA) ₂	27.94	1.06	1.3
CPA-1	Larihc-CF6-RN™	MeOH with 5 mM Ba(TFA) ₂	4.01	1.23	4.4
CPA-2	Larihc-CF6-RN™	EtOH with 5 mM Ba(ClO ₄) ₂	13.90	1.23	2.2
CPA-3	Larihc-CF6-RN™	EtOH with 5.2 mM Ba(TFA) ₂	4.95	1.14	1.7
CPA-4	Larihc-CF6-RN™	EtOH with 5.2 mM Ba(TFA) ₂	3.01	1.27	4.2
CPA-5	Larihc-CF6-RN™	MeOH with 1 mM Ba(OAc) ₂	12.10	1.06	1.6
CPA-6	Larihc-CF6-RN™	MeOH with 1 mM Ba(OAc) ₂	10.86	1.05	1.5
CPA-7	Larihc-CF6-PT™	EtOH with 5.2 mM Ba(TFA) ₂ *	6.78	1.08	1.8

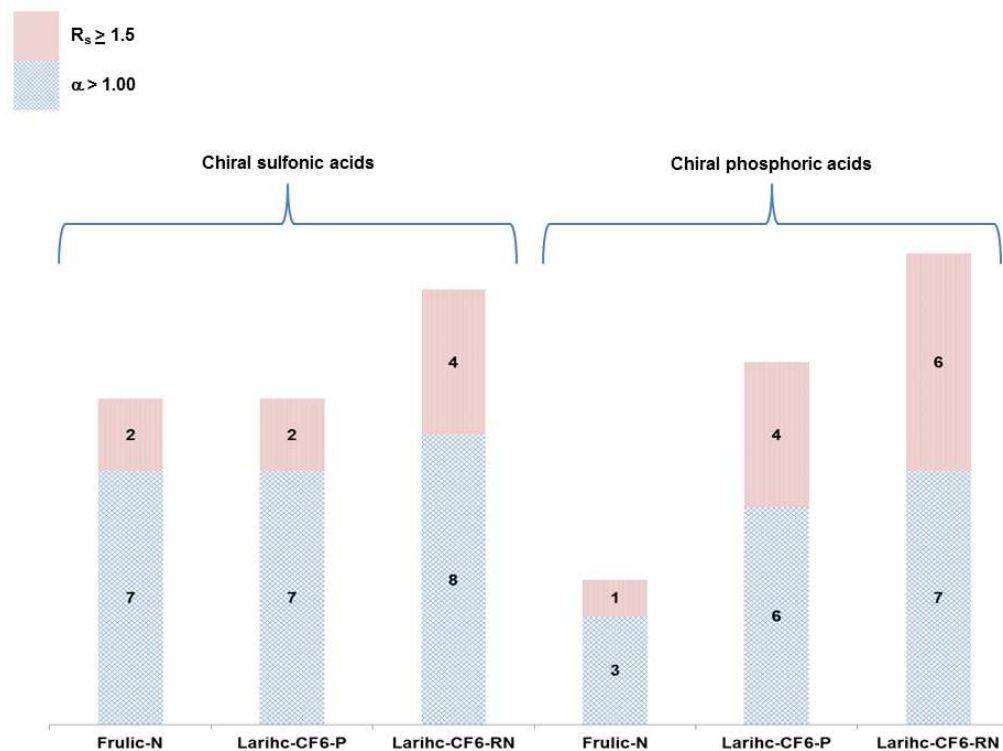


Figure 6-13 Overview of the performance of commercially available cyclodextran columns (complexed with barium) in separating chiral sulfonic and phosphoric acids.

6.5 Conclusion

The selectivity of cyclodextran-based CSPs has been significantly expanded to an entirely new class of anionic compounds. Preliminary tests for carboxylates are also promising. This has been achieved by exploiting a unique ion pairing behavior of a simple inorganic metal ion (Ba^{2+}). Once the CSPs have been conditioned and evaluated in the polar organic mode (methanol or ethanol) with a barium salt in the mobile phase, $\log k$ vs. $\log [X]$ plots are linear with negative slopes and behave as anion exchangers. Sterically hindered sulfonates or phosphates elute earlier than the less sterically hindered ones. The presence of additional hydrogen bond acceptors on the analyte also increases retention. $Ba(OAc)_2$ mobile phase additive affords shorter retention which, for CPA-1 and

CSA-5, is entropy driven while $\text{Ba}(\text{ClO}_4)_2$ affords longer retention which is enthalpy driven and $\text{Ba}(\text{TFA})_2$ is intermediate. Enantioselectivity improves in the order of $\text{OAc}^- < \text{TFA}^- < \text{ClO}_4^-$. The scale up of a separation of CSA-5 to preparative scale LC has also been successfully demonstrated. Barium complexed cyclofructans behave as hydrophilic analogues of reversed-phase ion-pairing LC systems.

Chapter 7

7.1 General summary

In Chapter 2, new stationary phases based upon ionic liquids were synthesized for SFC. The cationic portion was immobilized on silica gel while the counter anion could be varied. Six immobilized ionic liquids were synthesized and showed varying degrees of retention for beta-blockers and other acidic and basic drugs. The presence of aromatic groups on the stationary phase afforded greater analyte retention as did the presence of nitrogen in the pyridinium and imidazolium based stationary phases. Stationary phases containing phosphonium ion moieties generally provided less retention. The phases could be tuned by varying the nature of the counter anion. Perchlorate enhanced the retention of beta-blockers while acetate enhanced the retention of acidic drugs. In general TFA afforded the lowest analyte retention. The combinations of immobilized ionic liquids and the counter anions could conceivably lead to either strongly or weakly retentive phases.

Chapter 3 described the HPLC analysis of the antioxidants present in rosemary using a hydroxypropyl-beta cyclodextrin (Cyclobond RSP) stationary phase. In particular the paper focused on the degradation of carnosol, carnosic acid and rosmarinic acid, as individual components in ethanolic solutions and also as mixtures, and their dependence on temperature and light exposure over a 13 day period. Temperature, predictably, increased degradation while exposure to light produced unique degradation products, some of which could not be identified. Rosmarinic acid did not degrade appreciably in the study. While alone in ethanol carnosol degraded rapidly, and carnosic acid degraded noticeably more slowly. When mixed together they displayed the opposite trend. This was attributed partly to carnosic acid's ability to compensate for degrading carnosol by replenishing it and partly to its ability to protect it by a mechanism which is still not known. The antioxidants were found to be relatively stable in fish oil.

Chapter 4 attempted to address the issue of flinderole B's optical activity and stereoisomeric state as it is found in nature. Synthetic flinderole B enantiomers were isolated using preparative HPLC and a Chirobiotic V column. Specific rotations were determined and found to be vastly different from that which had been reported for naturally occurring flinderole B. While this does not prove that flinderole B is present in nature as a racemate, it does provide room for the possibility which has been claimed for a few compounds in the literature.

Chapter 5 dealt with the enantiomeric separations of flinderoles and borreverines by HPLC using Chirobiotic V/V2 columns as well as by CE using cyclodextrin chiral selectors. The Chirobiotic V2 was shown to have excellent enantioselectivity in the polar organic mode, affording baseline separations for all of the compounds except flinderole C. Flinderole C, however, was baseline separated only on the Chirobiotic V column in the reversed phase mode, thus indicating the complementary nature of these two columns. Chiral CE was not as successful as chiral HPLC and only two baseline separations were observed. Generally the hydroxypropyl cyclodextrins showed the best diastereoselectivity/ enantioselectivity for flinderoles, while sulphated α -cyclodextrin exhibited excellent baseline separations for the borreverines. This work can now be used to fully address the remaining questions left unanswered in chapter 4 by analyzing naturally occurring flinderoles and borreverines.

Chapter 6 introduced a novel use of commercially available cyclofructan 6 CSPs. The complexation of cyclofructan with barium cations in the polar organic mode transforms the neutral oligosaccharide into a cationic complex which exhibits increased enantioselectivity for chiral anionic compounds. Enantioselectivity was shown for a group of chiral sulfonic and phosphoric acids. Large, sterically hindered sulfonates and phosphates were less retained than the smaller unhindered ones by reason of

accessibility of the ionic moiety. The mechanism of retention was described as ion interaction – a mixture of ion-pairing and anion exchange. Thermodynamic studies using van't Hoff plots showed that kosmotropic barium salts, e.g. acetate, afford entropy driven retention while chaotropic barium salts, e.g. perchlorate, afford enthalpy driven retention. Furthermore, a rarely observed entropy driven separations was found for one of the chiral phosphoric acids. This work holds promise for the enantiomeric separation of chiral carboxylates as well as the selective retention of anionic analytes in a complex matrix of neutral molecules as is found in rosemary extracts and wine.

Appendix A

Names of co-contributing authors

- Chapter 2: Jonathan Paul Smuts, Eranda Wanigasekera and Daniel W. Armstrong.
- Chapter 3: Ying Zhang, Jonathan Paul Smuts, Edra Dodbia, Rekha Rangarajan, John C. Lang and Daniel W. Armstrong.
- Chapter 4: Ravikrishna Vallakati, Jonathan P. Smuts, Daniel W. Armstrong and Jeremy A. May.
- Chapter 5: Jonathan Paul Smuts, Yun-Cheol Na, Ravikrishna Vallakati, Adam Přibylka, Jeremy A. May and Daniel W. Armstrong.
- Chapter 6: Jonathan P. Smuts, Xi-Qi Hao, Zhaobin Han, Curran Parpia, Michael Krische and Daniel W. Armstrong.

Appendix B
Rights and permissions

**SPRINGER LICENSE
TERMS AND CONDITIONS**

Nov 05, 2013

This is a License Agreement between Jonathan P Smuts ("You") and Springer ("Springer") provided by Copyright Clearance Center ("CCC"). The license consists of your order details, the terms and conditions provided by Springer, and the payment terms and conditions.

All payments must be made in full to CCC. For payment instructions, please see information listed at the bottom of this form.

License Number	3262551063537
License date	Nov 05, 2013
Licensed content publisher	Springer
Licensed content publication	Analytical and Bioanalytical Chemistry
Licensed content title	Enantioseparation of flinderoles and borreverines by HPLC on Chirobiotic V and V2 stationary phases and by CE using cyclodextrin selectors
Licensed content author	Jonathan P. Smuts
Licensed content date	Jan 1, 2013
Volume number	405
Issue number	28
Type of Use	Thesis/Dissertation
Portion	Full text
Number of copies	3
Author of this Springer article	Yes and you are the sole author of the new work
Order reference number	
Title of your thesis / dissertation	The use of supercritical fluid chromatography (SFC) and liquid chromatography (LC) for the separation of pharmaceutical products and chiral phosphoric and sulfonic acids
Expected completion date	Dec 2013
Estimated size(pages)	200
Total	0.00 USD
Terms and Conditions	

Introduction

The publisher for this copyrighted material is Springer Science + Business Media. By clicking "accept" in connection with completing this licensing transaction, you agree that the following terms and conditions apply to this transaction (along with the Billing and Payment terms and conditions established by Copyright Clearance Center, Inc. ("CCC"), at the time that you opened your Rightslink account and that are available at any time at <http://myaccount.copyright.com>).

**SPRINGER LICENSE
TERMS AND CONDITIONS**

Nov 05, 2013

This is a License Agreement between Jonathan P Smuts ("You") and Springer ("Springer") provided by Copyright Clearance Center ("CCC"). The license consists of your order details, the terms and conditions provided by Springer, and the payment terms and conditions.

All payments must be made in full to CCC. For payment instructions, please see information listed at the bottom of this form.

License Number	3262550920036
License date	Nov 05, 2013
Licensed content publisher	Springer
Licensed content publication	Analytical and Bioanalytical Chemistry
Licensed content title	Comparison of stationary phases for packed column supercritical fluid chromatography based upon ionic liquid motifs: a study of cation and anion effects
Licensed content author	Jonathan Smuts
Licensed content date	Jan 1, 2011
Volume number	400
Issue number	2
Type of Use	Thesis/Dissertation
Portion	Full text
Number of copies	3
Author of this Springer article	Yes and you are the sole author of the new work
Order reference number	
Title of your thesis / dissertation	The use of supercritical fluid chromatography (SFC) and liquid chromatography (LC) for the separation of pharmaceutical products and chiral phosphoric and sulfonic acids
Expected completion date	Dec 2013
Estimated size(pages)	200
Total	0.00 USD
Terms and Conditions	

Introduction

The publisher for this copyrighted material is Springer Science + Business Media. By clicking "accept" in connection with completing this licensing transaction, you agree that the following terms and conditions apply to this transaction (along with the Billing and Payment terms and conditions established by Copyright Clearance Center, Inc. ("CCC"), at the time that you opened your Rightslink account and that are available at any time at <http://myaccount.copyright.com>).



ACS Publications Title:

High quality. High impact.

Degradation Study of Carnosic Acid, Carnosol, Rosmarinic Acid, and Rosemary Extract (Rosmarinus officinalis L.) Assessed Using HPLC

Logged in as:
Jonathan Smuts
Account #:
3000587642

[Logout](#)

Authors: Ying Zhang, Jonathan P. Smuts, Edra Dodbibá, Rekha Rangarajan, John C. Lang, and Daniel W. Armstrong

Publication: Journal of Agricultural and Food Chemistry

Publisher: American Chemical Society

Date: Sep 1, 2012

Copyright © 2012, American Chemical Society

PERMISSION/LICENSE IS GRANTED FOR YOUR ORDER AT NO CHARGE

This type of permission/license, instead of the standard Terms & Conditions, is sent to you because no fee is being charged for your order. Please note the following:

- Permission is granted for your request in both print and electronic formats, and translations.
- If figures and/or tables were requested, they may be adapted or used in part.
- Please print this page for your records and send a copy of it to your publisher/graduate school.
- Appropriate credit for the requested material should be given as follows: "Reprinted (adapted) with permission from (COMPLETE REFERENCE CITATION), Copyright (YEAR) American Chemical Society." Insert appropriate information in place of the capitalized words.
- One-time permission is granted only for the use specified in your request. No additional uses are granted (such as derivative works or other editions). For any other uses, please submit a new request.

[BACK](#)[CLOSE WINDOW](#)

**ELSEVIER LICENSE
TERMS AND CONDITIONS**

Nov 05, 2013

This is a License Agreement between Jonathan P Smuts ("You") and Elsevier ("Elsevier") provided by Copyright Clearance Center ("CCC"). The license consists of your order details, the terms and conditions provided by Elsevier, and the payment terms and conditions.

All payments must be made in full to CCC. For payment instructions, please see information listed at the bottom of this form.

Supplier	Elsevier Limited The Boulevard, Langford Lane Kidlington, Oxford, OX5 1GB, UK
Registered Company Number	1982084
Customer name	Jonathan P Smuts
Customer address	2353 Highlands Creek rd Carrollton, TX 75007
License number	3262550406878
License date	Nov 05, 2013
Licensed content publisher	Elsevier
Licensed content publication	Tetrahedron Letters
Licensed content title	On the biosynthesis and optical activity of the flinderoles
Licensed content author	Ravikrishna Vallakati, Jonathan P. Smuts, Daniel W. Armstrong, Jeremy A. May
Licensed content date	30 October 2013
Licensed content volume number	54
Licensed content issue number	44
Number of pages	3
Start Page	5892
End Page	5894
Type of Use	reuse in a thesis/dissertation
Portion	full article
Format	both print and electronic
Are you the author of this Elsevier article?	No
Will you be translating?	No
Order reference number	

Title of your thesis/dissertation	The use of supercritical fluid chromatography (SFC) and liquid chromatography (LC) for the separation of pharmaceutical products and chiral phosphoric and sulfonic acids
Expected completion date	Dec 2013
Estimated size (number of pages)	200
Elsevier VAT number	GB 494 6272 12
Permissions price	0.00 USD
VAT/Local Sales Tax	0.0 USD / 0.0 GBP
Total	0.00 USD
Terms and Conditions	

INTRODUCTION

1. The publisher for this copyrighted material is Elsevier. By clicking "accept" in connection with completing this licensing transaction, you agree that the following terms and conditions apply to this transaction (along with the Billing and Payment terms and conditions established by Copyright Clearance Center, Inc. ("CCC"), at the time that you opened your Rightslink account and that are available at any time at <http://myaccount.copyright.com>).

GENERAL TERMS

2. Elsevier hereby grants you permission to reproduce the aforementioned material subject to the terms and conditions indicated.

3. Acknowledgement: If any part of the material to be used (for example, figures) has appeared in our publication with credit or acknowledgement to another source, permission must also be sought from that source. If such permission is not obtained then that material may not be included in your publication/copies. Suitable acknowledgement to the source must be made, either as a footnote or in a reference list at the end of your publication, as follows:

"Reprinted from Publication title, Vol /edition number, Author(s), Title of article / title of chapter, Pages No., Copyright (Year), with permission from Elsevier [OR APPLICABLE SOCIETY COPYRIGHT OWNER]." Also Lancet special credit - "Reprinted from The Lancet, Vol. number, Author(s), Title of article, Pages No., Copyright (Year), with permission from Elsevier."

4. Reproduction of this material is confined to the purpose and/or media for which permission is hereby given.

5. Altering/Modifying Material: Not Permitted. However figures and illustrations may be altered/adapted minimally to serve your work. Any other abbreviations, additions, deletions and/or any other alterations shall be made only with prior written authorization of Elsevier Ltd. (Please contact Elsevier at permissions@elsevier.com)

6. If the permission fee for the requested use of our material is waived in this instance, please be advised that your future requests for Elsevier materials may attract a fee.

References

- (1) Okada, T.; Usui, T. *J. Chem. Soc., Faraday Trans.* **1996**, *92*, 4977-4981.
- (2) Klesper, E.; Corwin, A. H.; Turner, D. A. *J. Org. Chem.* **1962**, *27*, 700-1.
- (3) Berger, T. A.; Wilson, W. H. *Anal. Chem.* **1993**, *65*, 1451-5.
- (4) Berger, T. A.; Deye, J. F. *J. Chromatogr.* **1991**, *547*, 377-92.
- (5) Berger, T. A.; Deye, J. F. *Chromatographia* **1990**, *30*, 57-60.
- (6) Berger, T. A.; Deye, J. F. *Anal. Chem.* **1990**, *62*, 1181-5.
- (7) Novotny, M. *J. Chromatogr. Libr.* **1985**, *30*, 105-20.
- (8) Peaden, P. A.; Fjeldsted, J. C.; Lee, M. L.; Springston, S. R.; Novotny, M. *Anal. Chem.* **1982**, *54*, 1090-3.
- (9) Novotny, M.; Springston, S. R.; Peaden, P. A.; Fjeldsted, J. C.; Lee, M. L. *Anal. Chem.* **1981**, *53*, 407A-408A, 410A, 412A, 414A.
- (10) Mukhopadhyay, R. *Analytical Chemistry* **2008**, *80*, 3091-3094.
- (11) Sutton, M. *Chem. World* **2013**, *10*, 52-55.
- (12) Suttowitz, S. B. *Journal of Natural Products* **2003**, *67*, 136-138.
- (13) Kingston David, G. I. In *Human Medicinal Agents from Plants*; American Chemical Society, 1993, pp 138-148.
- (14) Badio, B.; Garraffo, H. M.; Spande, T. F.; Daly, J. W. *Med. Chem. Res.* **1994**, *4*, 440-8.
- (15) Gilpin, R. K.; Gilpin, C. S. *Analytical Chemistry* **2011**, *83*, 4489-4507.
- (16) Gilpin, R. K.; Gilpin, C. S. *Analytical Chemistry* **2009**, *81*, 4679-4694.
- (17) Cielecka-Piontek, J.; Zalewski, P.; Jelinska, A.; Garbacki, P. *Chromatographia* **2013**, *76*, 1429-1437.
- (18) Guillarme, D.; Dong, M. W. *Am. Pharm. Rev.* **2013**, *16*, 36, 38-43.
- (19) Maurer, H. H. *J. Chromatogr. A* **2013**, *1292*, 19-24.
- (20) Thevis, M.; Thomas, A.; Pop, V.; Schaenzer, W. *J. Chromatogr. A* **2013**, *1292*, 38-50.
- (21) Dejaegher, B.; Vander, H. Y. *J. Sep. Sci.* **2010**, *33*, 698-715.
- (22) Hsieh, Y. *J. Sep. Sci.* **2008**, *31*, 1481-1491.
- (23) Hao, Z.; Xiao, B.; Weng, N. *J. Sep. Sci.* **2008**, *31*, 1449-1464.
- (24) Dejaegher, B.; Mangelings, D.; Vander, H. Y. *J. Sep. Sci.* **2008**, *31*, 1438-1448.
- (25) Boehm, R. E.; Martire, D. E.; Armstrong, D. W. *Analytical Chemistry* **1988**, *60*, 522-528.
- (26) Pirkle, W. H.; Pochapsky, T. C. *Chem. Rev.* **1989**, *89*, 347-62.
- (27) Rogozhin, S. V.; Davankov, V. A. *Journal of the Chemical Society D: Chemical Communications* **1971**, 490a-490a.
- (28) US4043979A, 1977.
- (29) Lindner, K. R.; Mannschreck, A. *J. Chromatogr.* **1980**, *193*, 308-10.
- (30) Pirkle, W. H.; Hyun, M. H.; Bank, B. *J. Chromatogr.* **1984**, *316*, 585-604.
- (31) Pirkle, W. H.; Tsipouras, A. *J. Chromatogr.* **1984**, *291*, 291-8.
- (32) Pirkle, W. H.; Hyun, M. H. *J. Org. Chem.* **1984**, *49*, 3043-6.
- (33) Pirkle, W. H.; Welch, C. J.; Hyun, M. H. *J. Org. Chem.* **1983**, *48*, 5022-6.
- (34) Pirkle, W. H.; Schreiner, J. L. *J. Org. Chem.* **1981**, *46*, 4988-91.
- (35) Pirkle, W. H.; House, D. W.; Finn, J. M. *J. Chromatogr.* **1980**, *192*, 143-58.
- (36) Chang, C. A.; Wu, Q.; Armstrong, D. W. *J. Chromatogr.* **1986**, *354*, 454-8.
- (37) Armstrong, D. W.; DeMond, W.; Alak, A.; Hinze, W. L.; Riehl, T. E.; Bui, K. H. *Anal. Chem.* **1985**, *57*, 234-7.
- (38) Armstrong, D. W.; Alak, A.; Bui, K.; DeMond, W.; Ward, T.; Riehl, T. E.; Hinze, W. L. *J. Inclusion Phenom.* **1984**, *2*, 533-45.

- (39) Armstrong, D. W.; DeMond, W. *J. Chromatogr. Sci.* **1984**, *22*, 411-15.
- (40) Stalcup, A. M.; Armstrong, D. W.; Ed. Sante, 1990, pp 607-16.
- (41) Stalcup, A. M.; Chang, S. C.; Armstrong, D. W.; Pitha, J. *J. Chromatogr.* **1990**, *513*, 181-94.
- (42) Armstrong, D. W.; Li, W.; Chang, C. D.; Pitha, J. *Anal. Chem.* **1990**, *62*, 914-23.
- (43) Armstrong, D. W.; Faulkner, J. R., Jr.; Han, S. M. *J. Chromatogr.* **1988**, *452*, 323-30.
- (44) Han, S. M.; Armstrong, D. W. *J. Chromatogr.* **1987**, *389*, 256-60.
- (45) Armstrong, D. W.; Ward, T. J.; Armstrong, R. D.; Beesley, T. E. *Science (Washington, D. C., 1883-)* **1986**, *232*, 1132-5.
- (46) Allenmark, S.; Bomgren, B.; Andersson, S. *Prep Biochem* **1984**, *14*, 139-47.
- (47) Yuki, H.; Okamoto, Y.; Okamoto, I. *J. Am. Chem. Soc.* **1980**, *102*, 6356-8.
- (48) Okamoto, Y.; Kawashima, M.; Hatada, K. *J. Am. Chem. Soc.* **1984**, *106*, 5357-9.
- (49) Armstrong, D. W.; Tang, Y.; Chen, S.; Zhou, Y.; Bagwill, C.; Chen, J.-R. *Anal. Chem.* **1994**, *66*, 1473-84.
- (50) Mandl, A.; Nicoletti, L.; Lammerhofer, M.; Lindner, W. *J. Chromatogr. A* **1999**, *858*, 1-11.
- (51) Laemmerhofer, M.; Lindner, W. *J. Chromatogr. A* **1996**, *741*, 33-48.
- (52) Han, X.; Wang, C.; He, L.; Beesley, T. E.; Armstrong, D. W. *Anal. Bioanal. Chem.* **2007**, *387*, 2681-2697.
- (53) Han, X.; He, L.; Zhong, Q.; Beesley, T. E.; Armstrong, D. W. *Chromatographia* **2006**, *63*, 13-23.
- (54) Zhong, Q.; Han, X.; He, L.; Beesley, T. E.; Trahanovsky, W. S.; Armstrong, D. W. *J. Chromatogr. A* **2005**, *1066*, 55-70.
- (55) Sun, P.; Wang, C.-L.; Breitbach, Z. S.; Zhang, Y.; Armstrong, D. W. *Anal. Chem. (Washington, DC, U. S.)* **2009**, *81*, 10215-10226.
- (56) Fjeldsted, J. C.; Lee, M. L. *Anal. Chem.* **1984**, *56*, 619A-620A, 622A, 624A, 627A, 628A.
- (57) Smith, R. D.; Felix, W. D.; Fjeldsted, J. C.; Lee, M. L. *Anal. Chem.* **1982**, *54*, 1883-5.
- (58) Smith, R. M. *J. Chromatogr. A* **1999**, *856*, 83-115.
- (59) Taylor, L. T. *Anal. Chem. (Washington, DC, U. S.)* **2010**, *82*, 4925-4935.
- (60) Taylor, L. T. *J. Supercrit. Fluids* **2009**, *47*, 566-573.
- (61) Berger, T. A. *J. Chromatogr. A* **1997**, *785*, 3-33.
- (62) Berger, T.; Berger, B. *LCGC North Am.* **2010**, *28*, 344-357.
- (63) Zheng, J.; Taylor, L. T.; Pinkston, J. D. *Chromatographia* **2006**, *63*, 267-276.
- (64) Cazenave-Gassiot, A.; Boughtflower, R.; Caldwell, J.; Hitzel, L.; Holyoak, C.; Lane, S.; Oakley, P.; Pullen, F.; Richardson, S.; Langley, G. J. *J. Chromatogr. A* **2009**, *1216*, 6441-6450.
- (65) Ashraf-Khorassani, M.; Taylor, L. T. *J. Sep. Sci.* **2010**, *33*, 1682-1691.
- (66) Yip, H. S. H.; Ashraf-Khorassani, M.; Taylor, L. T. *Chromatographia* **2007**, *65*, 655-665.
- (67) Berger, T. A.; Fogleman, K.; Staats, T.; Bente, P.; Crocket, I.; Farrell, W.; Osonubi, M. *J. Biochem. Biophys. Methods* **2000**, *43*, 87-111.
- (68) Berger, T. A.; Wilson, W. H. *J. Biochem. Biophys. Methods* **2000**, *43*, 77-85.
- (69) Bailey, C. J.; Ruane, R. J.; Wilson, I. D. *J. Chromatogr. Sci.* **1994**, *32*, 426-9.
- (70) Bui, H.; Masquelin, T.; Perun, T.; Castle, T.; Dage, J.; Kuo, M.-S. *J. Chromatogr. A* **2008**, *1206*, 186-195.
- (71) Steuer, W.; Baumann, J.; Erni, F. *J. Chromatogr.* **1990**, *500*, 469-79.
- (72) Perkins, J. R.; Games, D. E.; Startin, J. R.; Gilbert, J. *J. Chromatogr.* **1991**, *540*, 239-56.
- (73) West, C.; Lesellier, E. *J. Chromatogr. A* **2007**, *1169*, 205-219.

- (74) Bhoir, I. C.; Patil, S. T.; Sundaresan, M. *Talanta* **1999**, *48*, 1179-1189.
- (75) Lesellier, E.; Tchaplal, A. *J. Chromatogr. A* **2005**, *1100*, 45-59.
- (76) Matsubara, A.; Bamba, T.; Ishida, H.; Fukusaki, E.; Hirata, K. *J. Sep. Sci.* **2009**, *32*, 1459-1464.
- (77) Schoenmakers, P. J.; Verhoeven, F. C. C. J. G.; Van, d. B. H. M. *J. Chromatogr.* **1986**, *371*, 121-34.
- (78) Bamba, T.; Fukusaki, E.; Kajiyama, S.; Ute, K.; Kitayama, T.; Kobayashi, A. *J. Chromatogr. A* **2001**, *911*, 113-117.
- (79) Harris, C. M. *Anal. Chem.* **2002**, *74*, 87A-91A.
- (80) Mukhopadhyay, R. *Anal. Chem. (Washington, DC, U. S.)* **2008**, *80*, 3091-3094.
- (81) Bonhote, P.; Dias, A.-P.; Papageorgiou, N.; Kalyanasundaram, K.; Graetzel, M. *Inorg. Chem.* **1996**, *35*, 1168-78.
- (82) Sun, J.; Forsyth, M.; MacFarlane, D. R. *J. Phys. Chem. B* **1998**, *102*, 8858-8864.
- (83) Parshall, G. W. *J. Amer. Chem. Soc.* **1972**, *94*, 8716-19.
- (84) Williams, S. D.; Schoebrechts, J. P.; Selkirk, J. C.; Mamantov, G. *J. Am. Chem. Soc.* **1987**, *109*, 2218-19.
- (85) G. Huddleston, J.; D. Rogers, R. *Chemical Communications* **1998**, 1765-1766.
- (86) Karodia, N.; Guise, S.; Newlands, C.; Andersen, J.-A. *Chemical Communications* **1998**, 2341-2342.
- (87) Berthod, A.; Ruiz-Angel, M. J.; Carda-Broch, S. *J. Chromatogr. A* **2008**, *1184*, 6-18.
- (88) Anderson, J. L.; Armstrong, D. W. *Anal. Chem.* **2005**, *77*, 6453-6462.
- (89) Wanigasekara, E.; Perera, S.; Crank, J. A.; Sidisky, L.; Shirey, R.; Berthod, A.; Armstrong, D. W. *Anal. Bioanal. Chem.* **2010**, *396*, 511-524.
- (90) Liu, S.-J.; Zhou, F.; Zhao, L.; Xiao, X.-H.; Liu, X.; Jiang, S.-X. *Chem. Lett.* **2004**, *33*, 496-497.
- (91) Sun, Y.; Stalcup, A. M. *J. Chromatogr. A* **2006**, *1126*, 276-282.
- (92) Qiu, H.; Jiang, S.; Liu, X. *J. Chromatogr. A* **2006**, *1103*, 265-270.
- (93) Qiu, H.; Jiang, S.; Liu, X.; Zhao, L. *J. Chromatogr. A* **2006**, *1116*, 46-50.
- (94) Sun, Y.; Cabovska, B.; Evans, C. E.; Ridgway, T. H.; Stalcup, A. M. *Anal. Bioanal. Chem.* **2005**, *382*, 728-734.
- (95) Wang, Q.; Baker, G. A.; Baker, S. N.; Colon, L. A. *Analyst (Cambridge, U. K.)* **2006**, *131*, 1000-1005.
- (96) Chou, F.-M.; Wang, W.-T.; Wei, G.-T. *J. Chromatogr. A* **2009**, *1216*, 3594-3599.
- (97) He, L.; Zhang, W.; Zhao, L.; Liu, X.; Jiang, S. *J. Chromatogr. A* **2003**, *1007*, 39-45.
- (98) Ruiz-Angel, M. J.; Carda-Broch, S.; Berthod, A. *J. Chromatogr. A* **2006**, *1119*, 202-208.
- (99) Marszall, M. P.; Kalisz, R. *Crit. Rev. Anal. Chem.* **2007**, *37*, 127-140.
- (100) Masuda, F.; Watanabe, Y.; Ikegami, T.; Tanaka, N. *Chromatography* **2009**, *30*, 89-90.
- (101) Lai, G.; Peng, J.; Li, J.; Qiu, H.; Jiang, J.; Jiang, K.; Shen, Y. *Tetrahedron Lett.* **2006**, *47*, 6951-6953.
- (102) Gruttadauria, M.; Riela, S.; Aprile, C.; Meo, P. L.; D'Anna, F.; Noto, R. *Adv. Synth. Catal.* **2006**, *348*, 82-92.
- (103) Yang, Y.; Beele, B.; Bluemel, J. *J. Am. Chem. Soc.* **2008**, *130*, 3771-3773.
- (104) Tundo, P.; Venturello, P. *Tetrahedron Lett.* **1980**, *21*, 2581-4.
- (105) Tundo, P.; Venturello, P. *J. Am. Chem. Soc.* **1979**, *101*, 6606-13.
- (106) Tundo, P. *Journal of the Chemical Society, Chemical Communications* **1977**, 641-642.
- (107) Modrogan, E.; Valkenberg, M. H.; Hoelderich, W. F. *J. Catal.* **2009**, *261*, 177-187.

- (108) Takahashi, T.; Watahiki, T.; Kitazume, S.; Yasuda, H.; Sakakura, T. *Chemical Communications* **2006**, 1664-1666.
- (109) Bristow, P. A. *Liquid Chromatography in Practice*; H.E.T.P., 1976, p 270 pp.
- (110) Sommer, J.; Yang, Y.; Rambow, D.; Blumel, J. *Inorg Chem* **2004**, *43*, 7561-3.
- (111) Hampe, E. M.; Rudkevich, D. M. *Tetrahedron* **2003**, *59*, 9619-9625.
- (112) Strubinger, J. R.; Song, H.; Parcher, J. F. *Anal. Chem.* **1991**, *63*, 98-103.
- (113) Strubinger, J. R.; Song, H.; Parcher, J. F. *Anal. Chem.* **1991**, *63*, 104-8.
- (114) Zheng, J.; Glass, T.; Taylor, L. T.; Pinkston, J. D. *J. Chromatogr. A* **2005**, *1090*, 155-164.
- (115) Yanishlieva, N. V.; Marinova, E.; Pokorny, J. *Eur. J. Lipid Sci. Technol.* **2006**, *108*, 776-793.
- (116) Ternes, W.; Bigge, E. *Riv. Ital. EPPOS* **1998**, 252-259.
- (117) Rac, M.; Ostric, B. *Rev. Fr. Corps Gras* **1955**, *2*, 796-803.
- (118) Etter, S. C. *J. Herbs, Spices Med. Plants* **2004**, *11*, 121-159.
- (119) Wang, H.; Liu, F.; Yang, L.; Zu, Y.; Wang, H.; Qu, S.; Zhang, Y. *Food Chem.* **2011**, *128*, 93-99.
- (120) Medina, I.; Gonzalez, M. J.; Pazos, M.; Della, M. D.; Sacchi, R.; Gallardo, J. M. *Eur. Food Res. Technol.* **2003**, *217*, 301-307.
- (121) Ramalho, V. C.; Jorge, N. *Rev. Inst. Adolfo Lutz* **2006**, *65*, 15-20.
- (122) Hras, A. R.; Hadolin, M.; Knez, Z.; Bauman, D. *Food Chem.* **2000**, *71*, 229-233.
- (123) Trojakova, L.; Reblova, Z.; Nguyen, H. T. T.; Pokorny, J. *J. Food Lipids* **2001**, *8*, 1-13.
- (124) Shahidi, F.; Pegg, R. B.; Saleemi, Z. O. *J. Food Lipids* **1995**, *2*, 145-53.
- (125) Jिंगgang Yin, W. H., John C. Lang, Edward Chaum. In *ARVO 2012: Fort Lauderdale, FL, 2012*.
- (126) Daniel T. Organisciak, R. M. D., Christine M. Rapp, Rekha Rangarajan, John C. Lang. In *ARVO 2012: Fort Lauderdale, FL, 2012*.
- (127) Richheimer, S. L.; Bernart, M. W.; King, G. A.; Kent, M. C.; Bailey, D. T. *J. Am. Oil Chem. Soc.* **1996**, *73*, 507-14.
- (128) Pokorny, J. *EJEAFChe, Electron. J. Environ., Agric. Food Chem.* **2008**, *7*, 3320-3324.
- (129) Nakatani, N.; Inatani, R. *Agric. Biol. Chem.* **1981**, *45*, 2385-6.
- (130) Bandara, M. S.; Tanino, K. K.; Acharya, S. N.; Research Signpost, 2007, pp 173-194.
- (131) Johnson, J. J. *Cancer Lett. (N. Y., NY, U. S.)* **2011**, *305*, 1-7.
- (132) Aruoma, O. I.; Spencer, J. P. E.; Rossi, R.; Aeschbach, R.; Khan, A.; Mahmood, N.; Munoz, A.; Murcia, A.; Butler, J.; Halliwell, B. *Food Chem. Toxicol.* **1996**, *34*, 449-456.
- (133) Folin, O.; Ciocalteu, V. *J. Biol. Chem.* **1927**, *73*, 627-50.
- (134) Lowry, O. H.; Rosebrough, N. J.; Farr, A. L.; Randall, R. J. *J. Biol. Chem.* **1951**, *193*, 265-75.
- (135) Okamura, N.; Fujimoto, Y.; Kuwabara, S.; Yagi, A. *J. Chromatogr. A* **1994**, *679*, 381-6.
- (136) Herrero, M.; Plaza, M.; Cifuentes, A.; Ibanez, E. *J. Chromatogr. A* **2010**, *1217*, 2512-2520.
- (137) Ramirez, P.; Garcia-Risco, M. R.; Santoyo, S.; Senorans, F. J.; Ibanez, E.; Reglero, G. *J. Pharm. Biomed. Anal.* **2006**, *41*, 1606-1613.
- (138) Ramirez, P.; Santoyo, S.; Garcia-Risco, M. R.; Senorans, F. J.; Ibanez, E.; Reglero, G. *J. Chromatogr. A* **2007**, *1143*, 234-242.
- (139) Saenz-Lopez, R.; Fernandez-Zurbano, P.; Tena, M. T. *J. Chromatogr. A* **2002**, *953*, 251-256.

- (140) Bonoli, M.; Pelillo, M.; Lercker, G. *Chromatographia* **2003**, *57*, 505-512.
- (141) Doolaee, E. H. A.; Raes, K.; Smet, K.; Andjelkovic, M.; Van, P. C.; De, S. S.; Verhe, R. *J. Agric. Food Chem.* **2007**, *55*, 7283-7287.
- (142) Basaga, H.; Tekkaya, C.; Acikel, F. *Food Sci. Technol. (London)* **1997**, *30*, 105-108.
- (143) Schwarz, K.; Ternes, W. *Z. Lebensm.-Unters. Forsch.* **1992**, *195*, 99-103.
- (144) Schwarz, K.; Ternes, W.; Schmauderer, E. *Z. Lebensm.-Unters. Forsch.* **1992**, *195*, 104-7.
- (145) Irmak, S.; Solakyildirim, K.; Hesenov, A.; Erbatur, O. *J. Anal. Chem.* **2010**, *65*, 899-906.
- (146) Jose, d. B. M.; Benavente-Garcia, O.; Marin, P. M.; Marin, A. M.; Castillo, J. *Nutrafoods* **2006**, *5*, 41-48.
- (147) Hossain, M. B.; Rai, D. K.; Brunton, N. P.; Martin-Diana, A. B.; Barry-Ryan, C. *J. Agric. Food Chem.* **2010**, *58*, 10576-10581.
- (148) Almela, L.; Sanchez-Munoz, B.; Fernandez-Lopez, J. A.; Roca, M. J.; Rabe, V. *J. Chromatogr. A* **2006**, *1120*, 221-229.
- (149) Pretsch, E.; Buehlmann, P.; Affolter, C. *Structure Determination of Organic Compounds: Tables of Spectral Data, 3rd Completely Revised and Enlarged Edition*; Springer-Verlag, 2000, p 421 pp.
- (150) Scott, A. I. *The Interpretation of Ultraviolet Spectra of Natural Products*; Pergamon Press, 1962, p 500 pp.
- (151) Woodward, R. B. *J. Am. Chem. Soc.* **1942**, *64*, 72-5.
- (152) Masuda, T.; Inaba, Y.; Takeda, Y. *J. Agric. Food Chem.* **2001**, *49*, 5560-5565.
- (153) Nagakura, S.; Kuboyama, A. *J. Am. Chem. Soc.* **1954**, *76*, 1003-5.
- (154) Gonzalez, A. G.; Andres, L. S.; Aguiar, Z. E.; Luis, J. G. *Phytochemistry* **1992**, *31*, 1297-305.
- (155) Wenkert, E.; Fuchs, A.; McChesney, J. D. *J. Org. Chem.* **1965**, *30*, 2931-4.
- (156) Masuda, T.; Inaba, Y.; Maekawa, T.; Takeda, Y.; Tamura, H.; Yamaguchi, H. *J. Agric. Food Chem.* **2002**, *50*, 5863-5869.
- (157) Houlihan, C. M.; Ho, C. T.; Chang, S. S. *JAOCS, J. Am. Oil Chem. Soc.* **1985**, *62*, 96-8.
- (158) Verdine, G. L. *Nature (London)* **1996**, *384*, 11-13.
- (159) Jones, S. B.; Simmons, B.; Mastracchio, A.; MacMillan, D. W. C. *Nature (London, U. K.)* **2011**, *475*, 183-188.
- (160) Fernandez, L. S.; Jobling, M. F.; Andrews, K. T.; Avery, V. M. *Phytother Res* **2008**, *22*, 1409-12.
- (161) Fernandez, L. S.; Buchanan, M. S.; Carroll, A. R.; Feng, Y. J.; Quinn, R. J.; Avery, V. M. *Org. Lett.* **2009**, *11*, 329-332.
- (162) Fernandez, L. S.; Sykes, M. L.; Andrews, K. T.; Avery, V. M. *Int. J. Antimicrob. Agents* **2010**, *36*, 275-279.
- (163) Tillequin, F.; Koch, M.; Rabaron, A. *J. Nat. Prod.* **1985**, *48*, 120-3.
- (164) Tillequin, F.; Koch, M.; Pousset, J. L.; Cave, A. *J. Chem. Soc., Chem. Commun.* **1978**, 826-8.
- (165) Tillequin, F.; Rousselet, R.; Koch, M.; Bert, M.; Sevenet, T. *Ann Pharm Fr* **1979**, *37*, 543-8.
- (166) Purushothaman, K. K.; Sarada, A. *Phytochemistry* **1981**, *20*, 351-2.
- (167) Balde, A. M.; Pieters, L. A.; Gergely, A.; Wray, V.; Claeys, M.; Vlietinck, A. J. *Phytochemistry* **1991**, *30*, 997-1000.
- (168) Tillequin, F.; Koch, M.; Bert, M.; Sevenet, T. *J. Nat. Prod.* **1979**, *42*, 92-5.

- (169) Kong, Y. C.; Cheng, K. F.; Cambie, R. C.; Waterman, P. G. *J. Chem. Soc., Chem. Commun.* **1985**, 47-8.
- (170) Dethe, D. H.; Erande, R. D.; Ranjan, A. *J. Am. Chem. Soc.* **2011**, *133*, 2864-2867.
- (171) Pousset, J. L.; Kerharo, J.; Maynard, G.; Monseur, X.; Cave, A.; Goutarel, R. *Phytochemistry* **1973**, *12*, 2308-10.
- (172) Cheng, K. F.; Kong, Y. C.; Chan, T. Y. *J. Chem. Soc., Chem. Commun.* **1985**, 48-9.
- (173) Wenkert, E.; Moeller, P. D. R.; Piettre, S. R.; McPhail, A. T. *J. Org. Chem.* **1988**, *53*, 3170-8.
- (174) Chan, W. L.; Ho, D. D.; Lau, C. P.; Wat, K. H.; Kong, Y. C.; Cheng, K. F.; Wong, T. T.; Chan, T. Y. *Eur. J. Med. Chem.* **1991**, *26*, 387-94.
- (175) Sheu, J. H.; Chen, Y. K.; Hong, Y. L. V. *Tetrahedron Lett.* **1991**, *32*, 1045-6.
- (176) Sheu, J. H.; Chen, Y. K.; Hong, Y. L. V. *J. Org. Chem.* **1993**, *58*, 5784-7.
- (177) Lee, V.; Cheung, M.-K.; Wong, W.-T.; Cheng, K.-F. *Tetrahedron* **1996**, *52*, 9455-9468.
- (178) Vallakati, R.; May, J. A. *Synlett* **2012**, *23*, 2577-2581.
- (179) Vallakati, R.; May, J. A. *J. Am. Chem. Soc.* **2012**, *134*, 6936-6939.
- (180) Zeldin, R. M.; Toste, F. D. *Chem. Sci.* **2011**, *2*, 1706-1709.
- (181) Cheng, H.-G.; Lu, L.-Q.; Wang, T.; Yang, Q.-Q.; Liu, X.-P.; Li, Y.; Deng, Q.-H.; Chen, J.-R.; Xiao, W.-J. *Angew. Chem., Int. Ed.* **2013**, *52*, 3250-3254.
- (182) Wang, X.; Liu, Y.-S.; Nair, U. B.; Armstrong, D. W.; Ellis, B.; Williams, K. M. *Tetrahedron: Asymmetry* **1997**, *8*, 3977-3984.
- (183) Zeldin, R. M. *Gold(I)-catalyzed cycloisomerization reactions of allenes: An exploration of ligand effects and the total synthesis of flinderole B and C*. 2011.
- (184) Beesley, T. E. *LCGC North Am.* **2004**, 31.
- (185) Sztojkov-Ivanov, A.; Lazar, L.; Fulop, F.; Armstrong, D. W.; Peter, A. *Chromatographia* **2006**, *64*, 89-94.
- (186) Bosakova, Z.; Curinova, E.; Tesarova, E. *J. Chromatogr. A* **2005**, *1088*, 94-103.
- (187) Takacs-Novak, K.; Noszal, B.; Tokes-Kovesdi, M.; Szasz, G. *Int. J. Pharm.* **1993**, *89*, 261-3.
- (188) Berthod, A.; Nair, U. B.; Bagwill, C.; Armstrong, D. W. *Talanta* **1996**, *43*, 1767-1782.
- (189) Kosel, M.; Eap, C. B.; Amey, M.; Baumann, P. *J. Chromatogr. B: Biomed. Sci. Appl.* **1998**, *719*, 234-238.
- (190) El, D. S. *Chromatographia* **2010**, *71*, 783-787.
- (191) Nair, U. B.; Chang, S. S. C.; Armstrong, D. W.; Rawjee, Y. Y.; Eggleston, D. S.; McArdle, J. V. *Chirality* **1996**, *8*, 590-595.
- (192) Inc., A. S. T. In *A guide to using macrocyclic glycopeptide bonded phases for chiral LC separations*: USA, 2004.
- (193) Vallakati, R.; Smuts, J. P.; Armstrong, D. W.; May, J. A. *Tetrahedron Lett.* **2013**, *54*, 5892-5894.
- (194) Juvancz, Z.; Bodane, K. R.; Ivanyi, R.; Szente, L. *Electrophoresis* **2008**, *29*, 1701-1712.
- (195) Akiyama, T.; Itoh, J.; Yokota, K.; Fuchibe, K. *Angew. Chem., Int. Ed.* **2004**, *43*, 1566-1568.
- (196) Uraguchi, D.; Sorimachi, K.; Terada, M. *J. Am. Chem. Soc.* **2004**, *126*, 11804-11805.
- (197) Terada, M. *Chem. Commun. (Cambridge, U. K.)* **2008**, 4097-4112.
- (198) Li, G.-Q.; Gao, H.; Keene, C.; Devonas, M.; Ess, D. H.; Kurti, L. *J. Am. Chem. Soc.* **2013**, *135*, 7414-7417.

- (199) Sun, Z.; Winschel, G. A.; Borovika, A.; Nagorny, P. *J. Am. Chem. Soc.* **2012**, *134*, 8074-8077.
- (200) Zhang, H.; Wen, X.; Gan, L.; Peng, Y. *Org. Lett.* **2012**, *14*, 2126-2129.
- (201) Zamfir, A.; Tsogoeva, S. B. *Org. Lett.* **2010**, *12*, 188-191.
- (202) Storer, R. I.; Carrera, D. E.; Ni, Y.; MacMillan, D. W. C. *J. Am. Chem. Soc.* **2006**, *128*, 84-86.
- (203) McInturff, E. L.; Yamaguchi, E.; Krische, M. J. *J. Am. Chem. Soc.* **2012**, *134*, 20628-20631.
- (204) Zbieg, J. R.; Yamaguchi, E.; McInturff, E. L.; Krische, M. J. *Science (Washington, DC, U. S.)* **2012**, *336*, 324-327.
- (205) Kellogg, R. M.; Nieuwenhuijzen, J. W.; Pouwer, K.; Vries, T. R.; Broxterman, Q. B.; Grimbergen, R. F. P.; Kaptein, B.; La, C. R. M.; de, W. E.; Zwaagstra, K.; van, d. L. A. C. *Synthesis* **2003**, 1626-1638.
- (206) Bathori, N. B.; Nassimbeni, L. R. *Cryst. Growth Des.* **2012**, *12*, 2501-2507.
- (207) Loh, J. S. C.; Van, E. W. J. P.; Vlieg, E.; Gervais, C.; Grimbergen, R. F. P.; Kaptein, B. *Cryst. Growth Des.* **2006**, *6*, 861-865.
- (208) Kawamura, M.; Uchiyama, T.; Kuramoto, T.; Tamura, Y.; Mizutani, K. *Carbohydr. Res.* **1989**, *192*, 83-90.
- (209) Shizuma, M.; Takai, Y.; Kawamura, M.; Takeda, T.; Sawada, M. *J. Chem. Soc., Perkin Trans. 2* **2001**, 1306-1314.
- (210) Takai, Y.; Okumura, Y.; Tanaka, T.; Sawada, M.; Takahashi, S.; Shiro, M.; Kawamura, M.; Uchiyama, T. *J. Org. Chem.* **1994**, *59*, 2967-75.
- (211) Uchiyama, T.; Kawamura, M.; Uragami, T.; Okuno, H. *Carbohydr. Res.* **1993**, *241*, 245-8.
- (212) Yoshie, N.; Hamada, H.; Takada, S.; Inoue, Y. *Chem. Lett.* **1993**, *2*, 353-6.
- (213) Padivitage, N. L. T.; Dissanayake, M. K.; Armstrong, D. W. *Anal. Bioanal. Chem.* **2014**, *405*, 8837-8848.
- (214) Vozka, J.; Kalikova, K.; Roussel, C.; Armstrong, D. W.; Tesarova, E. *J. Sep. Sci.* **2013**, *36*, 1711-1719.
- (215) Gondova, T.; Petrovaj, J.; Kutschy, P.; Armstrong, D. W. *J. Chromatogr. A* **2013**, *1272*, 100-105.
- (216) Kozlik, P.; Simova, V.; Kalikova, K.; Bosakova, Z.; Armstrong, D. W.; Tesarova, E. *J. Chromatogr. A* **2012**, *1257*, 58-65.
- (217) Aranyi, A.; Bagi, A.; Illisz, I.; Pataj, Z.; Fueleop, F.; Armstrong, D. W.; Peter, A. *J. Sep. Sci.* **2012**, *35*, 617-624.
- (218) Padivitage, N. L. T.; Armstrong, D. W. *J. Sep. Sci.* **2011**, *34*, 1636-1647.
- (219) Sun, P.; Wang, C.; Padivitage, N. L. T.; Nanayakkara, Y. S.; Perera, S.; Qiu, H.; Zhang, Y.; Armstrong, D. W. *Analyst (Cambridge, U. K.)* **2011**, *136*, 787-800.
- (220) Qiu, H.; Loukotkova, L.; Sun, P.; Tesarova, E.; Bosakova, Z.; Armstrong, D. W. *J. Chromatogr. A* **2011**, *1218*, 270-279.
- (221) Sun, P.; Armstrong, D. W. *J. Chromatogr. A* **2010**, *1217*, 4904-4918.
- (222) Na, Y.-C. P.; Nilusha L. T.; Dissanayake, Milan K. and Armstrong, Daniel W. . *Supramolecular Chemistry* **2014**, *In press*.
- (223) Roumeliotis, P.; Unger, K. K.; Kurganov, A. A.; Davankov, V. A. *Journal of Chromatography A* **1983**, *255*, 51-66.
- (224) Bidlingmeyer, B. A.; Deming, S. N.; Price Jr, W. P.; Sachok, B.; Petrusek, M. *Journal of Chromatography A* **1979**, *186*, 419-434.
- (225) Gargano, A. F. G.; Kohout, M.; Macikova, P.; Laemmerhofer, M.; Lindner, W. *Anal. Bioanal. Chem.* **2013**, *405*, 8027-8038.

- (226) Pell, R.; Schuster, G.; Laemmerhofer, M.; Lindner, W. *J. Sep. Sci.* **2012**, *35*, 2521-2528.
- (227) Qiu, H.; Armstrong, D. W.; Berthod, A. *J. Chromatogr. A* **2013**, *1272*, 81-89.
- (228) Gritti, F.; Guiochon, G. *Anal. Chem.* **2006**, *78*, 4642-4653.
- (229) Durmaz, F.; Memon, F. N.; Memon, N. A.; Memon, S.; Memon, S.; Kara, H. *Chromatographia* **2013**, *76*, 909-919.
- (230) Okada, T. *Anal. Chem.* **1998**, *70*, 1692-1700.
- (231) Levitskaia, T. G.; Maya, L.; Van Berkel, G. J.; Moyer, B. A. *Inorganic Chemistry* **2006**, *46*, 261-272.
- (232) Roberts, J. M.; Diaz, A. R.; Fortin, D. T.; Friedle, J. M.; Piper, S. D. *Anal. Chem.* **2002**, *74*, 4927-4932.
- (233) Peruzzi, N.; Ninham, B. W.; Lo, N. P.; Baglioni, P. *J. Phys. Chem. B* **2012**, *116*, 14398-14405.
- (234) Bilanicová, D.; Salis, A.; Ninham, B. W.; Monduzzi, M. *The Journal of Physical Chemistry B* **2008**, *112*, 12066-12072.
- (235) Zhang, Y.; Cremer, P. S. *Curr. Opin. Chem. Biol.* **2006**, *10*, 658-663.
- (236) Staahlberg, J. *Anal. Chem.* **1994**, *66*, 440-9.
- (237) Lamb, J. D.; Drake, P. A. *J. Chromatogr.* **1989**, *482*, 367-80.
- (238) Fritz, J. S. *J. Chromatogr. A* **2005**, *1085*, 8-17.
- (239) Izatt, R. M.; Bradshaw, J. S.; Nielsen, S. A.; Lamb, J. D.; Christensen, J. J.; Sen, D. *Chem. Rev.* **1985**, *85*, 271-339.
- (240) Lamb, J. D.; Smith, R. G. *Talanta* **1992**, *39*, 923-30.
- (241) Smith, R. G.; Drake, P. A.; Lamb, J. D. *J. Chromatogr.* **1991**, *546*, 139-49.
- (242) Lamb, J. D.; Smith, R. G.; Jagodzinski, J. *J. Chromatogr.* **1993**, *640*, 33-40.

Biographical Information

Jonathan Paul Smuts obtained his Bachelor of Science degree, double major in chemistry and physics, in 1998 from the University of Cape Town, South Africa. He obtained a further Honours degree in chemistry in 1999 from the same institution. In 2000, he was employed by the leading South African petrochemical company, Sasol, as an analytical chemist focusing primarily on gas chromatography and ion chromatography. In 2006 Sasol sponsored his part-time Master of Science degree in analytical chemistry at the University of Stellenbosch, South Africa and in 2008 graduated with this degree. During this time love enraptured his soul and in April, 2008 the sublime impulse would eventually draw him away from South Africa to Texas, USA. In May of 2008 Jonathan and Kelly Smuts became husband and wife and in September, 2008 Jonathan became a graduate student at the University of Texas in Arlington. In 2009 he joined the Armstrong research group and focused his research on SFC and HPLC. His research interests are all forms of chromatography, chiral and achiral, with application towards petrochemicals, pharmaceuticals and natural products. He and Kelly have two children, Calvin and Elizabeth.